NOAA Technical Memorandum ERL ARL-225

THE DEFENSE SPECIAL WEAPONS AGENCY DIPOLE PRIDE 26 FIELD EXPERIMENT

Thomas B. Watson
Robert E. Keislar
Bradley Reese
David H. George

ARL/Field Research Division
Idaho Falls, Idaho

Christopher A. Biltoft

Meteorology and Obscurants Division
U.S. Army Dugway Proving Ground, Dugway, Utah

Air Resources Laboratory
Silver Spring, Maryland
May 1998

UNITED STATES DEPARTMENT OF COMMERCE

William M. Daley
Secretary

NATIONAL OCEANIC AND ATMOSPHERIC ADMINISTRATION

D. JAMES BAKER
Under Secretary for Oceans and Atmosphere/Administrator

Environmental Research Laboratories

James L. Rasmussen
Director

Notice

This document was prepared as an account of work sponsored by an agency of the United States Government. The views and opinions of the author expressed herein does not necessarily state or reflect those of the United States Government. Neither the United States Government, nor any of their employees, makes any warranty, express or implied, or assumes any legal liability or responsibility for the accuracy, completeness, or usefulness of any information, product, or process disclosed, or represents that its use would not infringe privately owned rights. Mention of a commercial company or product does not constitute an endorsement by NOAA/ERL. Use of information from this publication concerning proprietary products or the tests of such products for publicity or advertising purposes is not authorized.

CONTENTS

TABLES

FIGURES

ABSTRACT

The purpose of the DIPOLE PRIDE 26 (DP 26) tracer release field program was to obtain data on the transport of clouds resulting from sudden point releases of gaseous materials. The diffusion and dispersion of the inert chemical tracer, sulfur hexafluoride (SF_6), were measured under conditions simulating a release caused by a conventional weapons explosion. This data will be used for validation of models that predict exposure to toxic substances from these types of releases. DP 26 was held at the Department of Energy Nevada Test Site; tests began on November 4, 1996 and were conducted through November 20. A total of 21 SF_6 releases were made. An array of 90 whole air samplers in three lines and six continuous SF_6 analyzers were positioned down wind of the release site. The whole air samplers collected 15 minute integrated samples and were located approximately 1, 10, and 20 km from the release point. The continuous analyzers were located on the 10 km sampling line. The limit of detection for the continuous analyzers was 25 pptv and the limit of quantitation was 83 pptv. Data recovery from the whole air samplers was 93%. The limit of detection for the whole air samplers was 21 pptv and the limit of quantitation was 70 pptv. The data from the whole air samplers agreed within confidence limits with the results from continuous analyzers located at the same positions.

Meteorological measurements were made from a permanent network of towers positioned throughout the test area. Additional meteorological measurements were made using sonic anemometers, a radar wind profiler, radiosondes, and pibals. Infrared cameras and an FTIR spectrometer provided remote sensing measurements of the tracer clouds. The SF_6 tracer data combined with the extensive meteorological measurements make this data set a valuable resource for the evaluation of models designed to predict the results of sudden point source releases of gaseous substances.

The SF_6 concentration data and a three dimensional visualization program which graphically displays SF_6 concentration, wind flow, and the topography of Yucca Flat are available on compact disk. The supporting meteorological data are also available on magnetic or optical media.

INTRODUCTION

The destruction of targets containing chemical, biological, or radioactive materials can result in exposure of troops and civilians to dangerous levels of toxic substances. The Defense Special Weapons Agency (DSWA) has developed computer models to predict the results of using conventional weapons on targets containing hazardous materials. These tools are intended for use by commanders to help make battlefield decisions.

DSWA has developed the Second Order Closure, Integrated Puff (SCIPUFF) atmospheric transport and dispersion model, which is part of the Hazard Assessment and Consequence Analysis tool (HASCAL). The purpose of the Long Range Dispersion Model Validation program, Phase II, Subtest I, known as DIPOLE PRIDE 26 (DP 26), was to obtain data on transport to validate these models.

During DP 26, the diffusion and dispersion of the inert chemical tracer, sulfur hexafluoride (SF_6), were measured under conditions simulating a conventional weapons explosion. These tests were held at the Department of Energy (DOE) Nevada Test Site (NTS); they began on November 4, 1996 and were conducted through November 20. A total of 21 SF_6 releases were made (Table 1). Approximately 25 to 50 kg of SF_6 was released in a puff. An array of 90 whole air samplers and six continuous SF_6 analyzers were positioned down wind of the release. There were three sampling lines located approximately 1, 10, and 20 km from the northern release points. Thirty whole air samplers were located on each line at 300 meter intervals (see Figure 1 and Appendix 1 for details). The continuous analyzers were located on the 10 km sampling line. Chemical analysis of the samples and the results from the continuous analyzers provide the SF_6 concentration data necessary to calculate diffusion and dispersion parameters. Meteorological and remote sensor data were also collected.

Participants in DP 26 were DSWA; Dugway Proving Ground (DPG), Meteorology and Obscurants Division, West Desert Test Center; National Oceanic and Atmospheric Administration (NOAA) Air Resources Laboratory Field Research Division (ARLFRD) and Special Operations and Research Division (ARLSORD); Logicon, RDA; Aerospace Corporation; and the Department of Energy (DOE), Nevada Operations Office.

The data resulting from DP 26 can be used to validate models designed to predict the transport from sudden, point releases of gaseous materials over distances of 1 to 50 km. This technical memorandum provides an overview of the field experiment, describes the available tracer and meteorological data, and documents the experimental methods and data analysis procedures used in compiling the tracer data set.

Table 1: DIPOLE PRIDE 26 Test Summary.

Test #	Date (1996)	Trial* (JJJHHMM)	Sampler Start (PST)	Release Time (PST)	Release Point	Comments
1	11/4	3091441	14:00	14:41	S2	Missed grid
2	11/6	**********	8:00	**********	********	**No Release**
3	11/8	3130400	4:00	4:00	N3	Drainage
4	11/9	3140400	4:00	4:00	N3	Drainage
	11/9	3140530		5:38	N3	Drainage
5	11/11	3160400	4:30	4:40	N2	Drainage
6	11/12	3170400	4:00	4:00	N2	Drainage
7	11/12	3171300	13:00	13:00	S3	Up-Valley
	11/12	3171445		14:45	S3	Up-Valley
8	11/13	**********	9:30	**********	********	**No Release**
9	11/13	3181400	14:00	14:00	S2	Up-Valley
10	11/14	**********	9:00	**********	********	**No Release**
11	11/14	3191430	14:30	14:30	N2	Post-Frontal
	11/14	3191545		15:50	N2	Post-Frontal
12	11/15	3200900	9:00	9:00	N2	Post-Frontal
	11/15	3201030		10:30	N2	Post-Frontal

Test #	Date (1996)	Trial* (JJJHHMM)	Sampler Start (PST)	Release Time (PST)	Release Point	Comments
13	11/15	3201430	14:30	14:30	N2	Post-Frontal
14	11/16	3211300	13:00	13:00	S2	Up-Valley
15	11/18	3231130	11:30	11:30	S2	Up-Valley
	11/18	3231300		13:00	S2	Up-Valley
16	11/19	3241200	12:00	12:00	S3	Up-Valley
	11/19	3241330		13:30	S2	Up-Valley
17	11/20	3251200	12:00	12:00	S3	Pre-Frontal
	11/20	3251330		13:30	S2	Pre-Frontal

*Julian Day (JJJ) + intended release time (HHMM PST)

TEST SITE

Yucca Flat (37° N, 116° W) is a basin 30 km long and 12 km wide with the long axis oriented in the north-south direction. The lowest point of the basin, at an elevation of 1195 meters above mean sea level (MSL), is a seasonally dry lakebed known as Yucca Lake. The elevation of the basin increases from south to north at an average angle of 0.3°. The basin is surrounded by mountains; the mountains on the north and west sides have a minimum altitude of 1800 m MSL, and those on the east side have a minimum altitude of 1500 m MSL. There are passes at the northeast and southwest ends that form the main airflow channels (Figure 1).

The Yucca Flat site was chosen for this dispersion experiment because of the comparative homogeneity in terrain within the basin, and because of the mesoscale channeling of winds in a predictable, meridional (north-south) direction through the basin by the bordering mountains. In the absence of synoptic forcing (even as late in the year as this November test), a consistent, thermally-driven, diurnal pattern occurs: daytime heating of the higher terrain to the north causes up-valley southerly winds to develop by afternoon, while nocturnal cooling of this higher terrain causes northerly drainage flows to dominate after midnight. Under very stagnant conditions, the nocturnal drainage flow accumulates in a pool over Yucca Lake by morning. If weak to moderate synoptic forcing is present, mesoscale channeling of the meridional wind component generally reinforces one of the two thermally-driven diurnal flows, again imparting the desired wind orientation (Quiring). Under strong synoptic forcing, wind speeds may be outside experimental parameters (e.g., wind speed maximum set to avoid blowing dust or rapid dispersion of the plume before transport to sampling lines). These factors combine to provide a reasonable probability that tracer released from the appropriate north or south location will impact the grid on many test days.

SF_6 DISSEMINATION SYSTEM

The SF_6 gas release system used in DP 26 consists of two vertically mounted cylinders, solenoid-operated release valves, and a remote control panel. The cylinders have a volume of 0.15 m^3. The SF_6 is released through a 25-cm (10-inch) butterfly valve mounted on the top of the cylinder. During DP 26, one or both cylinders were filled with SF_6 gas to a pressure of approximately 150 psi. The two cylinders could be released individually or simultaneously. The release process lasted from 1 to 3 seconds. Each cylinder was equipped with a temperature sensor and a pressure transducer. This data was used to calculate the mass of SF_6 released during each test. The release system was mounted on the bed of a 5-ton flatbed truck. Details of the release system are presented in Appendix 7.

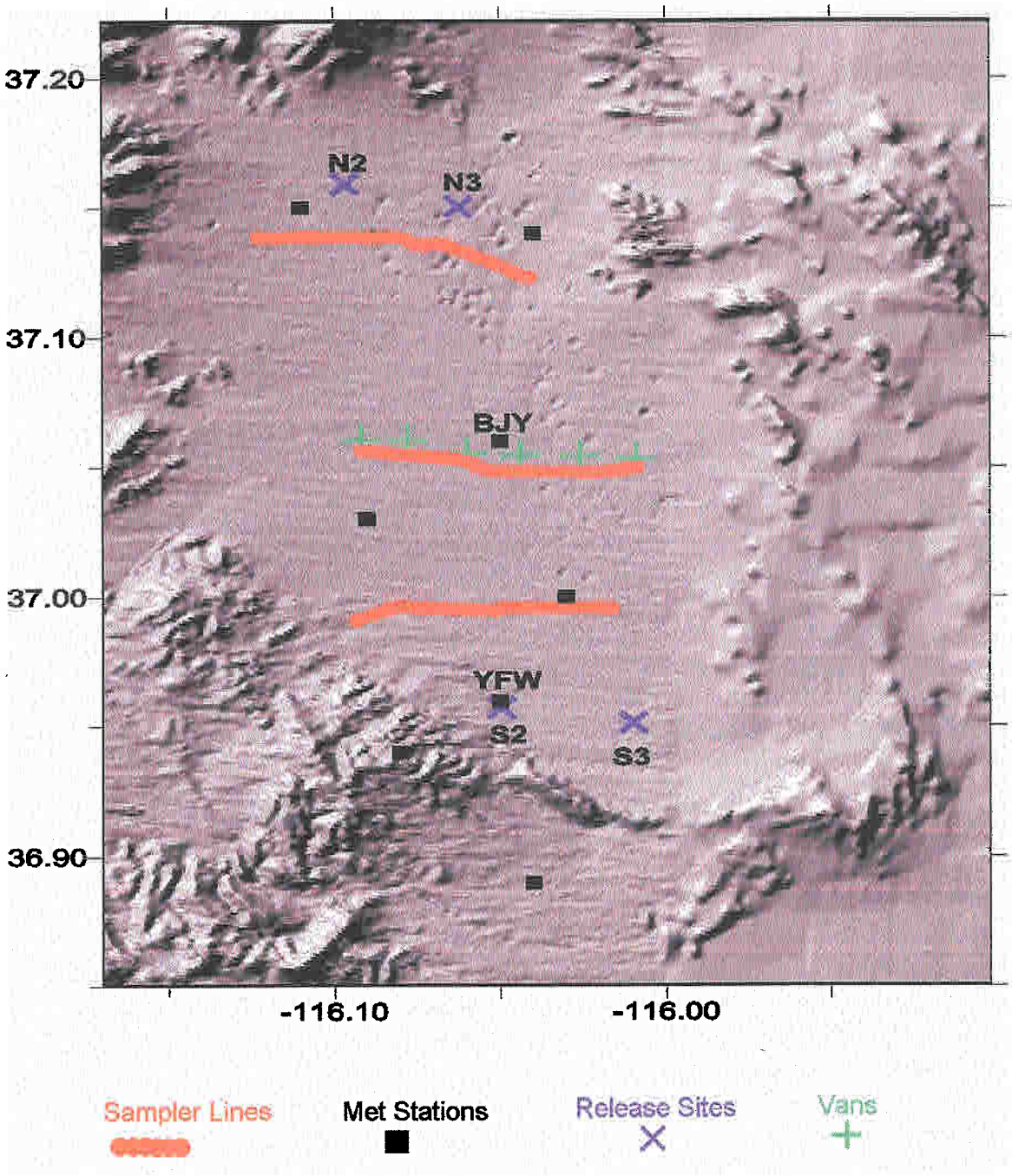

Figure 1: Yucca Flat topography with locations of release sites, samplers, vans, and meteorological stations. The display is 41 km (North–South) by 27 km (East-West)

TGA-4000 CONTINUOUS SF_6 ANALYZER

Continuous SF_6 concentration measurements were made using the TGA–4000 (Tracer Gas Analyzer) manufactured by Scientech Inc. of Pullman, Washington. This is a fast response instrument designed specifically to measure the concentration of SF_6 in ambient air. Six van-mounted instruments were deployed as shown in Figure 1 and listed in Appendix 1, Table A3.

The TGA–4000 consists of three units; a catalytic reactor, a dryer, and an electron capture detector (Figure 2). The electron capture detector (ECD) is very sensitive to halogenated compounds such as chlorofluorocarbons and SF_6. Its mass detection limit for halogenated compounds is on the order of one picogram. Unfortunately the detector also responds to oxygen. Therefore, oxygen must be removed from the sampled air before it reaches the detector. This is accomplished in two steps. First the oxygen is catalytically combined with hydrogen to produce water. This reaction is highly exothermic and must be carefully controlled by limiting the hydrogen supply. Second, a Nafion® semi-permeable membrane dryer removes the water from the sample stream. Dry, Ultra-High Purity (UHP, less than 1 ppbv halocarbons) nitrogen flows on one side of the membrane and the reacted ambient air, now mostly nitrogen and water, flows on the other. A water concentration gradient is established across the membrane. Nafion® is selectively permeable to water; it allows water to diffuse along the gradient through the membrane and into the dry nitrogen. The resulting sample stream acts as a carrier gas transporting any SF_6 present to the detector. The presence of hydrogen and the high temperature in the catalytic reactor destroy any halogenated hydrocarbons which could be sensed by the ECD and result in interfering signals. SF_6 is unaffected by these conditions.

Sampling and Calibration

The TGA-4000 was incorporated into an air sampling and calibration system (Figure 3), which consists of three subunits; a pump and filter to deliver the sampled air to the continuous analyzer, a dynamic dilution system for delivering calibration mixtures to the analyzer, and the analyzer itself.

The dynamic dilution system allows multi-point calibrations of the analyzer with a single calibration standard by changing the amount of calibration gas mixed into the ambient air flow. The calibration standard is introduced into the air stream and its flow rate

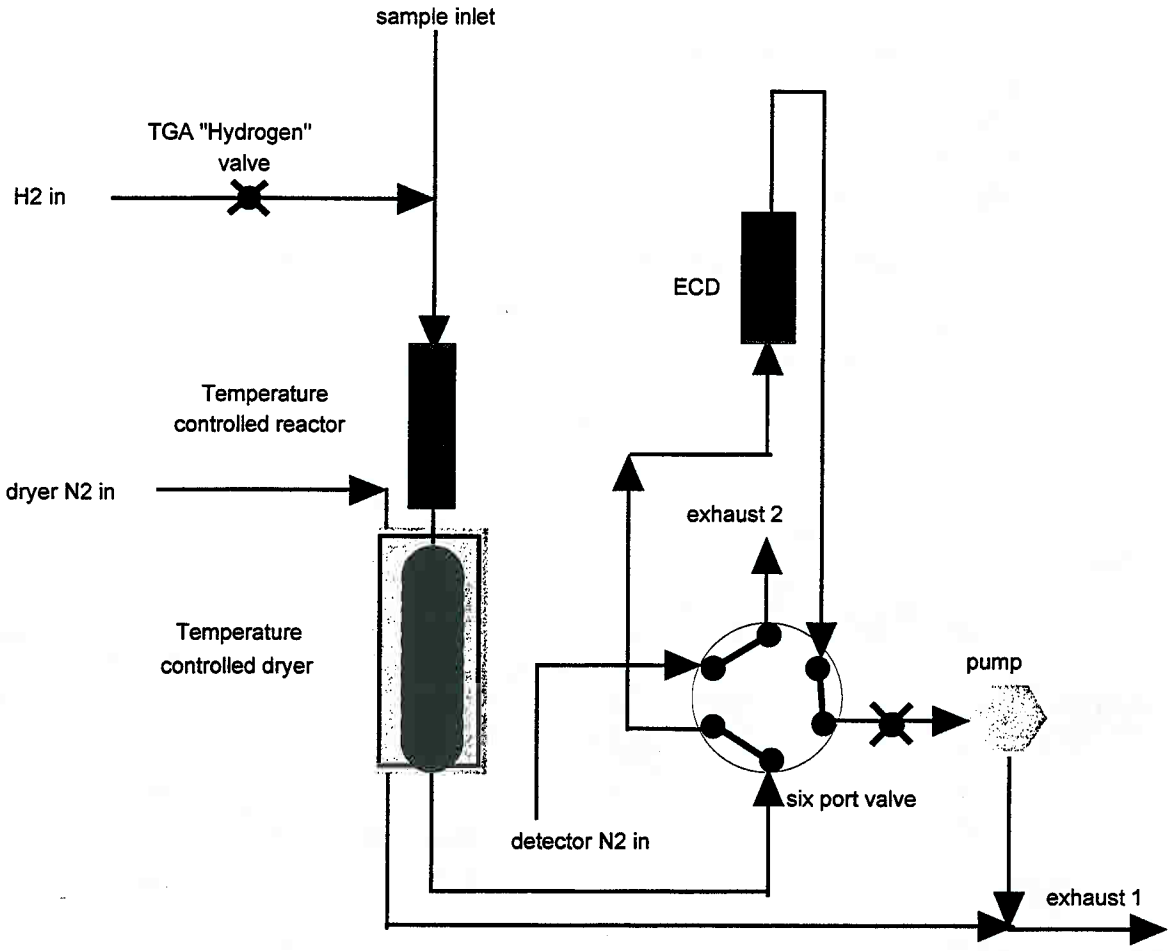

Figure 2: Schematic of the TGA-4000 (six port valve shown in the sample position).

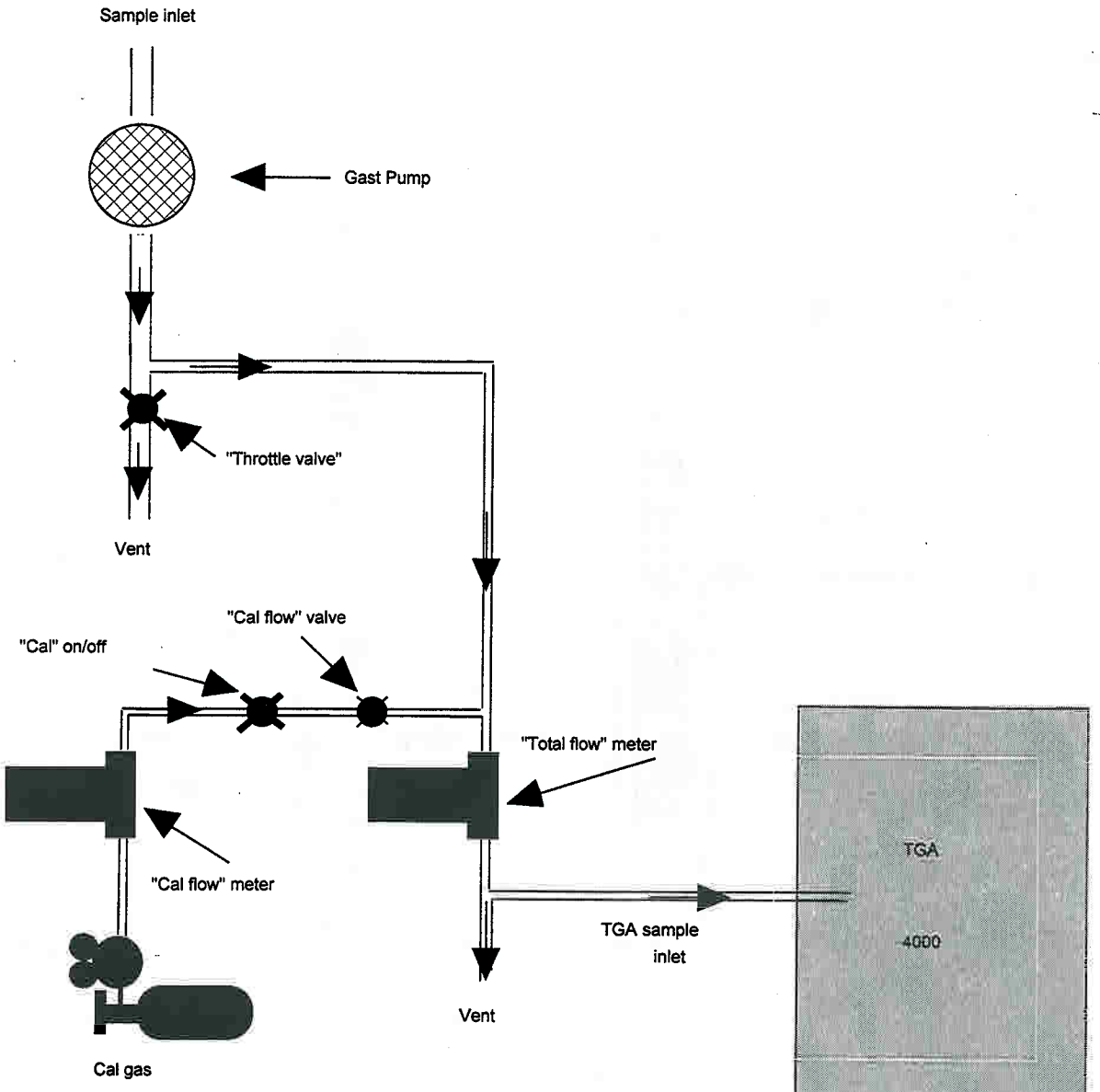

Figure 3: Schematic of the TGA-4000 sample acquisition and calibration system.

measured. The total flow to the instrument is measured. The concentration of SF_6 delivered to the analyzer is given by:

$$\text{Concentration } SF_6 = \left(\frac{\text{flow of calibration standard}}{\text{total flow}}\right)(\text{concentration calibration standard})$$

By varying the flow of the calibration standard while keeping the total flow constant, a number of different concentrations can be supplied to the instrument. The flows were regulated with needle valves and measured with mass flow meters (Omega Engineering, Stamford CT). The flow meters were calibrated in the laboratory and found to have an accuracy of ± 2%. This value is in agreement with the manufacturer's specifications.

Data Acquisition

The TGA signal along with real time GPS position, data from the flow controllers, instrument temperatures, ambient pressure, and valve positions are collected by a CR-10 data logger (Campbell Scientific, Logan UT) at a rate of 4 Hz. The data are transferred to a laptop computer where they are stored and the TGA signal is graphically displayed. A description of the data files is given in Appendix 5.

TGA-4000 Performance Statistics

Two quantities that are useful for evaluating instrument performance are the limit of detection (LOD) and the limit of quantitation (LOQ). The LOD is the lowest concentration at which there is 99% certainty that the analyte is detected. The LOQ is the minimum concentration, which can be measured with a relative error of ± 30% at the 95% confidence level (Taylor,1987). The LOD is defined as three times the standard deviation obtained as the concentration goes to zero (σ_0). The quantity σ_0 can be estimated by extrapolation to zero concentration of the standard deviations calculated for repeated measurements of a series of calibration concentrations or from a measurement of the signal noise. The LOQ is defined as 10 times σ_0. The LOD and LOQ, as determined from instrument performance during DP 26, are given in Table 2. The value of σ_0 was determined from analysis of signal noise. The confidence limits determined from laboratory measurements of calibration standards treated as unknowns are given in Table 2a.

The response time for the TGA-4000 has been measured as 0.86 s (Benner and Lamb, 1985).

Table 2: Performance Statistics for TGA-4000 during DP 26.

Unit	σ_0 (pptv)	LOD (pptv)	LOQ (pptv)
1	11	33	110
2	7	21	70
3	14	42	140
4	5	15	50
5	6	18	60
6	7	21	70
Mean	8	25	83

Table 2a: Performance Statistics for TGA-4000 from Laboratory Measurements.

Standard concentration (pptv)	Mean measured concentration (pptv)	Standard deviation (pptv)	95% confidence (2σ) limit (pptv)	Relative 95% confidence limit
40	32.3	3.56	7	0.18
200	180	10.8	22	0.11
813	745	26.5	43	0.05
1560	1470	34.4	69	0.04
5000	5231	167	334	0.07

SF_6 WHOLE AIR SAMPLING

The FRD whole air sampling method can be applied to permanent atmospheric gases and intentionally released tracers such as SF_6. It is built around programmable air samplers which fill twelve, one-liter Tedlar® bags housed in a removable cartridge. The sampler is contained in a waxed cardboard box 50 cm long, 30 cm high, and 40 cm wide, and weighs 4 kg. (9 pounds). An aluminum handle allows the sampler to be suspended from a bracket. The sampler has been successfully deployed in all types of weather conditions, including sub-zero blizzards, thunderstorms, and high winds (Watson, 1995). A programmable microprocessor controls the sampling. The control unit activates a pumping cycle at equally spaced intervals during the period of interest. Each bag has its own pump. The check valve in the pump seals the bag before and after filling. One-hundred to three-hundred cycles are required to fill a bag, depending on the ambient temperature. Each cycle lasts several seconds and transports from one to three ml of air into a sample bag, resulting in the collection of a whole air sample in which the concentration of the species of interest is integrated over the sampling period. The sampler can be programmed to fill bags during time periods ranging from ten minutes to several days. The bags are filled sequentially so that a single sampler can collect twelve consecutive, integrated samples before the cartridge must be changed. The unit is powered by a single "D" cell, which has sufficient capacity to fill 60 sample bags.

A large number of samples are generated during an intensive sampling study. DP 26, for example, produced over 23,000 samples including quality control samples and calibration standards. FRD has developed an automated gas analysis system (Figure 4), to minimize sample handling and analytical time, making it practical to analyze large numbers of samples.

At the core of the system is a chromatograph. Here the components of the air sample are separated and the species of interest detected. The separations are performed using two, quarter-inch stainless steel columns packed with 5Å molecular sieves (Supelco, Inc., Bellefonte, PA). The SF_6 is detected with an electron capture detector (Valco instruments Co. Inc., Houston, TX, model 140BN). During DP 26, the carrier gas was UHP nitrogen obtained from several sources and was further purified using a model CAT-1 catalytic combustion filter and a GP-1 molecular sieve, Drierite trap (Trace Analytical, Menlo Park, CA) and a high capacity gas purifier to remove oxygen and water (Supelco, Inc.). The sample injection valve, the sample loop, and the column were contained in an oven maintained at 50^{o} C. The sample loop volume was 5 cm^3.

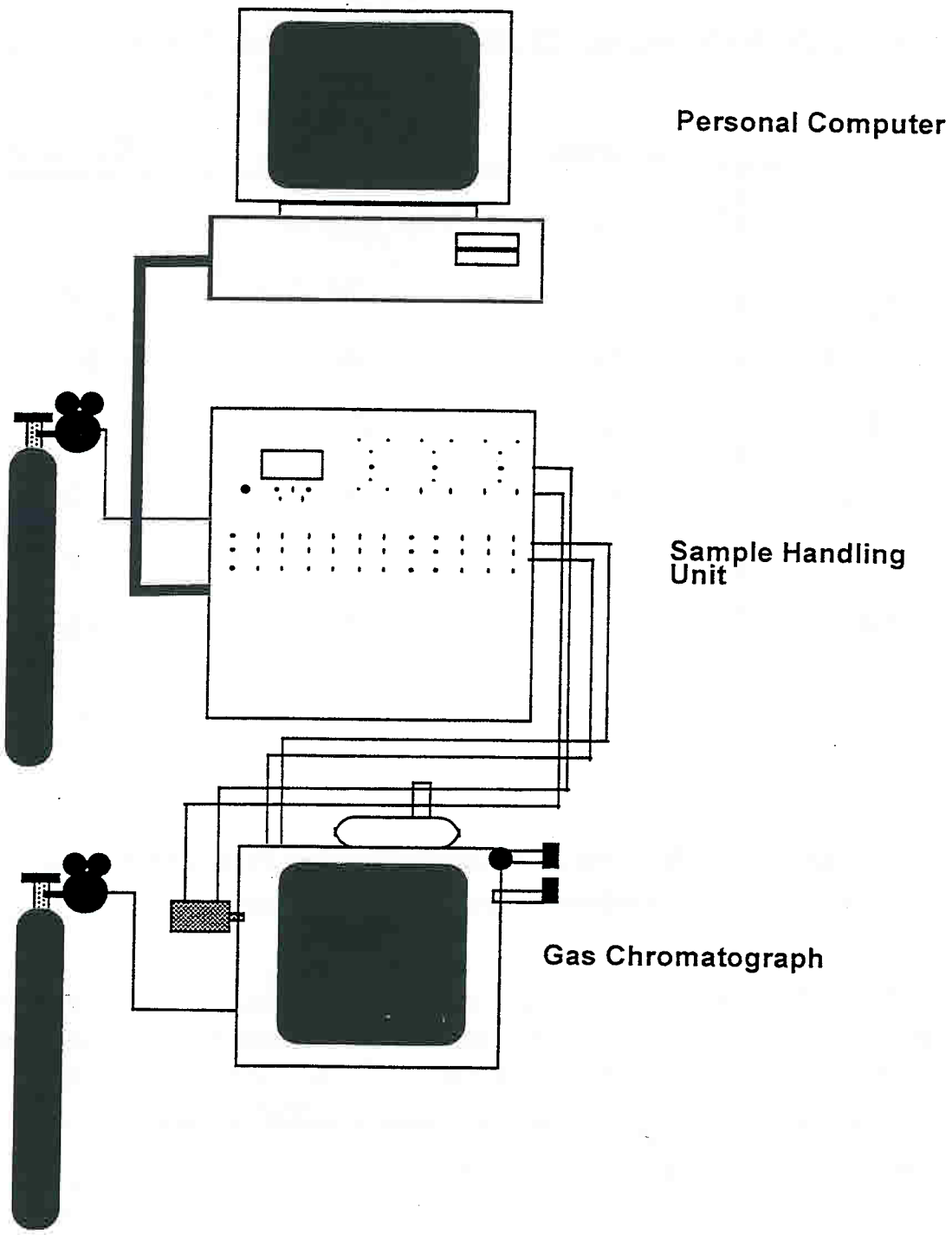

Figure 4: The whole air sample analytical system.

A personal computer (PC) controls the system operation and records oven temperature and pressure in the sample loop as well as the raw detector signal. The PC also processes the signal. This consists of integration of the peak of interest and correction to standard temperature and pressure. Concentrations are calculated based on calibration data. The chromatograms, peak areas, calculated concentrations, and sample identification are all displayed on a monitor. All sample cartridges are labeled with a bar code. The code is read into the PC using a laser scanner. The data is stored on disk in both raw and processed forms.

A third subsystem is a gas handling unit, which sequentially introduces aliquots from each bag of a sample cartridge into the gas chromatograph. Between samples the system is purged with nitrogen.

Calibration of the analytical system was performed using SF_6 in ultra zero air (Scott-Marin, Riverside, CA) at the beginning of each analytical shift and after every 120 (ten sample cartridges) analyses. Control charts were also constructed for the entire experiment and for each test within the experiment. Three analytical systems were used to analyze the DIPOLE PRIDE tests. They were run continuously throughout the program. A single test took approximately 15 hours to analyze; all tests were analyzed within 36 hours of sample collection.

The precision of the analytical method was determined using a linear fit of the standard deviation of the instrument response to each calibration standard versus concentration. The intercept of this fit is an estimation of the standard deviation at zero concentration or the baseline noise, σ_0. The LOD ($3\sigma_0$) and LOQ (σ_0) determined in this manner for each GC system are found in Table 3.

The precision of the analysis method can also be estimated from the reanalysis of samples. During DP26, 1275 samples were analyzed twice. The results were highly correlated. A linear fit between the two analyses resulted in a line with a slope of 1.01± 0.01, an intercept of 2 ± 1 pptv, and a correlation coefficient (r^2) of 0.99 (Figure 5). The mean difference between the two analyses was 8 pptv with a standard deviation of 30 pptv. Since both the absolute and relative differences in the measurements are a function of the concentration of SF_6 being measured, a more meaningful measure of precision is the absolute and relative differences between duplicate samples over a series of concentration ranges. The mean absolute difference is defined as the absolute value of the difference between the first analysis and the second analysis. The mean absolute relative difference is defined as the mean absolute difference divided by the average of first and second analyses. These quantities, over six concentration ranges, are given in Table 4. This replicate analysis data places a somewhat higher value on the analytical LOQ of 50 pptv.

Table 3: Performance Statistics for Gas Chromatographs Estimated From Calibration Standards.

Unit	σ_0 (pptv)	LOD (pptv)	LOQ (pptv)
1	5	15	50
2	1	3	10
3	2	6	20
Means	3	8	27

Table 4: Performance Statistics for Gas Chromatographs Estimated From Replicate Analyses.

[SF_6] range (pptv)	Mean absolute difference (pptv)	Standard deviation (pptv)	mean absolute relative difference	standard deviation	relative 95% confidence level (2σ)	Number of points
<LOD=8	2	3	0.29	0.30	0.6	937
<LOQ=27	5	6	0.36	0.42	0.84	137
LOQ to 50	5	6	0.17	0.25	0.50	56
50 to 100	8	9	0.11	0.15	0.30	40
100 to 500	18	24	0.08	0.12	0.24	56
500 – 1000	41	50	0.06	0.06	0.12	13
> 1000	104	117	0.04	0.05	0.10	36

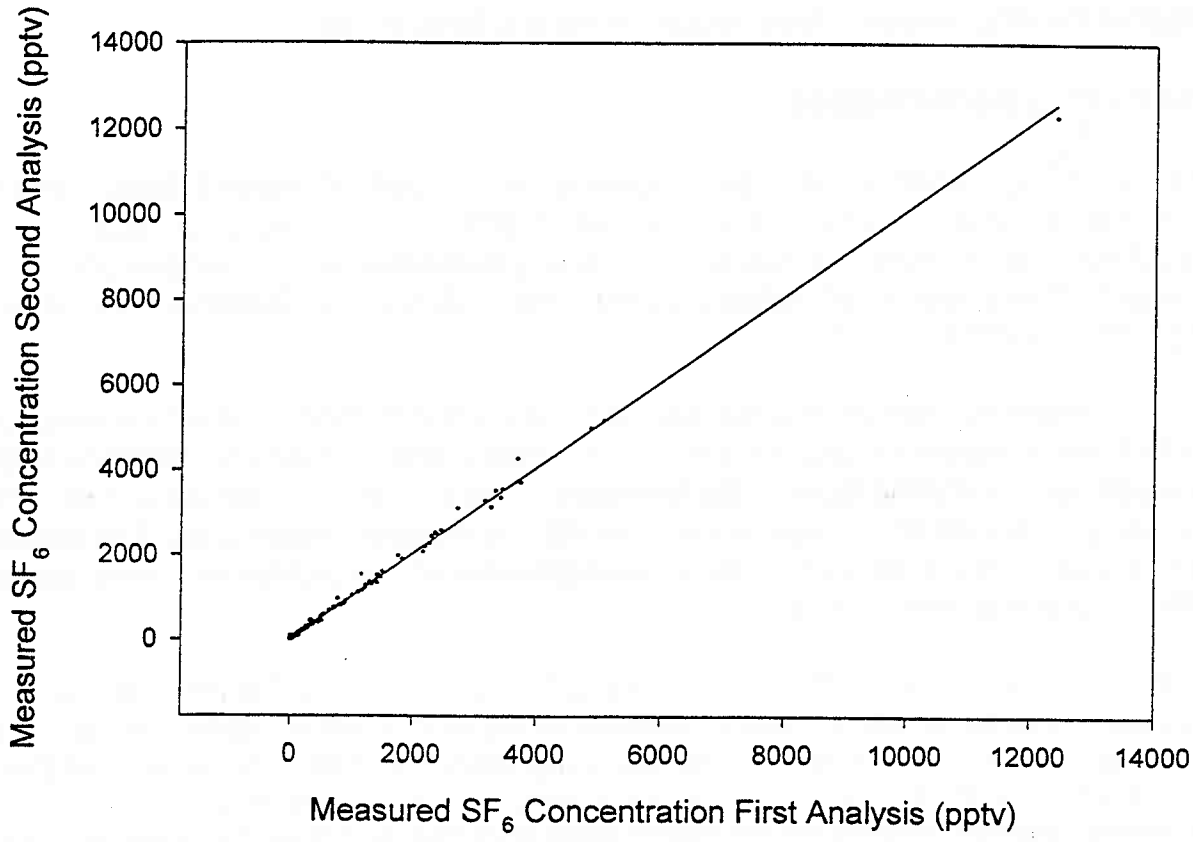

Figure 5: Comparison of reanalysis of samples. The solid line is a linear fit to the data: $y = (1.01 \pm 0.01)\,x + (0.6 \pm 0.7)$, $r^2 = 0.997$, N=1275.

Sampler Programming During DP 26

The samplers were programmed to execute 225 pumping cycles during each 15-minute sampling period. The line farthest from the release point (line 100 for southern releases, and line 300 for northern releases) was delayed by one half hour from the start of the SF_6 release. Sampler start times are listed in Table 1.

Sampling performance

During DP 26, 19,688 ambient air samples were collected. Sampler failures, incorrectly handled cartridges, or analytical errors made 1,386 of these samples unusable. The resulting data recovery rate was 93%. The SF_6 plume missed the sampler grid during Tests 1. There was no SF_6 release during Tests 2, 8, and 10. Samples from Tests 8 and 10 were not analyzed.

The precision and accuracy of the laboratory analytical method does not necessarily reflect the precision and accuracy of the SF_6 measurements made by collecting field samples and analyzing them in the laboratory. The processes of sampling and sample handling introduce additional uncertainties into the measured quantities. The accuracy and precision of the sampling method were determined using dynamic blanks, dynamic spikes, and duplicate samples.

A dynamic blank is a sample collected using the standard sampling protocol but in isolation from the ambient levels of analyte. Analysis of these samples is a measure of residual analyte concentrations in the sampling system and can identify contamination problems. Blanks also provide a means of measuring the baseline noise of the sampling method. During DP 26, blanks were collected by connecting the inlet lines of a sampler to Tedlar® bags containing UHP air. The sampler was then downloaded with the same program used for all samplers.

A dynamic spike is a sample where a known concentration of analyte is supplied to the sampler. Analysis of the resulting cartridge is a measure of the accuracy of the sampling method. During DP 26, spikes were collected by supplying samplers with calibration standards in a manner similar to the blank samples.

Samplers deployed at the same location are known as duplicates. The concentrations measured in duplicate samples should agree within analytical and sampling confidence limits.

One blank sampler, one spike sampler, and two duplicate samplers were located at sampling stations 115, 215, and 315 on each sampling line (see Appendix 1 for sampler locations).

The blanks provide a measurement that is equivalent to a baseline noise measurement of an analytical instrument as well as a means of detecting contamination. Analysis of the results from 455 blank samples showed that the mean level of SF_6 measured in these samples was 4 pptv with a standard deviation of 7 pptv, indicating that there was no contamination (Figure 6). From this result we determined that the noise level of the sampling method was 7 pptv resulting in an LOD of 21 pptv and an LOQ of 70 pptv. These values are higher than the equivalent values determined for the analytical method and are the limiting values for the coupled sampling and analysis system.

The spike samples provide a calibration of the sampling method that is equivalent to the calibration of an analytical instrument. Analysis was restricted to the results from six spike concentrations ranging from 2 to 200 ppbv SF_6 because this range could be analyzed with a single instrument attenuation. Comparison of the concentration values resulting from the analysis of 225 spiked samples to the concentration of the standards as reported by the supplier (Figure 7) resulted in a linear fit with a slope of 0.91 ± 0.02, an intercept of 1 ± 1 pptv, and a correlation coefficient (r^2) of 0.95. The standard deviation of the results for these spikes versus reported concentration was plotted and fit with a straight line (Figure 8). The resulting equation, $y=(0.15 \pm 0.02)\,x + (1.5 \pm 1.4)$ can be used to estimate the relative standard deviation of measurements over 100 pptv as 15%. This is an overestimation, particularly at high concentration levels, because the relative standard deviation will decrease as concentration increases.

The precision of the sampling method can also be estimated by comparing the results of 693 duplicate samples. Concentrations measured in the duplicate samples were highly correlated (Figure 9). A linear fit between concentrations obtained from these samples, weighted with the standard deviation given by the equation from Figure 8, resulted in a slope of 0.98 ± 0.003, an intercept of 0.2 ± 0.4, and a correlation coefficient (r^2) of 0.96. The mean difference between the duplicate samples was 7 pptv with a standard deviation of 50 pptv. This statistic is somewhat misleading because the absolute confidence limit is dependent on the concentration of SF_6 being measured. The relative difference between duplicate samples can be examined by grouping the data into concentration ranges. This was done for three ranges: 0 to 100, 100 to 500, and greater than 500 pptv. The ranges were chosen to include a sufficient number of points in each group to enable a meaningful statistical analysis and still provide enough groups to establish the concentration dependence. A relative difference for each range was then established by taking the absolute value of the difference between the two measurements, and dividing by their average (Table 5). Values less than the LOD of 21 pptv determined from the blanks were excluded from the calculation. This resulted in exclusion of background level measurements, which were the majority of the points. There were 21 points, or 3% of the total, where one measurement was greater than LOD but the other was less than LOD. In two cases, the measurement over LOD was

in the 100 to 500 pptv range. The reason for these outliers is not clear. For the 100 to 500 pptv range, all points with the noted exceptions, were included. One point was excluded in the calculation for range greater than 500 pptv. This point is the obvious outlier in Figure 9 at sample 1 = 2000 pptv and sample 2 = 700 pptv. The precision of the SF_6 whole air sampler data can be estimated from this analysis at the 95% (2σ) confidence level as ± 42% for the 0 to 100, ± 32% 100 to 500 pptv range and ± 12% for values over 500 pptv.

Table 5: Performance Statistics for the Whole Air Sampling Method over Three Concentration Ranges.

Concentration range (pptv)	Mean relative difference	95% confidence limit (2σ)	Number of points
< 100	0.22	0.42	35
100 – 500	0.16	0.32	19
>500	0.06	0.12	11

Table 6: Comparison of the Whole Air Sampling Method with TGA-4000 Continuous Analyzers.

Concentration range (pptv)	Mean relative difference	Number of points
< 100	0.27	16
100 - 500	0.26	17
>500	0.21	21

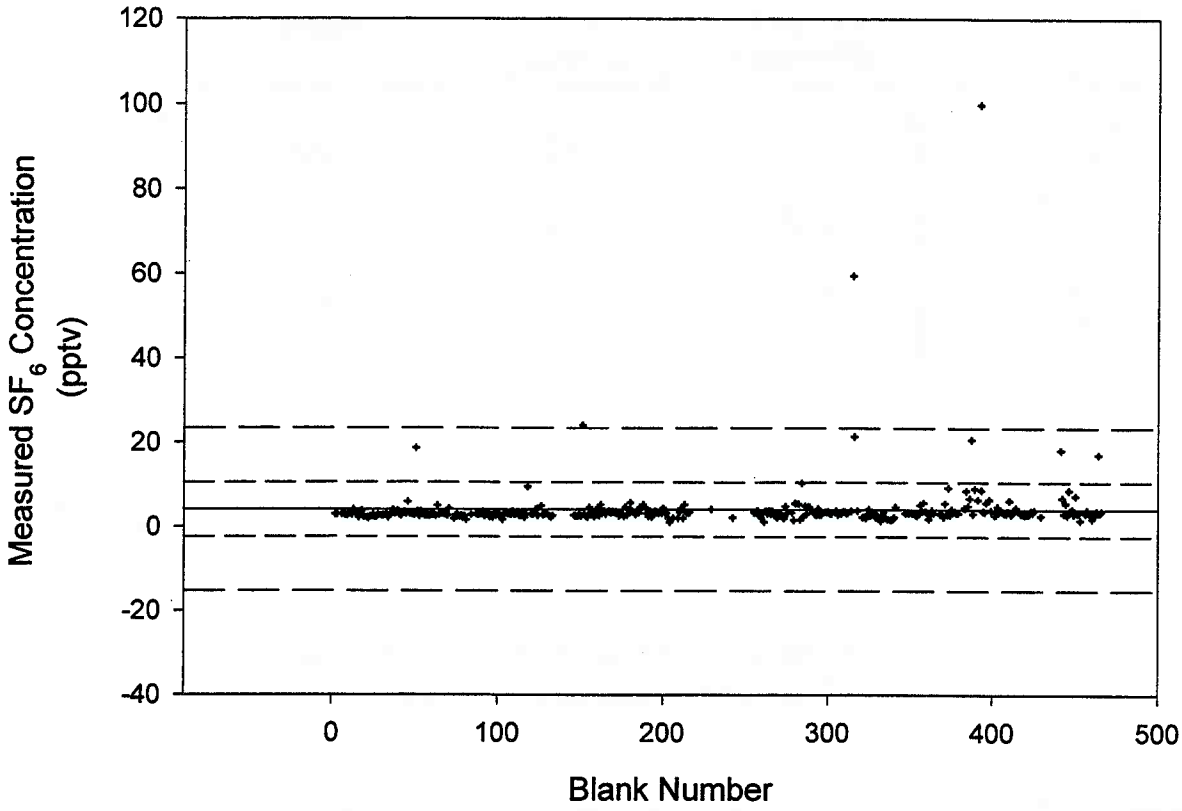

Figure 6: Results of analysis of blank samples. Mean is 4 pptv, standard deviation is 7 pptv, N= 455. The dashed lines are one and two standard deviations from the mean.

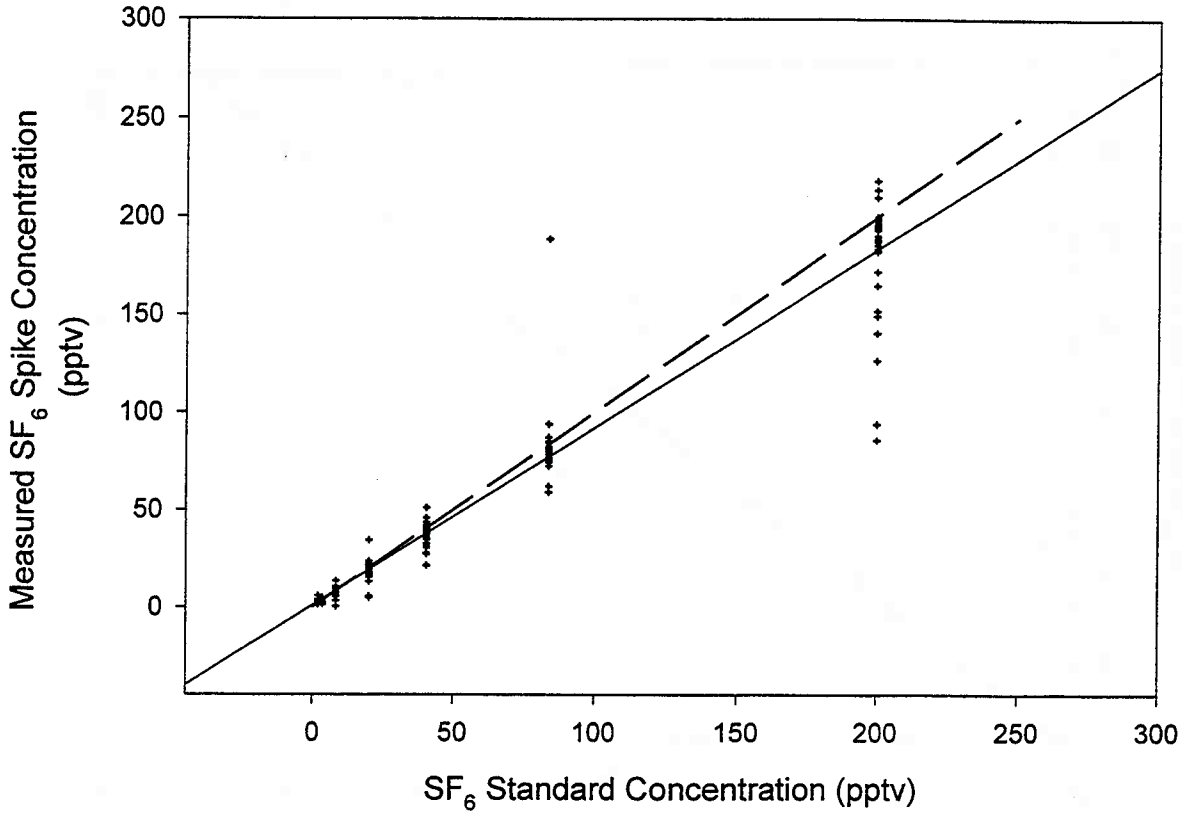

Figure 7: Comparison of reported concentration of calibration standards with results of analysis of spike samples. The solid line is a linear fit to the data with $y = (0.91 \pm 0.02)\, x + (1 \pm 1)$, $r^2 = 0.95$, $N = 225$. The dashed line is $y=x$.

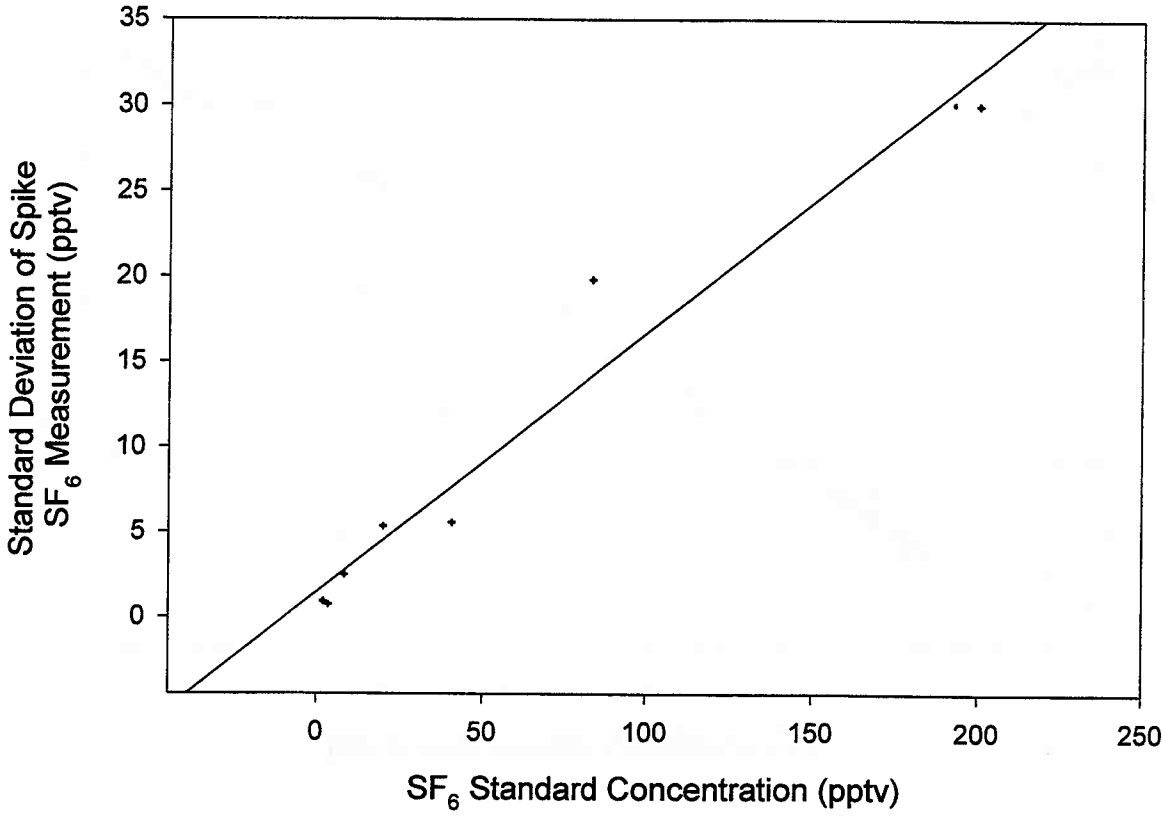

Figure 8: Standard deviation of measured spike concentrations versus calibration standard concentration. The solid line is a linear fit to the data with $y = (0.15 \pm 0.02)\, x + (1.5 \pm 1.4)$, $r^2 = 0.94$, N= 225.

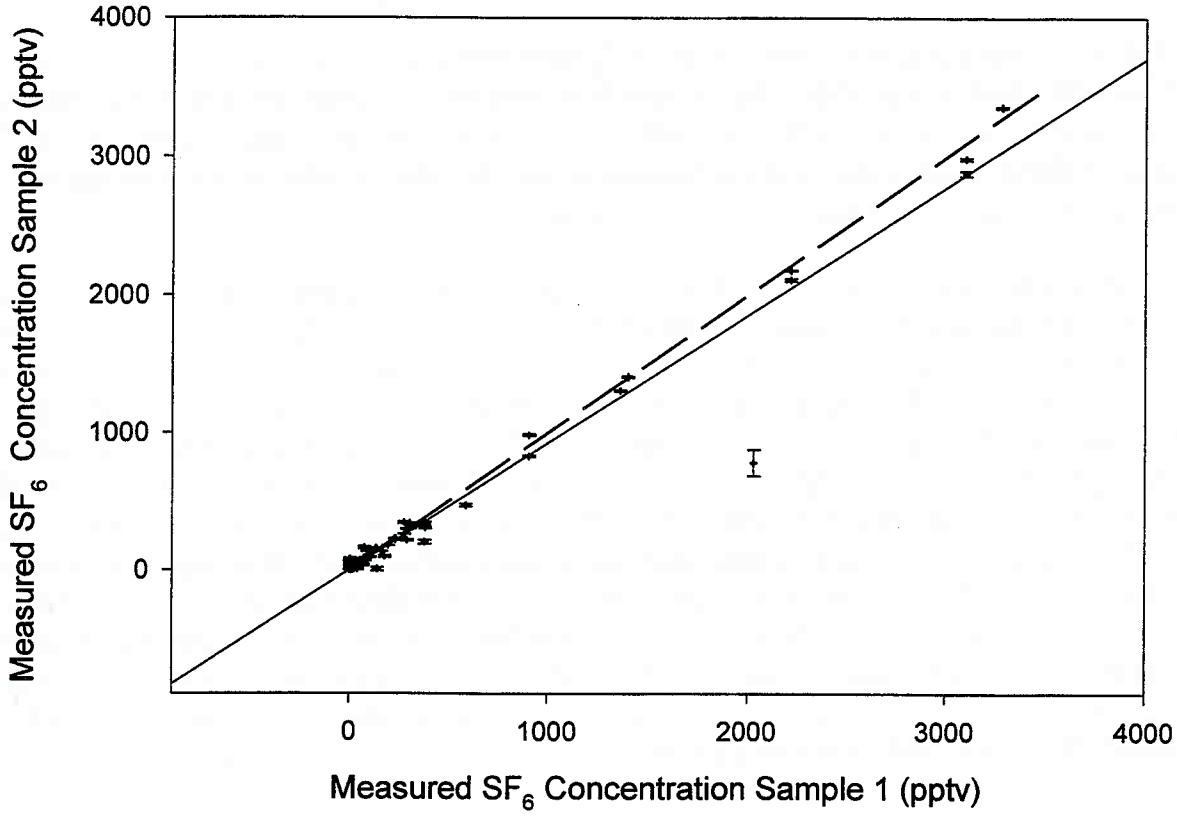

Figure 9: Comparison of results from duplicate samplers. The solid line is a linear fit to the data with $y = (0.98 \pm 0.003)\, x + (0.2 \pm 0.4)$, $r^2 = 0.96$, $N = 693$. The dashed line is $y=x$.

COMPARISON OF TGA RESULTS WITH WHOLE AIR SAMPLES

The whole air samplers integrate the SF_6 concentration over the sampling period. The TGA-4000 has a response time of less than one second and can accurately resolve concentration changes occurring over the course of ten seconds. Therefore, the TGA data must be integrated over the sampling period used in collecting the whole air samples before the results can be compared.

A correlation plot of the concentrations obtained from time integrated averages of the TGA-4000 continuous analyzers versus the analysis of 81 whole air samples stationed in the same locations (Figure 10) results in a linear fit with a slope of 0.99 ± 0.04, an intercept of 10 ± 24 pptv, and a correlation coefficient (r^2) of 0.88. The mean difference between the results of the two methods was 63 ± 35 pptv with a standard deviation of 150 pptv. Again, the comparison should be made over ranges of concentration. A comparison of Tables 2a, 5, and 6 show that the whole air samplers and the integrated TGA measurements are in agreement within confidence limits at concentrations under 500 pptv, mostly because of the uncertainty in the whole air samplers. Over 500 pptv, the relative mean difference of 0.21 is greater than the combined relative confidence limit of 0.19. This disagreement can be explained by the uncertainty in comparing the integrated TGA signal with the whole air sampler data and the relative small number of points, 21, examined in the comparison.

METEOROLOGICAL MEASUREMENTS AND EQUIPMENT

MEteorological Data Acquisition Stations (MEDA)

The NOAA Air Resources Laboratory Special Operations and Research Division (ARLSORD) maintains a network of meteorological measurement stations covering the Nevada Test Site. Data are transmitted every 15 minutes by radio from the stations to ARLSORD Headquarters and are stored in a computer data base. Each station reports measurements of temperature, atmospheric pressure, humidity, and wind speed and direction. Data from each fifteen minute interval consists of an instantaneous measurement of pressure, temperature and relative humidity taken immediately before transmission and a vector average of winds made from the five minute period immediately before transmission. Maximum and minimum wind speeds from the fifteen-minute period are also transmitted.

Sonic Anemometer/Thermometers

Sonic anemometers provide wind and temperature data by measuring the speed and the Doppler shift of sonic pulses sent and received between pairs of transducers. The transducer pairs are separated by 15 cm and are usually deployed in sets of three with one pair oriented along each of the coordinate (x, y, z) axes. This results in a measure of the horizontal (u and v) and vertical (w) wind velocity components. The instruments have sufficient temporal and spatial resolution to measure mean winds and fluctuations from the mean. Fluctuations are a measure of turbulence intensities and are necessary to quantify fluxes of heat and momentum. Protocols established by the American Society for Testing of Materials (ASTM, 1997) are used to calculate wind and sound velocity. Confidence limits are $\pm$ 3 cm s^{-1}.

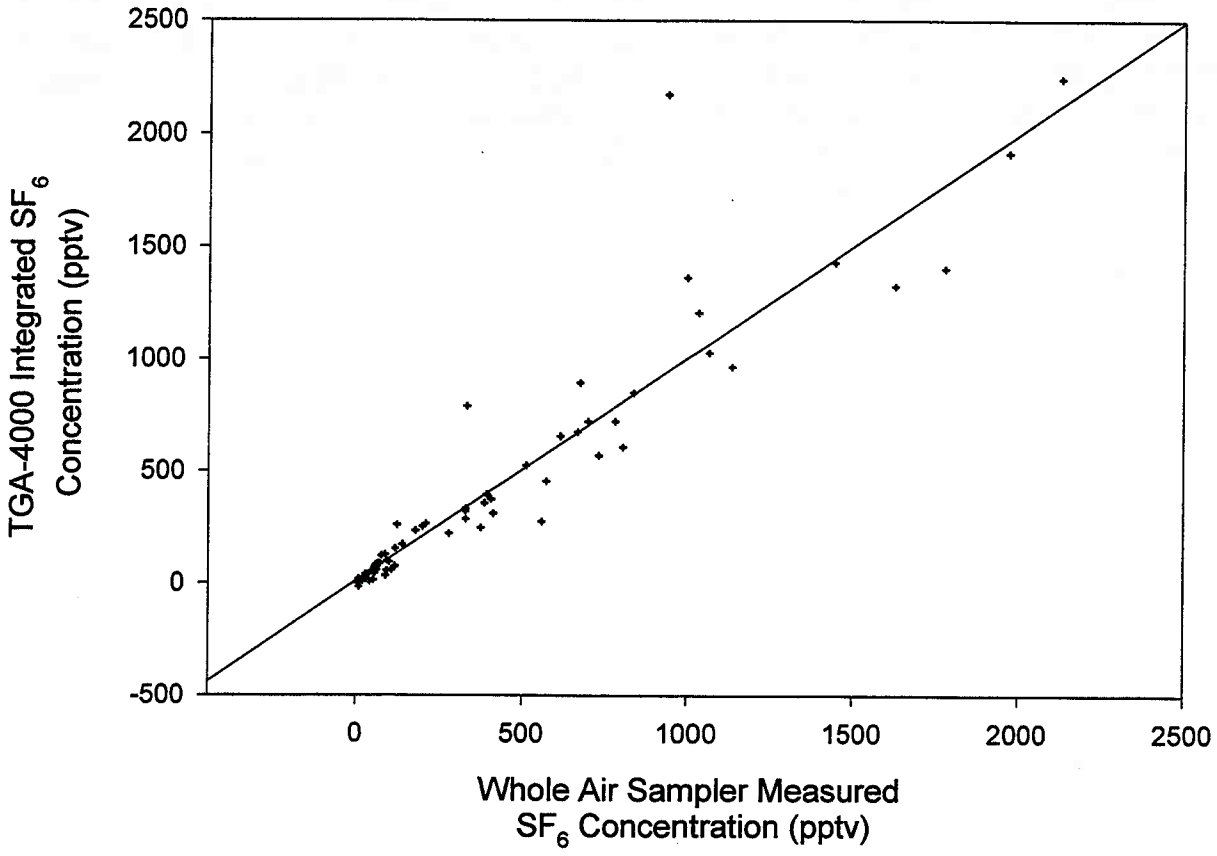

Figure 10: Comparison of TGA-4000 measurements with those of the whole air samplers. The line is a linear fit to the data with $y = (0.99 \pm 0.04)\,x + (10 \pm 24)$, $r^2 = 0.88$, $N = 81$.

Radiosonde

A radiosonde system consists of a balloon-borne instrument package that rises through the atmosphere, providing profiles of wind, temperature, humidity, and height at 10-second intervals throughout the flight. Data packets are transmitted via radio link to a base station where they are logged. Each profile reading is reduced to standard pressure levels (the mandatory levels) and significant inflection points (significant levels). The radiosonde system used at the NTS is the automatic radio-theodolite (ART), which includes a ground-based radio theodolite that tracks the ascending balloon and provides elevation and azimuth angles which, when used with time-synchronized pressure readings, are converted to profiles of wind speed and direction. The ART system used during DP 26 was stationed at the ARLSORD Yucca Flat Weather Station. Flights were made every three hours during the active test periods.

Pibal

The pilot balloon (pibal) is an optically tracked free balloon that is used to obtain profiles of wind speed and direction. Thirty gram (30-g) pibals were released by ARLSORD personnel to obtain boundary layer wind profiling during this test program. When filled to its design lift weight, a 30-g pibal has an ascent rate that is large in comparison with typical atmospheric vertical motions. Standard Tables are used to relate the flight time of a pibal to its height AGL. Optical tracking with a theodolite provides azimuth and elevation readings taken at 30-s intervals. These readings, combined with tabulated height versus time data, provide sufficient information to calculate layer-averaged wind speeds and directions. Pibal wind profiles are typically accurate to within ±2 m/s. The digital pibal (DIGIPI) Systems used at NTS feature shaft encoders which record theodolite angles every 30 seconds. The angular data are stored in a microcomputer, which then transmits these data to the central computer during a polling sequence. DIGIPI units were stationed at BJY and YFW providing hourly pibal flights during testing.

Radar Profiler

A 924 MHz wind profiler was operated by DPG at the BJY site to provide additional upper air data with 30-min resolution. The profiler was operated in two modes: the first mode provided winds with a nominal 60-meter vertical resolution from approximately 200-800 meters. The second mode provided 200-meter vertical resolution from approximately 315 meters up to, and occasionally beyond, 3 km AGL. Both modes were operated simultaneously. Some data is missing due to problems with the radar.

CHEMICAL REMOTE SENSING MEASUREMENTS

Infrared Imaging Radiometers

Infrared (IR) imaging radiometers are passive optical devices sensitive to energy in the 8- to 12-μm wavelength range. SF_6 has distinct absorption characteristics in this band. When the SF_6 puff passes across the field of view of the radiometer, it is visible because it has a different temperature than the background. If the SF_6 is colder than the background, the IR signal is attenuated because the SF_6 molecules absorb radiation. If the SF_6 is hotter than the background, the IR is enhanced. This change in IR level is proportional to both concentration and to the path length or thickness of the SF_6 cloud.

Infrared cameras were used to determine initial puff dimensions and to track the puffs as they traversed the sampling lines. DPG operated an Inframetrics Model 600L Imaging Radiometer near the release point to measure the size of the initial source cloud. This instrument has a thermal sensitivity of 0.05 °C, a scan rate of 50 Hz, and a 7-bit image resolution.

Aerospace Corporation operated three Agema Thermovision 900 digital IR cameras. These cameras were equipped with narrow band filters centered on the main SF_6 absorption band and were used to monitor the movement of the cloud as it crossed the sampling lines. A 15-Hz, non-interlaced scan rate and a thermal sensitivity of 0.08 °C characterize the Agema cameras. The spectral resolution and field of view varied with the filters and lenses used.

Fourier Transform Infrared Spectrometer

The Fourier Transform Infrared Spectrometer (FTIR) is a remote imaging device sensitive to IR radiation and capable of resolving molecular emission or absorption spectra. These instruments work best when the background within the field of view is constant and the target cloud is easily distinguishable from the background thermal signature. Consequently, the FTIRs were oriented towards the relatively cold clear sky to detect the arrival and passage of the relatively warm SF_6 puffs across the field of view. SF_6 can be identified by a unique absorption feature at 10.5 μm. When processed to remove background signal and noise, the SF_6 peak is resolved and can be used for quantitative determination of the concentration-pathlength of the SF_6 cloud (Polak et al., 1995).

The Aerospace Corporation operated two Intillitec M21 Chemical Agent Detector FTIR spectrometers during DP 26. This instrument has a spectral resolution of 1.5 cm^{-1}, a 5.25-Hz scan rate, a 25-milliradian field-of-view, and a sensitivity of 1.5 x 10^{-8} W cm^{-2} sr^{-1}/cm^{-1}. The spectrometers were mounted in the Aerospace Ram Van which remained stationary to intercept the SF_6, and in the Aerospace Tonka Van that followed the puff as it advected downrange.

SAMPLER AND RELEASE LOCATIONS

Generally, in the absence of strong synoptic forcing, the following surface wind climatology applies to Yucca Flat. During the early morning before the breakup of the nocturnal boundary layer, the winds in the Yucca Flat area are primarily from the north. In the afternoon, under normal synoptic conditions, winds are from the south. Sampling and release sites were selected to take advantage of these conditions.

Thirty samplers were located on each of three lines oriented in the east-west direction in the central part of the Yucca Flat basin. The lines were approximately ten kilometers apart. Samplers were spaced nominally 300 m apart (Figure 1, and Appendix 1, Table A1). Lines were numbered 100, 200, and 300, with the 100 line being the north most. The sampler coordinates were obtained using a differential GPS receiver. Forty-two locations were surveyed using GPS. The remaining locations were derived by interpolation. Three release sites were located approximately one half mile north of the 100-line, and three were approximately two miles south of the 300-line. With this configuration, tests could be run with both north and south winds by changing the location of the release system. Based on ARLSORD forecasts and data from the meteorological stations, one of the three north or south points was selected as the release location so that the SF_6 plume would be likely to travel over the center of the test grid. The continuous analyzers were located as described in Appendix 1, Table A3. Continuous analyzer locations for tests four through seventeen are also shown on Figure 1. All releases during DIPOLE PRIDE 26 were made from S_2, S_3, N_2, or N_3. S_1 and N_1 were not used.

DISSEMINATION MASS CALCULATIONS

The mass of SF_6 released during each trial can be calculated from the cylinder volume and the cylinder temperature and pressure. Dr. William Espander of Logicon RDA performed a series of mass calculations based on the Law of Corresponding States, a Virial equation, and a Martin-Hou (Mears et al., 1979) equation. While the results from these three methods were similar, Dr. Espander recommended the Martin-Hou method because it is based on actual SF_6 experimental data. Details of Dr. Espander's DIPOLE PRIDE 26 mass calculation procedures are presented in Appendix 3. Table A4 presents the results obtained using the Martin-Hou method.

RELEASE DIMENSIONS

Puff dimension estimates were obtained using an IR imager positioned 100 m east or west (crosswind from) of the disseminator. Puff dimensions varied with wind speed, stability, and the time delay between the two valve openings when the second release cylinder was used. This delay was usually on the order of tenths of a second. Useable images were not obtained for each release, and those that were available are subject to uncertainties in interpretation. Consequently, this report contains no trial-by-trial source dimension information. However, there was enough useful data to define general source dimension characteristics. Momentum of the exiting gas typically carried the puff centroid to a height of 6 ± 2 m, with a vertical dimension of 4 ± 0.5 m. The alongwind puff dimension averaged 7.5 ± 2 m.

PUFF WIDTH ESTIMATES

Cross Wind

As described above, there were 30 samplers on three lines that collected 12 fifteen minute integrated samples. Samplers on each line were 300 meters apart. This spacing provided a sufficient number of measurements above the SF_6 detection limit to generate histograms of the puffs in the cross wind or lateral dimension for each sampling line. A minimum of six points is desirable for this process. A Gaussian fit to these histograms was then used to determine the cross-wind puff width. Details of the calculations and the results are given in Appendix 4.

Along Wind

TGA-4000 measurements are used to calculate alongwind puff dispersion. The TGA-4000 units were stationed at 1500-m intervals along Sampling Line 2 (Pahute Mesa Road), providing continuous concentration-time measurements as each puff crossed this sampling line. The concentration time series from the unit found to be closest to the puff centroid was selected for alongwind dispersion calculations.

The GAUSq.XFM and Gausfit.XFM transforms and the Jandel Scientific SigmaPlot® graphing program were used to define alongwind puff dimensions in terms of sigma t. The transforms provided a Gaussian fit to the concentration-time histogram data, defined a sigma t and coefficients of skewness and kurtosis, and provided a goodness of fit measure analogous to that used for lateral dispersion calculations. The results are provided in Table A6. The TGA-4000 data provided sufficient temporal resolution for calculation of the centroid arrival at Sampling Line 2 and the transport speed, both of which are found in Table A6.

3D VISUALIZATION

Three dimensional animation sequences were generated using Interactive Data Language (IDL), version 4.0 (Research Systems, Inc., Boulder, CO). Yucca Flat surface features were derived from 1-degree USGS Digital Elevation Models (DEM).

The DEMs are contained in 1- by - 1 degree blocks. The data spacing within each 1-degree block is 3-arc seconds with 1201 elevations per block. The file size for each DEM block is approximately 10 Mbytes. The representation of Yucca Flat topography was created by combining 4 adjoining blocks into a single file, then extracting the elevations by sorting through the latitude and longitude values. The surface color scheme was chosen to highlight the difference in elevation of the surrounding topography, with red representing the highest points and black the lowest. Also depicted on the map are wind vectors from the meteorological sites (see below), a red X for the release location, the sampler locations, and corresponding SF_6 concentrations.

The first frame in each animation sequence was generated for the time of release, with each succeeding frame depicting the middle of each 15-minute sampling period. Scales to the right of each map show the wind vectors for 5 ms^{-1} north and west winds and the height of a 1 part per billion (ppbv) concentration. Instructions for viewing the 3D files are in Appendix 6.

Meteorological Data Display

During the course of preparation for the DIPOLE PRIDE study, ARLFRD developed the capability to process and display meteorological data from the on-site Nevada Test Site mesonet. Mesonet data was obtained from ARLSORD for MEDA (MEteorological Data Acquisition) stations in the Yucca Flat area. The following subsections describe the MEDA stations from which data was used and the treatment of that data.

Mesonet Site Locations

Table 7 lists the MEDA stations in the Yucca Flat area. Figure 1 shows the station locations in relation to the release site locations and the sampling lines. All MEDA stations have 10-meter tower winds. Station 16, BJY, provides 30-meter winds directly above Station 17 on the same tower. In the display, these two stations are offset by 0.01 degree of longitude (approximately 1 km) for the convenience of the viewer with the 10-meter winds artificially displaced to the west.

The MEDA Stations 1, 3, 6, 16, and 17 are on the "flat" of Yucca Flat, while Stations 2 and 9 are near the steppe of the bordering mountains to the northeast and northwest, respectively. Station 10 is on the mountain at the southeast rim, and Station 28 is south of Yucca Flat over a small pass. The north release sites are closest to Stations 2 and 9, and the southern release sites are closest to Station 6.

Mesonet Data Treatment

NTS MEDA data are not straight-forward 15-minute averages. For each 15-minute MEDA observation, wind speed and direction are given from a 5-minute vector average immediately preceding the reported MEDA observation time. Averaging is required to match the MEDA data to the 15-minute, time-integrated tracer concentration data. A FORTRAN program was written to convert 15-minute MEDA data into 15-minute averages. For each 15-minute tracer sampling period, weighting is assigned to the two relevant 15-minute MEDA observations as shown in Table 8.

Each generated average value was checked for missing data. Since wind data require vector averaging, either a missing wind direction or a missing wind speed will cause the value for that 15-minute sampling period to be recorded as missing. The MEDA reporting unit of knots was converted into meters per second for the display.

Table 7: MEDA Stations in the Yucca Flat DIPOLE PRIDE 26 Study Area.

MEDA #	Name	Lat (N)	Lon (W)	Elev (m)	Wind	Temp	RH	Pres	Precip
1	Area 1	37.0275	116.0917	1265	Yes	Yes	Yes	No	Yes
2	Area 2	37.1392	116.1058	1341	Yes	Yes	Yes	Yes	Yes
3	Area 3 South	37.0042	116.0317	1207	Yes	Yes	Yes	No	Yes
6	Yucca Flat	36.9583	116.0467	1195	Yes	Yes	Yes	Yes	Yes
9	Area 9	37.1358	116.0400	1290	Yes	Yes	Yes	No	Yes
10	The Monas-tery	36.9400	116.0792	1570	Yes	Yes	No	No	Yes
16	BJY Tower	37.0625	116.0525	1244	Yes	Yes	No	No	Yes
17	Buster Jangle Y	37.0625	116.0525	1244	Yes	Yes	Yes	Yes	Yes
28	Device Assem-bly	36.8925	116.0375	1107	Yes	Yes	Yes	No	Yes

Table 8: Weighting factors for MEDA observations affecting the Nth 15-minute tracer sampling period.

PARAMETER	WEIGHTING FOR MEDA OBSERVATION (N)	WEIGHTING FOR MEDA OBSERVATION (N+1)
Wind Speed	1/3	2/3
Wind Direction	1/3	2/3
Wind Speed Minimum	0	1
Wind Speed Maximum	0	1
Temperature	1/2	1/2
Pressure	1/2	1/2
Relative Humidity	1/2	1/2
Precipitation	0	1

ACKNOWLEDGMENT

The Defense Special Weapons Agency sponsored this research as part of the Transport and Model Validation Program. It was supported by funding number 8-ES-685-CPB-003/K4.

SOURCES FOR DATA SETS

SF_6 Tracer concentration data and 3-D Visualizations

Dr. Thomas B. Watson
NOAA Air Resources Laboratory
Field Research Division
1750 Foote Drive
Idaho Falls, ID. 83402
Voice: (208) 526-9397
Fax: (208) 526-2549
tom.watson@noaa.gov

Sonic Anemometer, and Radar Profiler Data

Dr. Christopher A. Biltoft
Meteorology and Obscurants Division
West Desert Test Center
U. S. Army Dugway Proving Ground
Dugway, Utah 84022-5000
Voice: (801) 831-5101
Fax: (801) 831-5289
biltoft@dugway-emh3.army.mil

MEDA Meteorological Network, Radiosonde, and Pibal Data

Dr. Darryl Randerson
NOAA Air Resources Laboratory
Special Operations Research Division
P. O. Box 94227
Las Vegas, NV 89193-4227
Voice: (702) 295-1233
Fax: (702) 295-3068
randerso@arl.nv.doe.gov

Chemical Remote Sensing Data

Dr. Ken Herr
The Aerospace Corporation
P. O. Box 92957
Las Angeles, CA 900059-2957
(310) 336-5620

REFERENCES

Annual Book of ASTM Standards, 1997. Standard practice for conversion units and factors relating to atmospheric analysis, *ASTM Standards*, Vol. 11.03 Atmospheric Analysis, D1914-91.

Benner, R. L., B. Lamb, 1985. A Fast Response Continuous Analyzer for Halogenated Atmospheric Tracers, *J. Atmos. Oceanic Technol.* **2:** 582-589.

Mears, W. H., E. Rosenthal, and J.V. Sinka,: 1979. Physical properties and virial coefficients of Sulfur Hexafluoride, *J. Phys. Chem.* 73:2254-2261.

Polak, M. L., J. L. Hall, and K. C. Herr, 1995. Passive Fourier-transform Infrared Spectroscopy of Chemical Plumes: An Algorithm for Quantitative Interpretation and Real-Time Background Level, *Appl. Optics*, **34:** 5406-5412.

Quiring, R. F. *Climatological Data Nevada Test Site and Nuclear Rocket Development Station.* Department of Commerce, Environmental Science Services Administration.

Taylor, J. K., 1987. *Quality Assurance of Chemical Measurements.* Lewis Publishers, Inc., Chelsea, Michigan, 129-146.

Watson, T. B.; 1995. Evaluation of an Intensive Sampling and Analysis Method for Carbon Monoxide, *J. Air and Waste Mgnt. Assoc.*, **45:** 29-35.

APPENDIX 1: NUMBERING AND COORDINATES FOR SAMPLING SITES, RELEASE SITES, AND VAN SITES

Table A1: Sampler Site Numbers and Locations.

Site #	Latitude	Longitude
101	37.13831	-116.12311
102	37.13817	-116.12033
103	37.13797	-116.11742
104	37.13828	-116.11456
105	37.13831	-116.11158
106	37.13830	-116.10848
107	37.13829	-116.10538
108	37.13828	-116.10228
109	37.13827	-116.09918
110	37.13826	-116.09607
111	37.13825	-116.09297
112	37.13808	-116.08989
113	37.13806	-116.08667
114	37.13819	-116.08356
115	37.13811	-116.08025
116	37.13700	-116.07789
117	37.13542	-116.07525
118	37.13522	-116.07228
119	37.13558	-116.06939
120	37.13506	-116.06647
121	37.13386	-116.06388
122	37.13267	-116.06129
123	37.13147	-116.05869
124	37.13000	-116.05631
125	37.12903	-116.05364
126	37.12765	-116.05103
127	37.12628	-116.04842
128	37.12464	-116.04619
129	37.12328	-116.04378
130	37.12267	-116.04100

Site #	Latitude	Longitude
201	37.05572	-116.09197
202	37.05543	-116.08908
203	37.05513	-116.08619
204	37.05484	-116.08331
205	37.05454	-116.08042
206	37.05425	-116.07753
207	37.05396	-116.07464
208	37.05366	-116.07175
209	37.05337	-116.06886
220	37.05307	-116.06597
211	37.05278	-116.06308
212	37.05178	-116.06025
213	37.05053	-116.05781
214	37.04928	-116.05536
215	37.04803	-116.05292
216	37.04800	-116.04988
217	37.04797	-116.04684
218	37.04794	-116.04380
219	37.04792	-116.04076
220	37.04789	-116.03772
221	37.04786	-116.03468
222	37.04783	-116.03164
223	37.04778	-116.02869
224	37.04769	-116.02583
225	37.04758	-116.02294
226	37.04761	-116.02008
227	37.04800	-116.01708
228	37.04844	-116.01433
229	37.04889	-116.01158
230	37.04933	-116.00883

Site #	Latitude	Longitude
301	36.99056	-116.09333
302	36.99167	-116.09093
303	36.99278	-116.08852
304	36.99389	-116.08611
305	36.99500	-116.08361
306	36.99611	-116.08111
307	36.99606	-116.07856
308	36.99550	-116.07572
309	36.99537	-116.07274
310	36.99525	-116.06976
311	36.99512	-116.06678
312	36.99499	-116.0638
313	36.99487	-116.06082
314	36.99474	-116.05784
315	36.99461	-116.05486
316	36.99442	-116.05183
317	36.99564	-116.04953
318	36.99562	-116.04696
319	36.99560	-116.04440
320	36.99559	-116.04184
321	36.99557	-116.03927
322	36.99555	-116.03671
323	36.99554	-116.03414
324	36.99552	-116.03158
325	36.99550	-116.02902
326	36.99549	-116.02645
327	36.99547	-116.02389
328	36.99545	-116.02132
329	36.99543	-116.01876
330	36.99542	-116.01619

Table A2: Release Site Numbers and Locations (Release locations N_1 and S_1 were not used).

Site #	Latitude	Longitude
N2	37.1586	-116.0967
N3	37.1500	-116.0625
S2	36.9570	-116.0498
S3	36.9512	-116.00998

Table A3: Continuous Analyzer Locations by Sampler Station Number.

Test #	Van 1	Van 2	Van 3	Van 4	Van 5	Van 6
1	220	320	110	120	310	210
2	225	320	210	220	------	205
3	230	220	215	------	210	201
4	230	224	212	218	206	201
5	230	224	212	218	206	201
6	230	224	212	218	206	201
7	230	224	212	218	206	201
8	230	224	212	218	206	201
9	230	224	212	218	206	201
10	230	224	212	218	206	201
11	230	224	212	218	206	201
12	230	224	212	218	206	201
13	230	224	212	218	206	201
14	230	224	212	218	206	201
15	230	224	212	218	206	201
16	230	224	212	218	206	201
17	230	224	212	218	206	201

APPENDIX 2: WEATHER SUMMARY AND CHARTS

Weather during the DIPOLE PRIDE 26 field experiment, November 4-20,1996, can be characterized roughly by a "trough-high-trough-zonal" upper-air pattern. The following 500-mb analysis charts show this pattern.

The first test on November 4 was held as a shakedown exercise. There was a trough over Nevada that imparted a westerly component to the surface winds resulting in the SF_6 cloud missing the sampling grid as it was transported to the east. By November 6 an upper-air high set in to dominate the synoptic scale for the next 4-5 days; northerly releases were successfully conducted for Tests 3-6 during early morning drainage flow conditions for this period. Test 4 included two separate releases in a moderate drainage flow.

An upper trough moved in for Test 7 on November 12. Channeled southwesterly winds and up-valley flow combined to produce sufficient wind speeds for two successful southerly releases that afternoon. With the passage of a surface front, the next 2 days were characterized by persistent northerly flows, even in the afternoons. Wind speeds were sufficiently high during Tests 11 and 12 for two separate northerly releases during each test.

Tests 14-16 from November 16 through November 19 were conducted under zonal flow off the Pacific Ocean with a weak high attempting to build. Test 14 had a west-northwesterly component but up-valley forcing dominated in the afternoon. With Tests 15 and 16, the west-southwesterly upper-air flow, the up-valley component, and flow from a building surface high over the four corners, provided a driving force for sufficient southerly wind speeds for two releases per test. By Test 17, another trough was moving on-shore, but again, the southwesterly flow was channeled to provide sufficient wind speeds for two releases. DP 26 ended with a major precipitation event that resulted in cancellation of the last release on November 21.

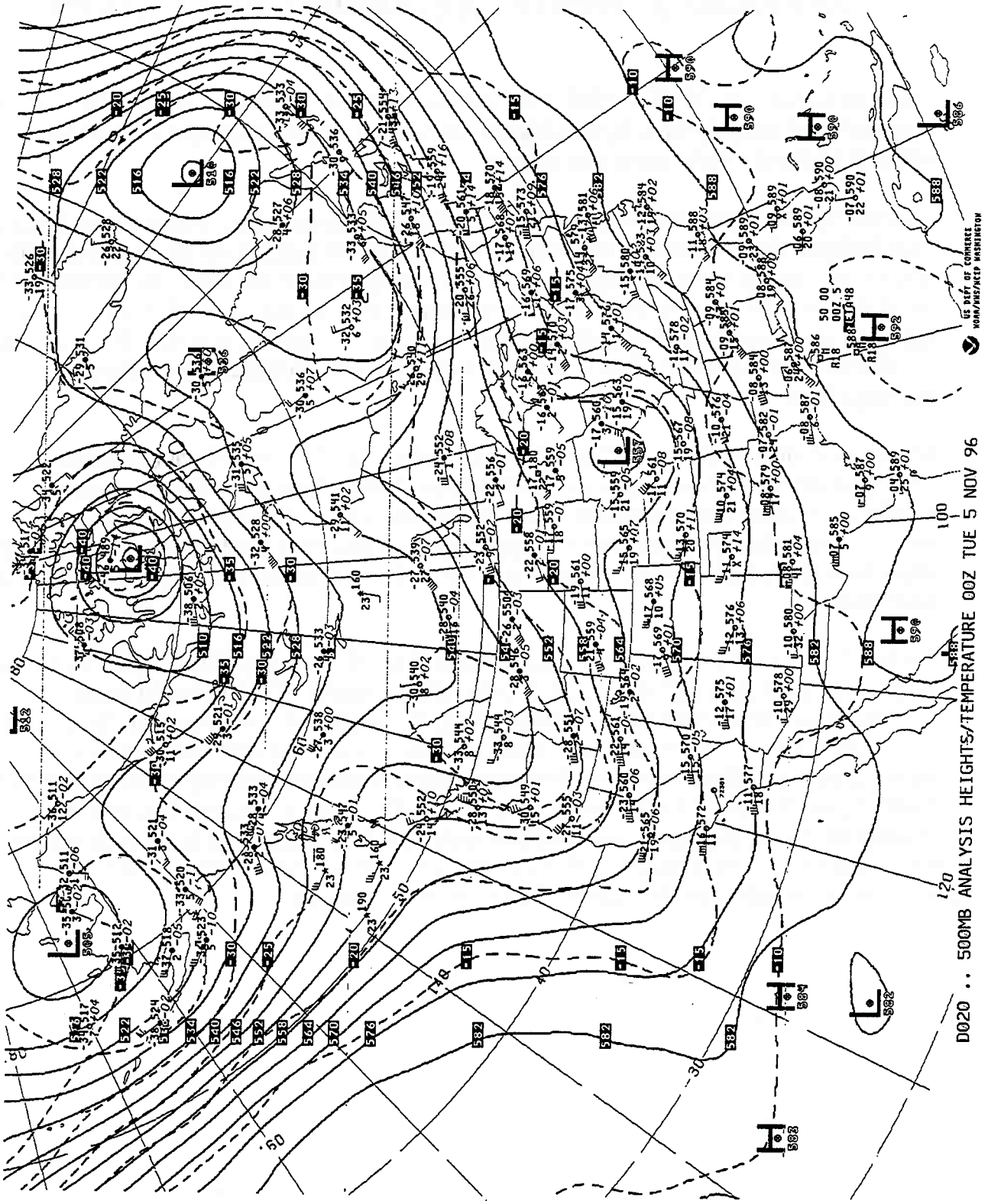

Figure A3-1: 500 mb weather map temporally closest to Test #1.

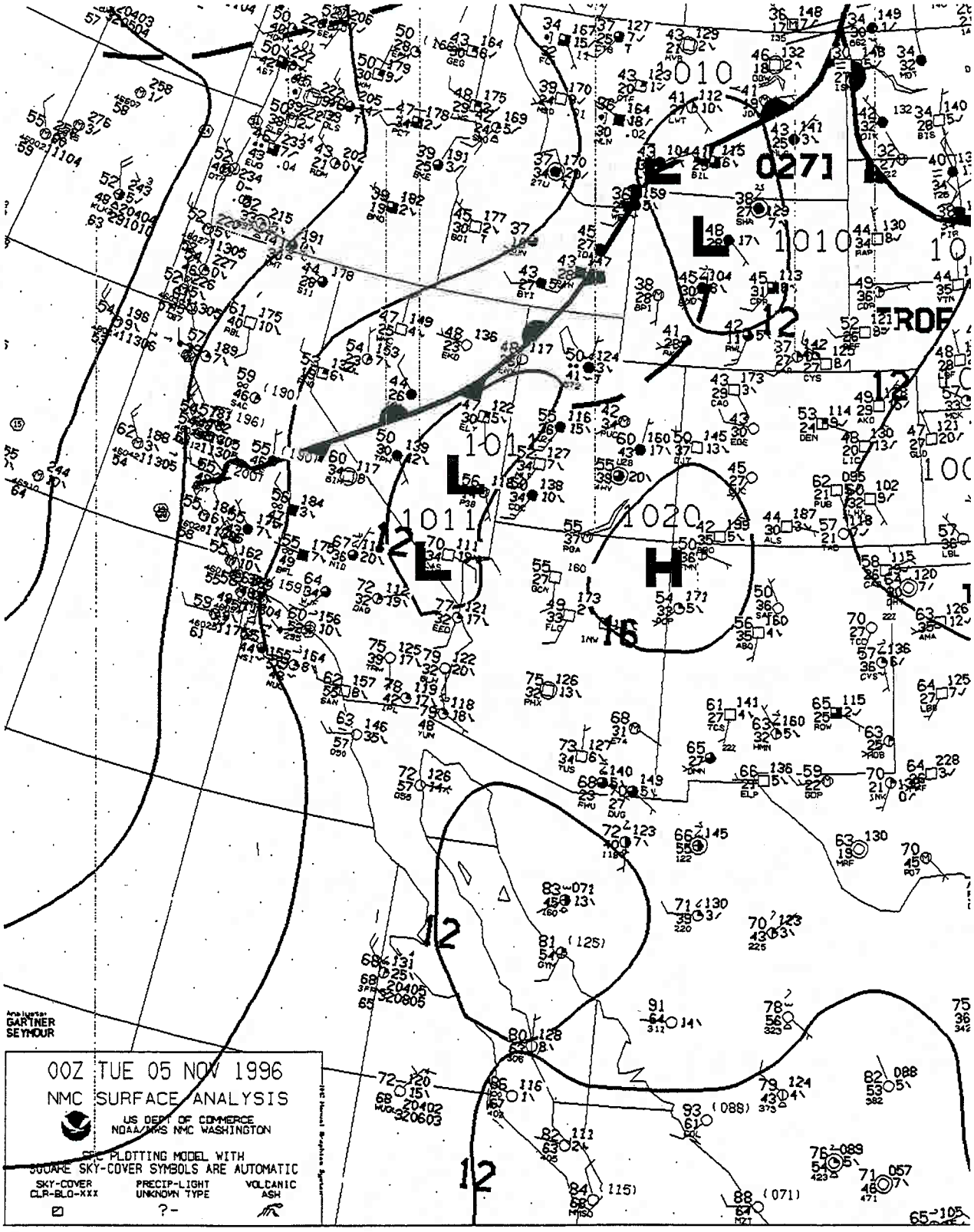

Figure A3-2: Selected portion of surface weather map temporally closest to Test #1.

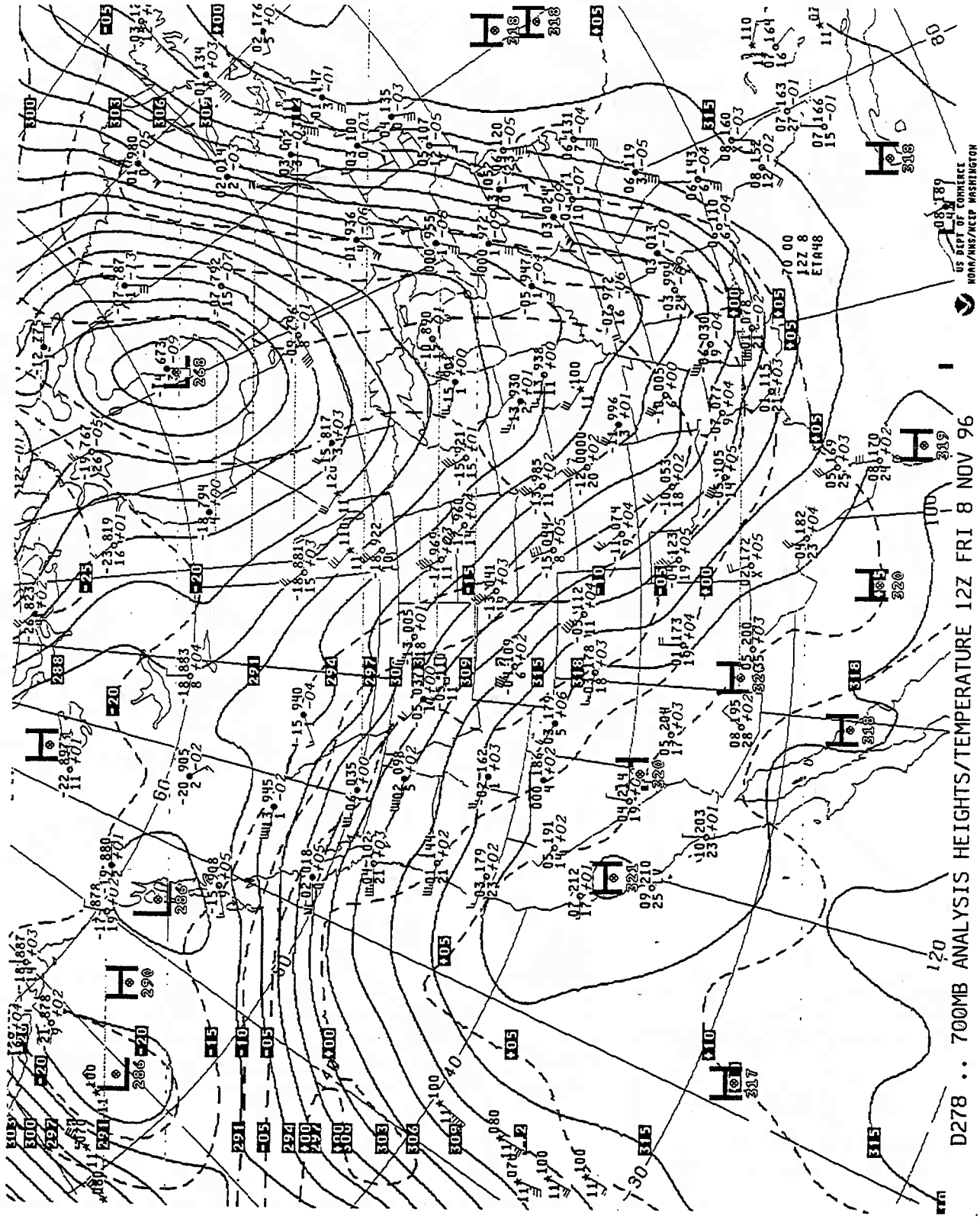

Figure A3-3: 700 mb weather map temporally closest to Test #3, (the 12Z 500-mb chart for 11/8/96 was unavailable).

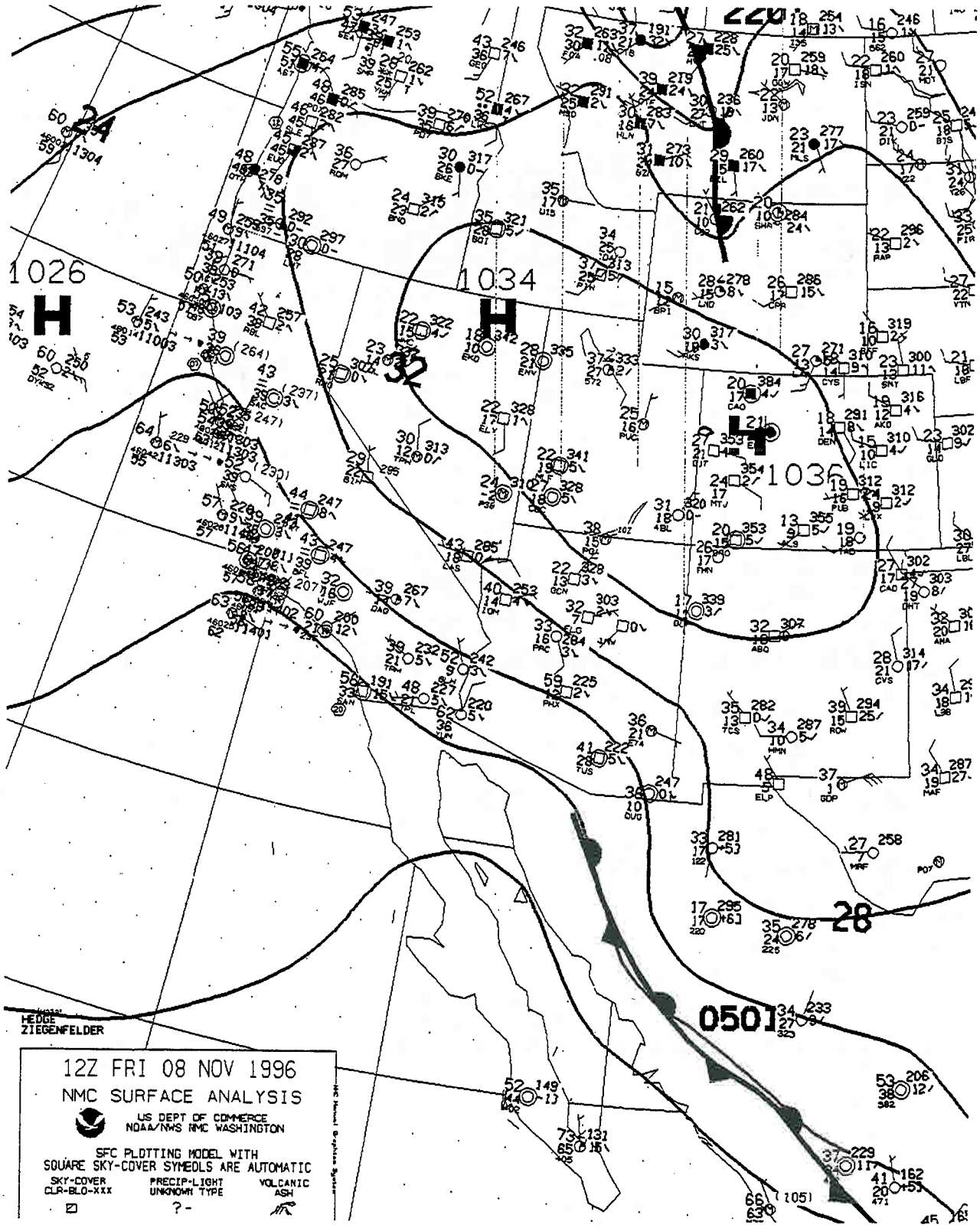

Figure A3-4: Selected portion of surface weather map temporally closest to Test #3.

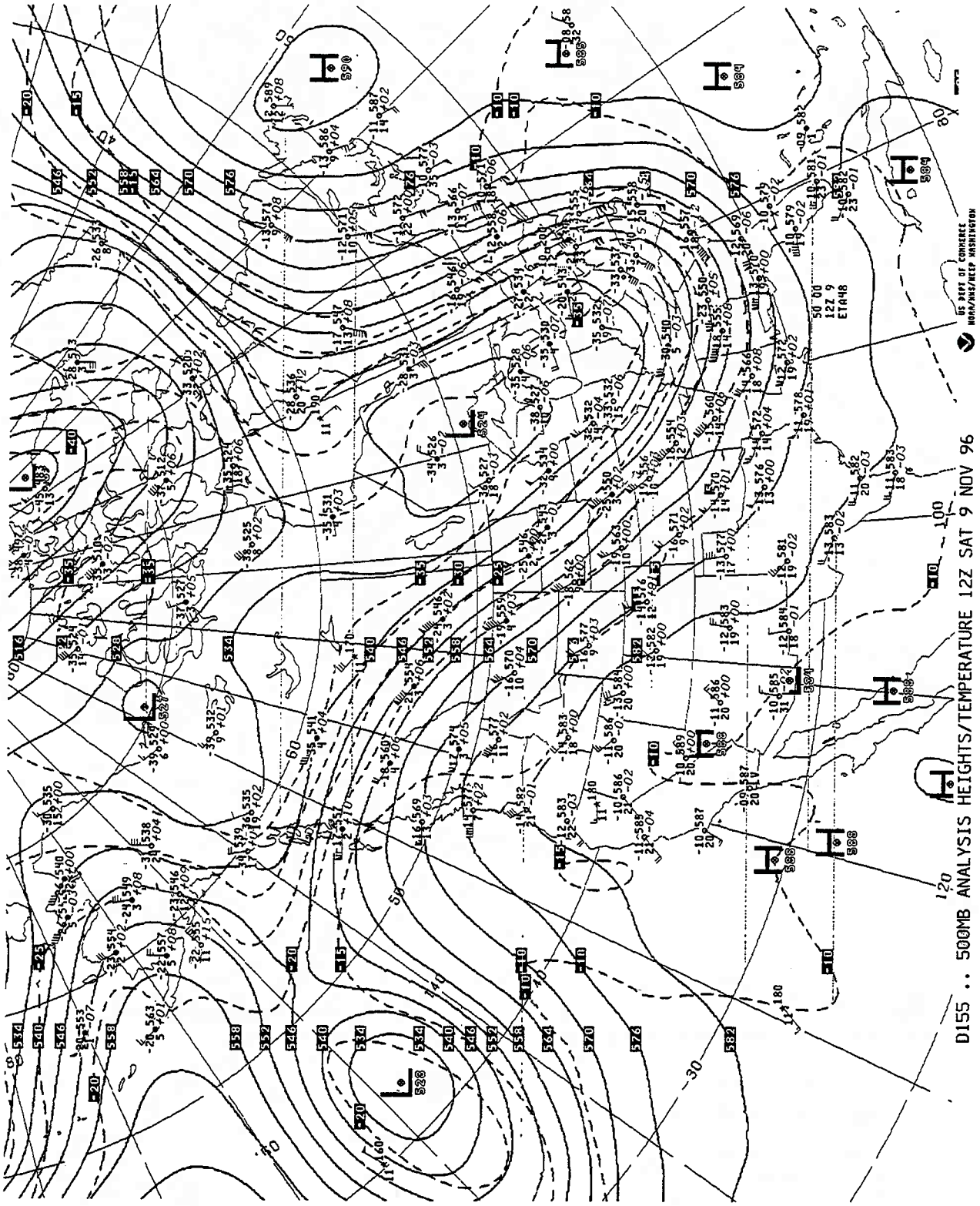

Figure A3-5: 500 mb weather map temporally closest to Test #4.

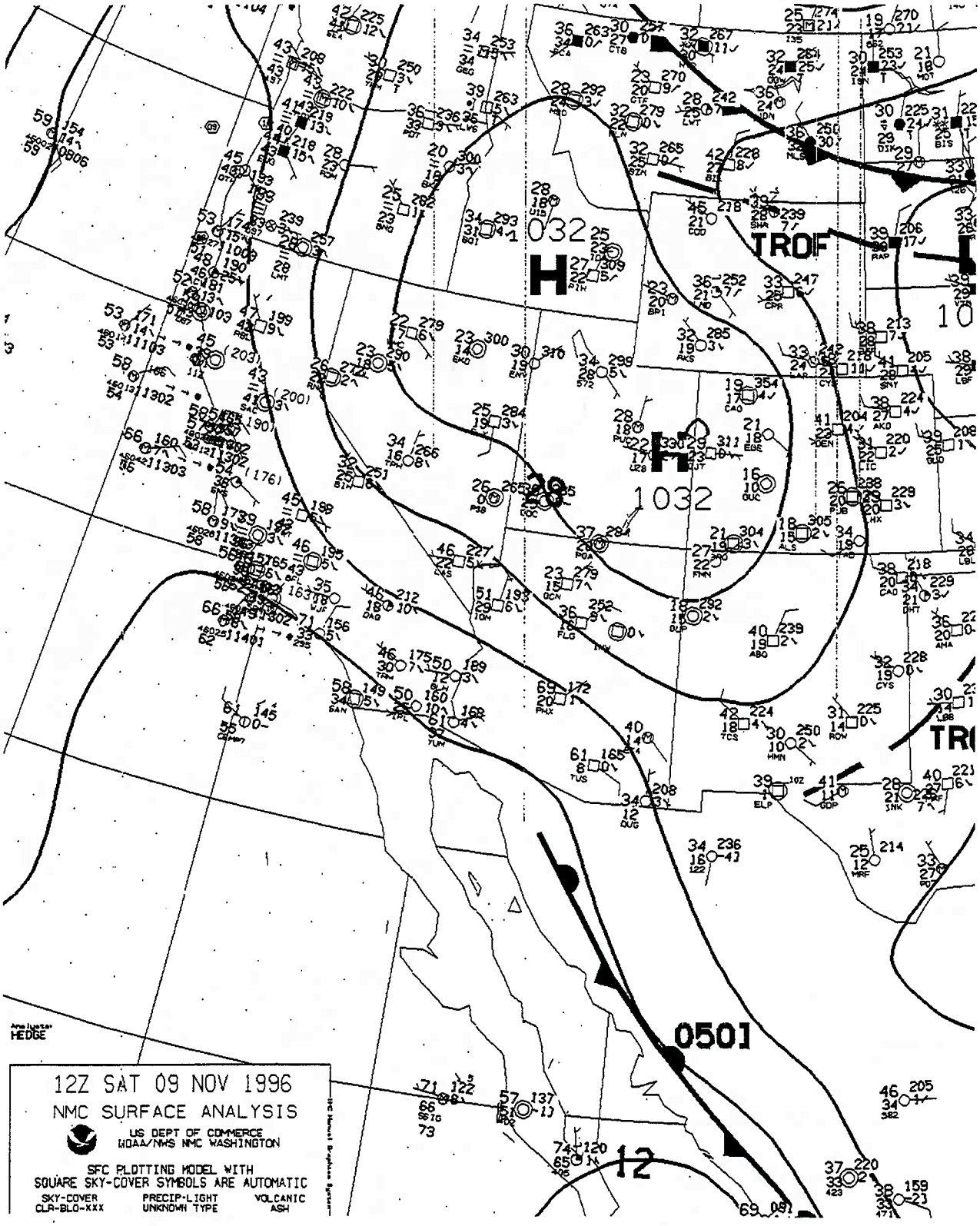

Figure A3-6: Selected portion of surface weather map temporally closest to Test #4, Trial 3140400.

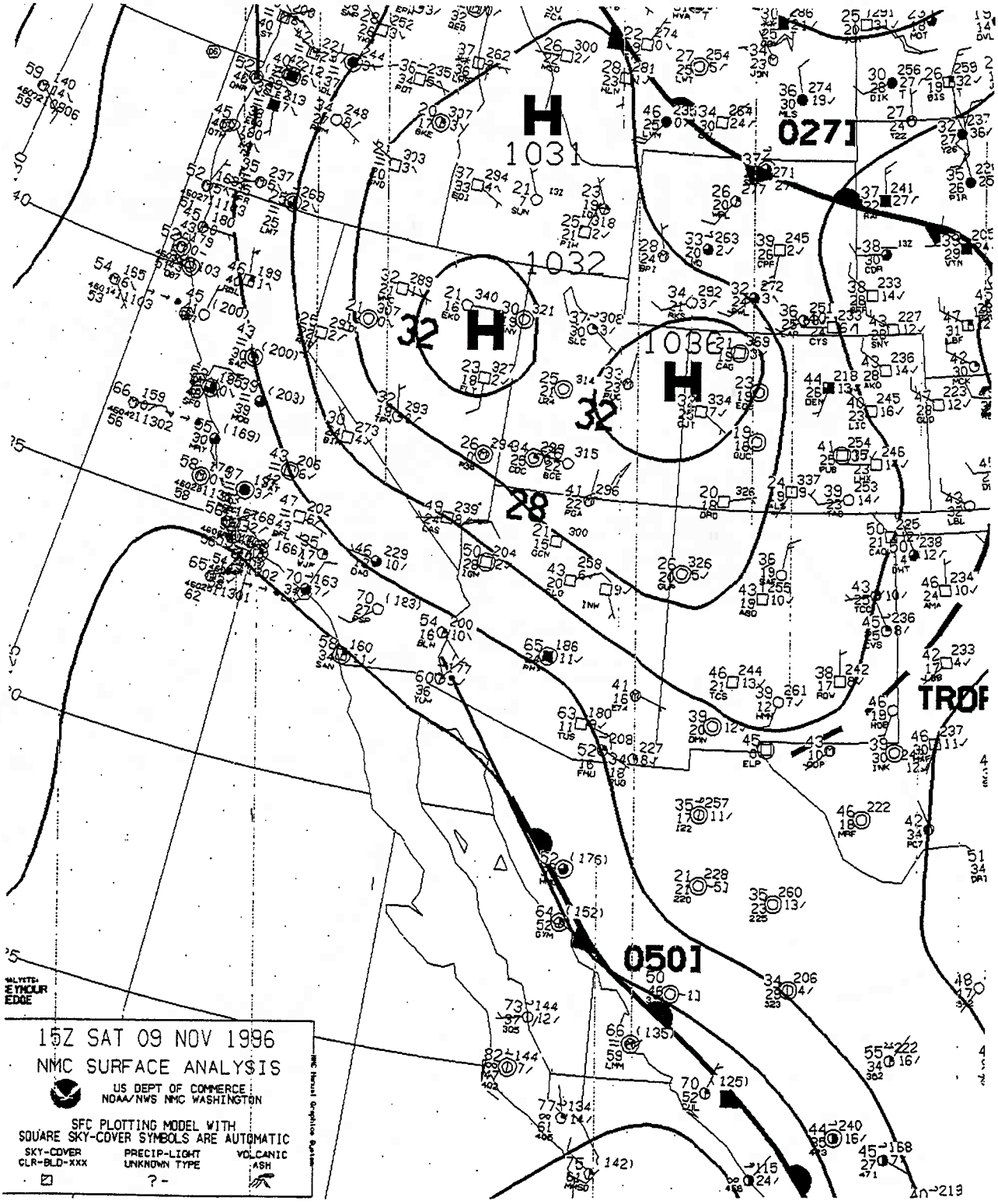

Figure A3-7: Selected portion of surface weather map temporally closest to Test #4, Trial 3140530.

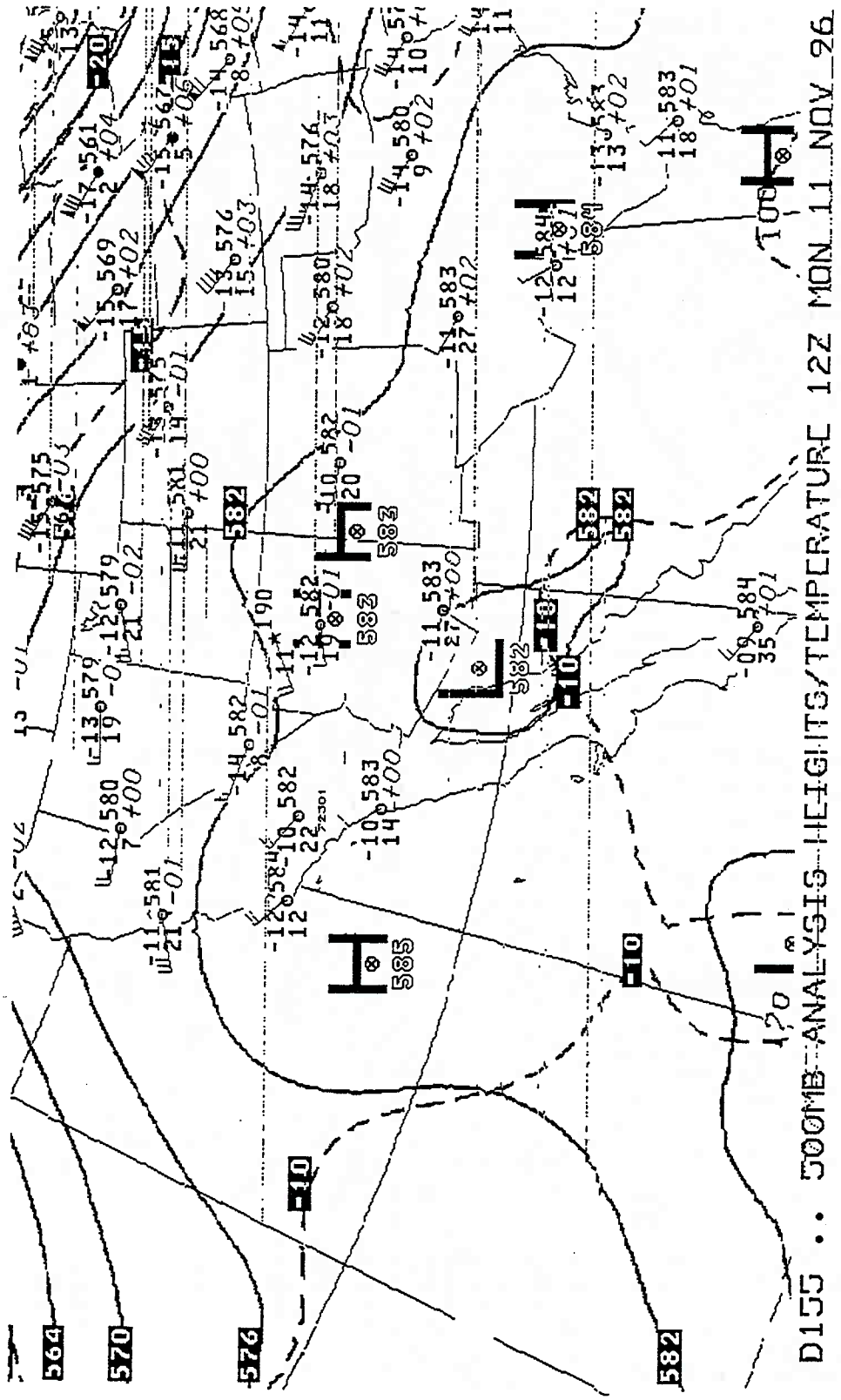

Figure A3-8: 500 mb weather map temporally closest to Test #5, (upper portion of map missing. See Figure A3-9 below).

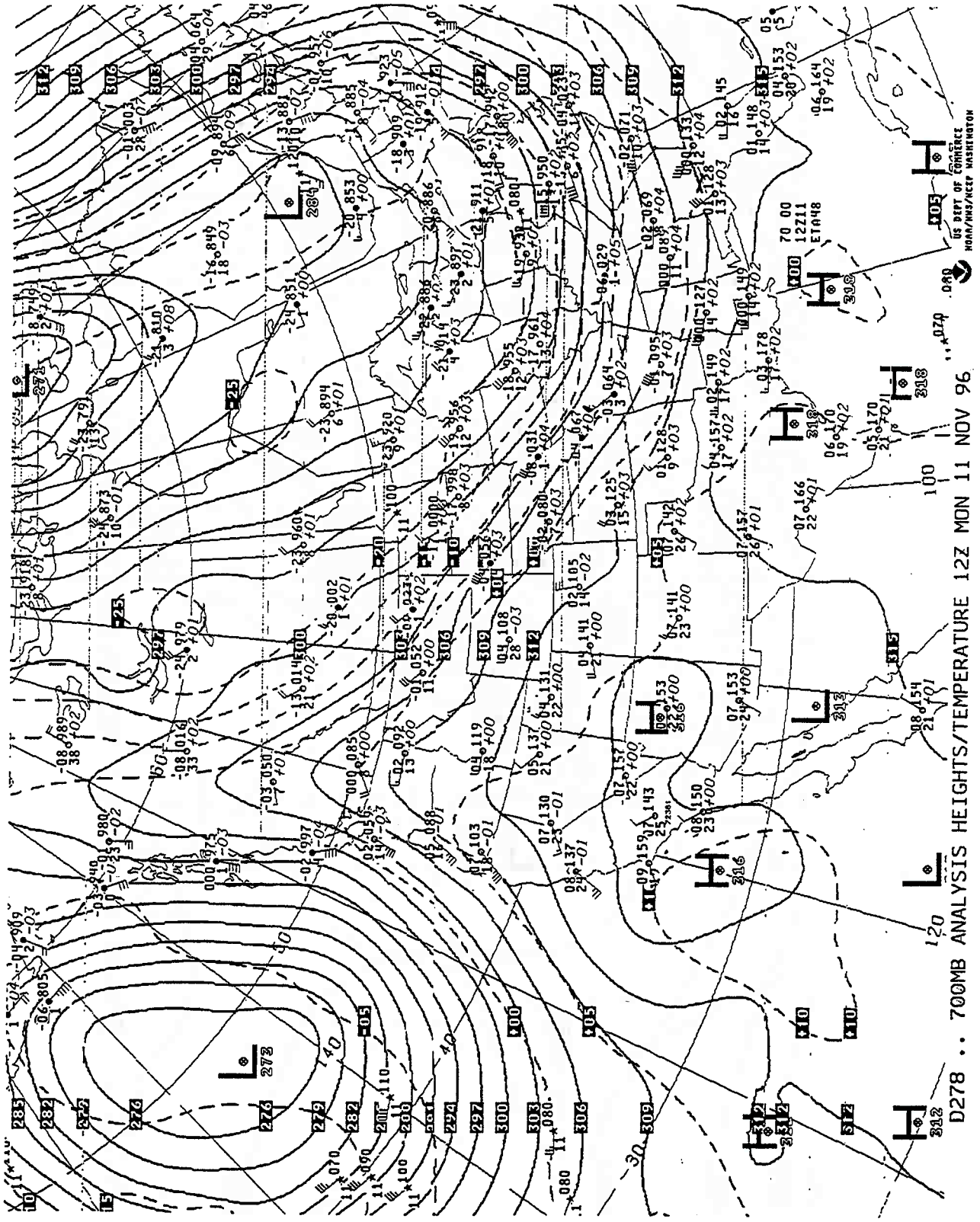

Figure A3-9: 700 mb weather map temporally closest to Test #5, (presented here as upper air substitute for missing portion of 500 mb chart in Figure A3-8).

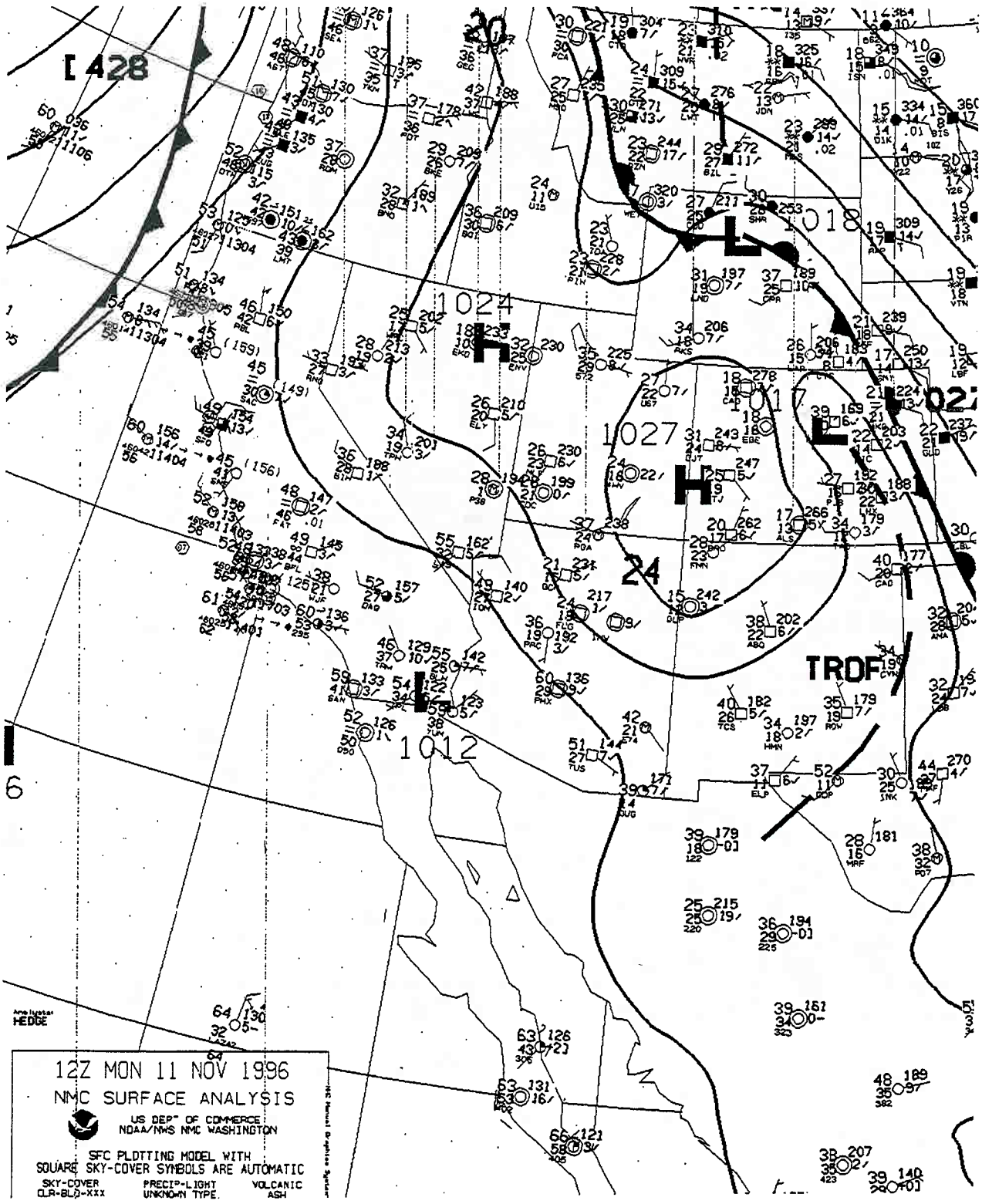

Figure A3-10: Selected portion of surface weather map temporally closest to Test #5.

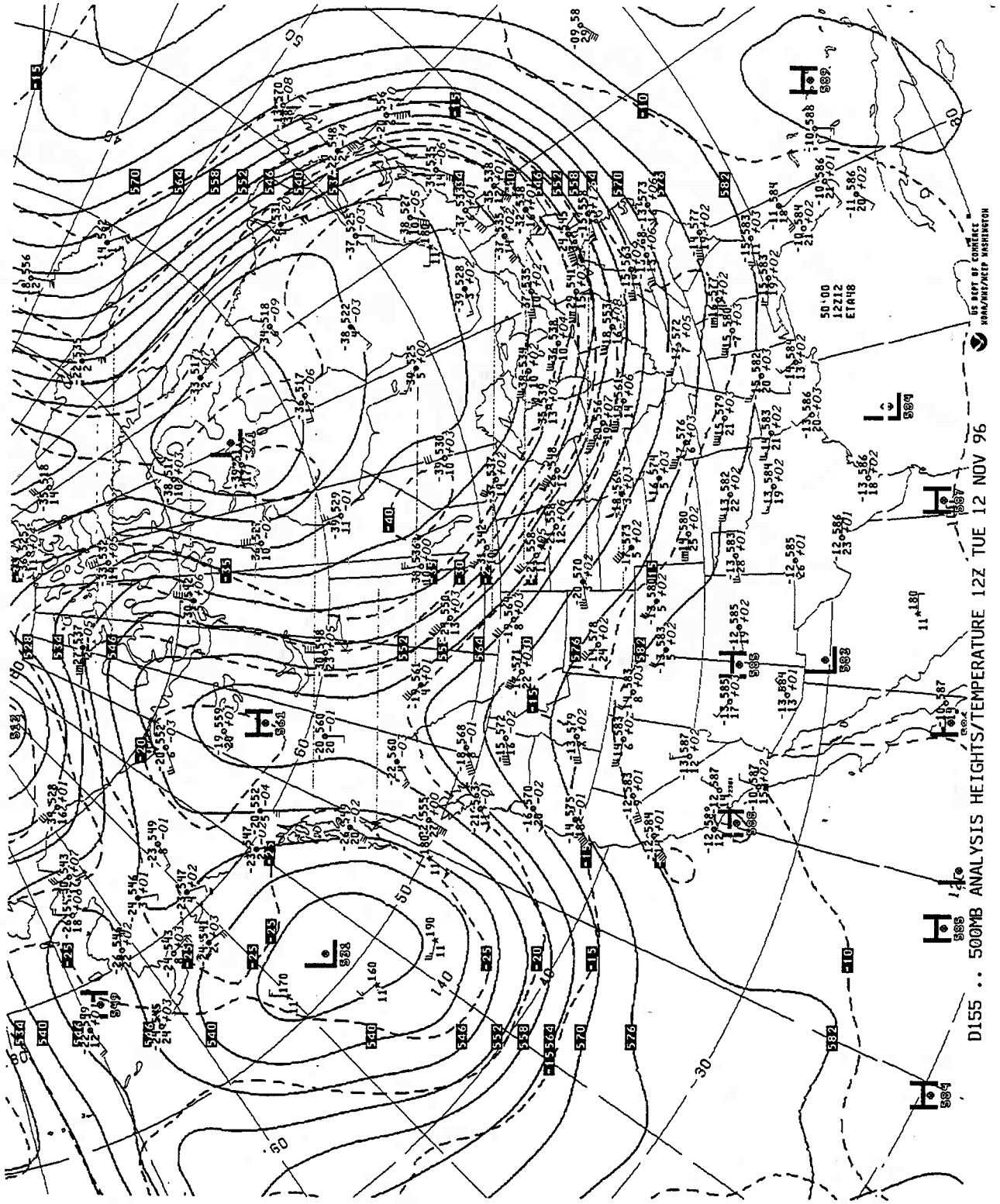

Figure A3-11: 500 mb weather map temporally closest to Test #6.

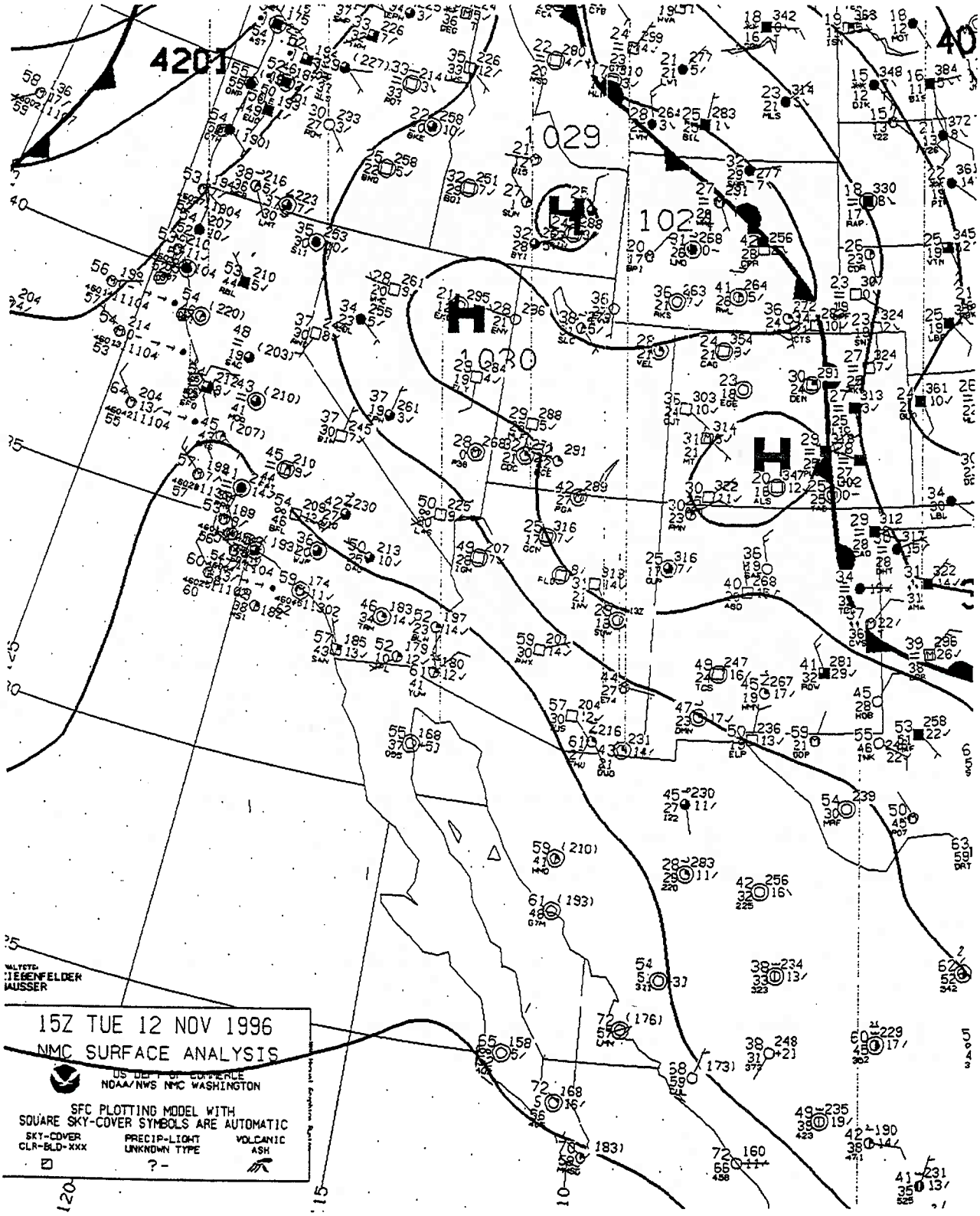

Figure A3-12: Selected portion of surface weather map temporally closest to Test #6, (the 12Z surface map was unavailable).

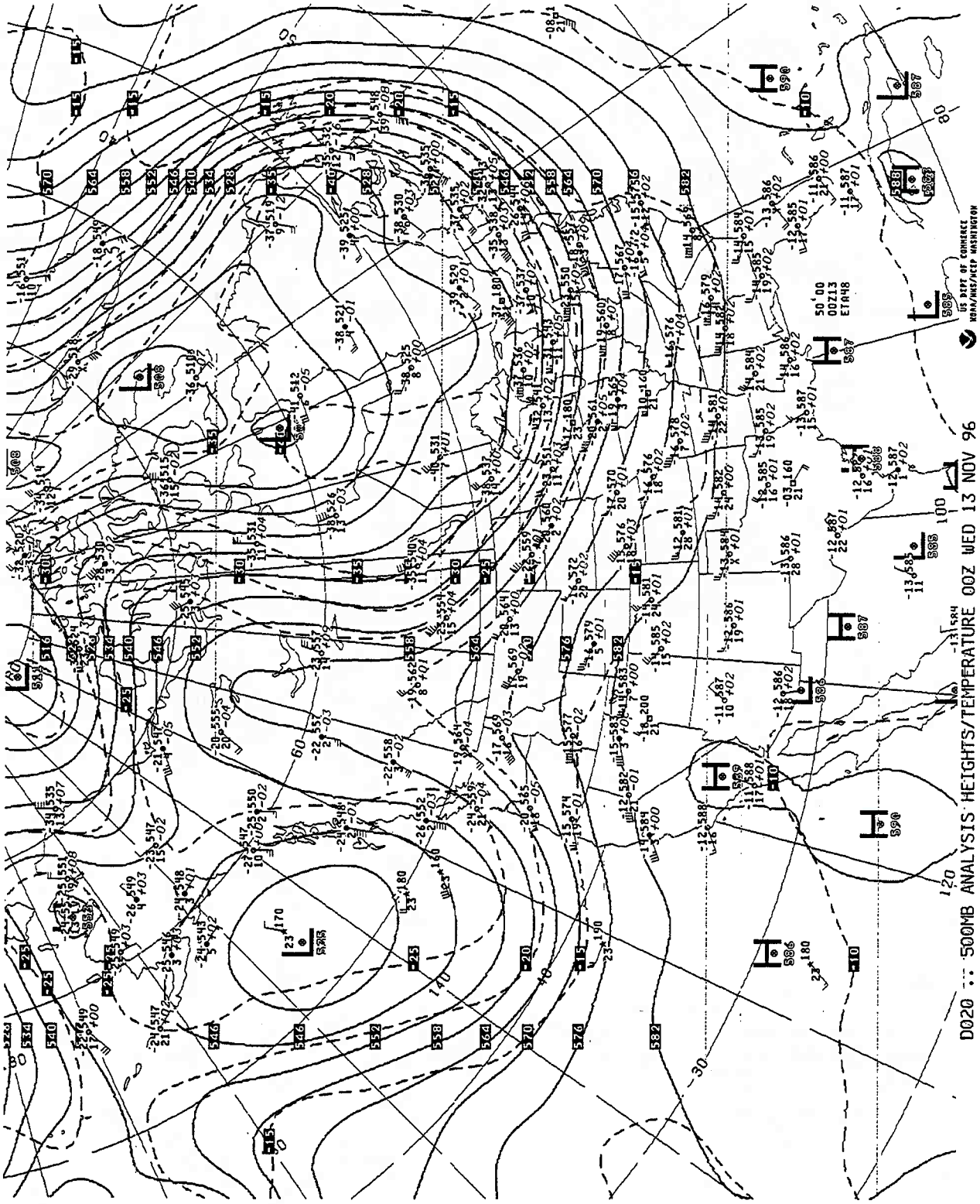

Figure A3-13: 500 mb weather map temporally closest to Test #7.

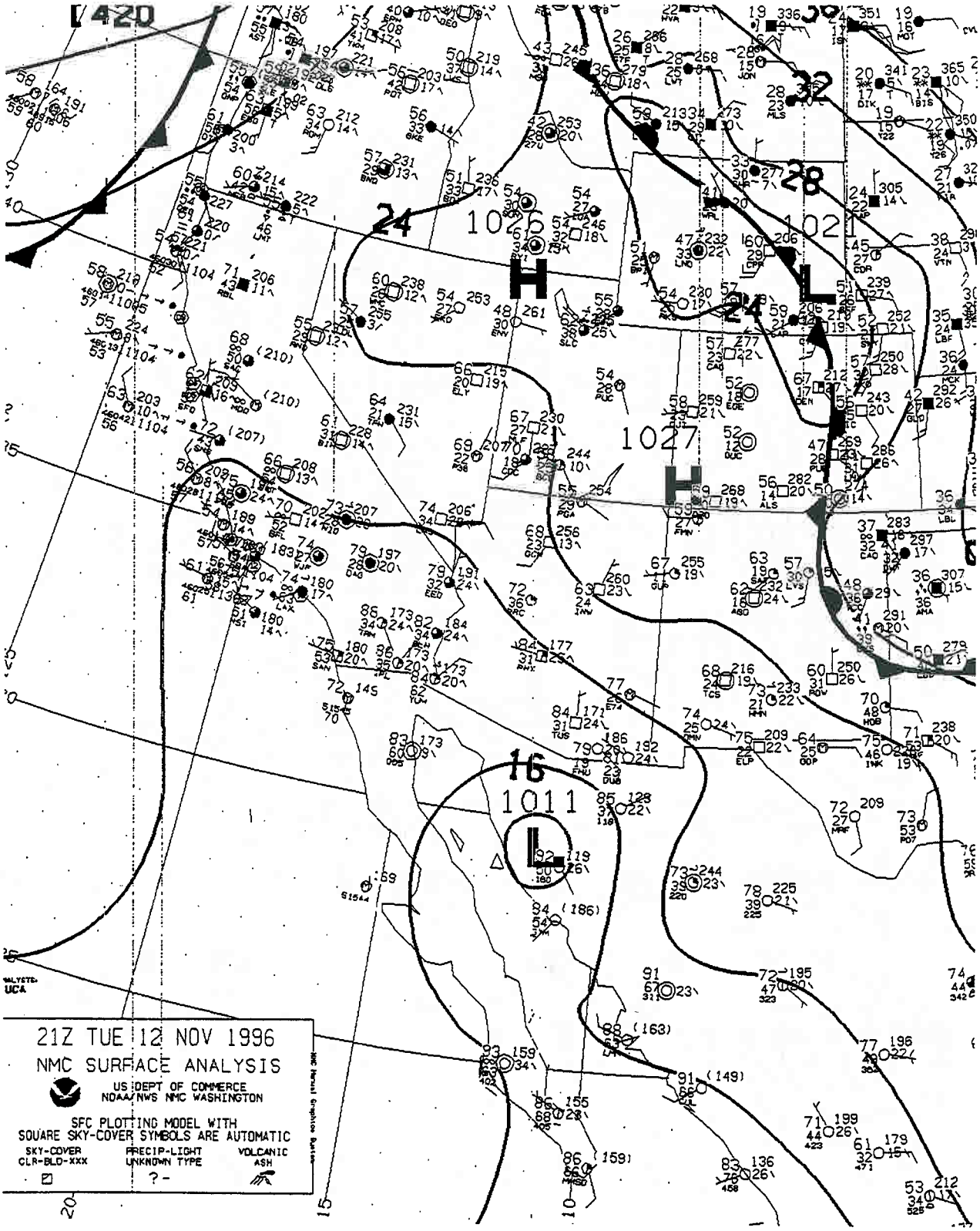

Figure A3-14: Selected portion of surface weather map temporally closest to Test #7.

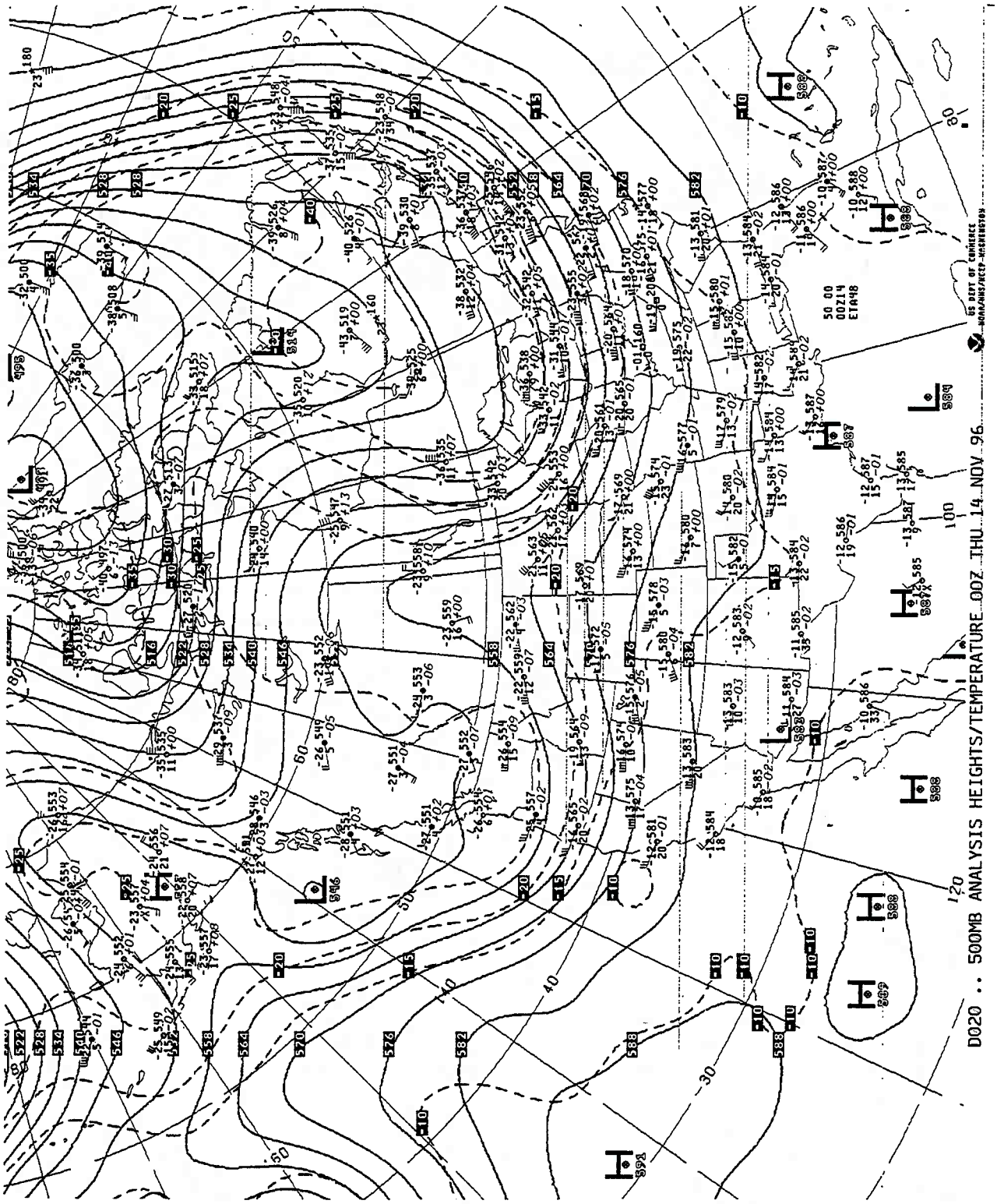

Figure A3-15: 500 mb weather map temporally closest to Test #9.

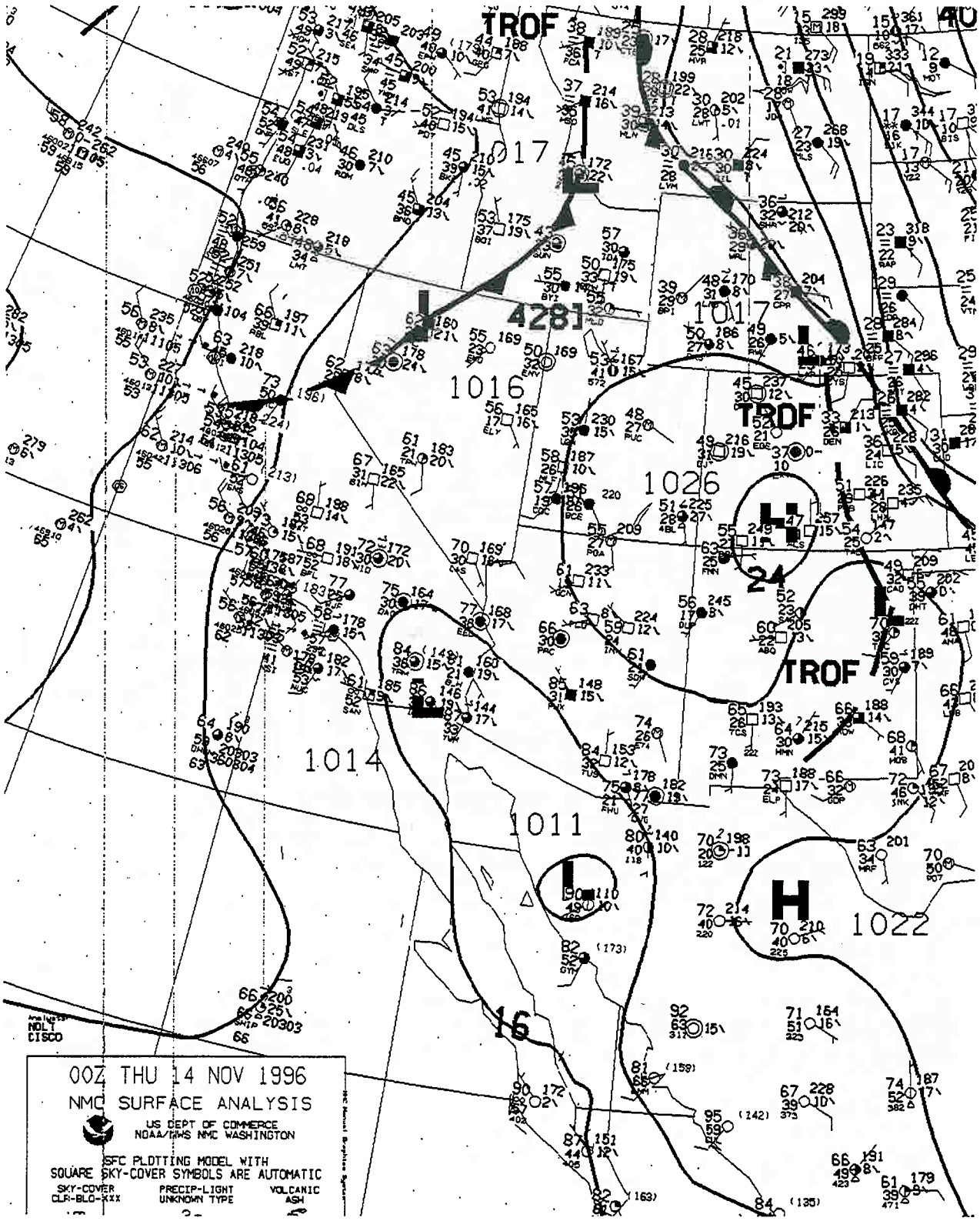

Figure A3-16: Selected portion of surface weather map temporally closest to Test #9.

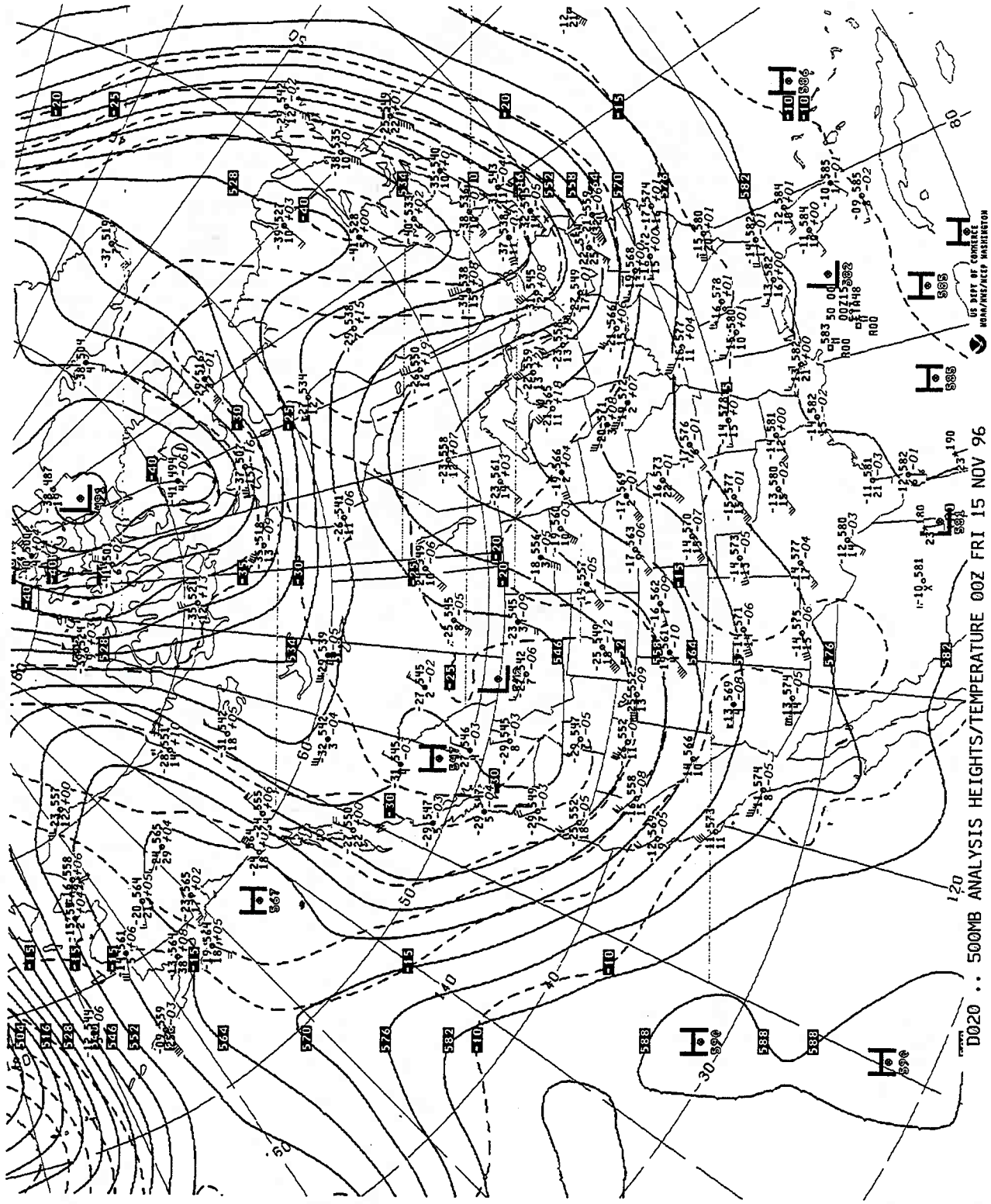

Figure A3-17: 500 mb weather map temporally closest to Test #11.

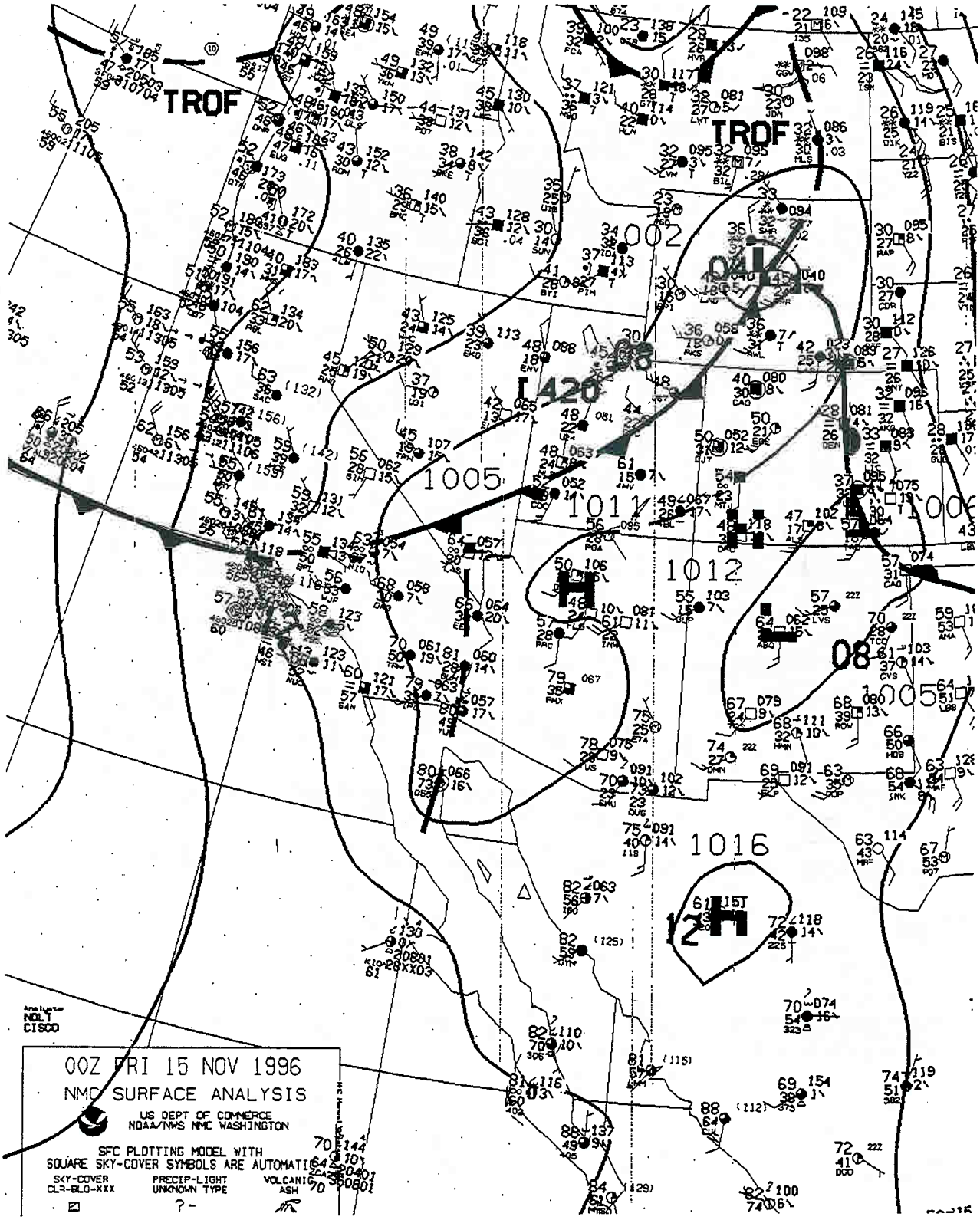

Figure A3-18: Selected portion of surface weather map temporally closest to Test #11.

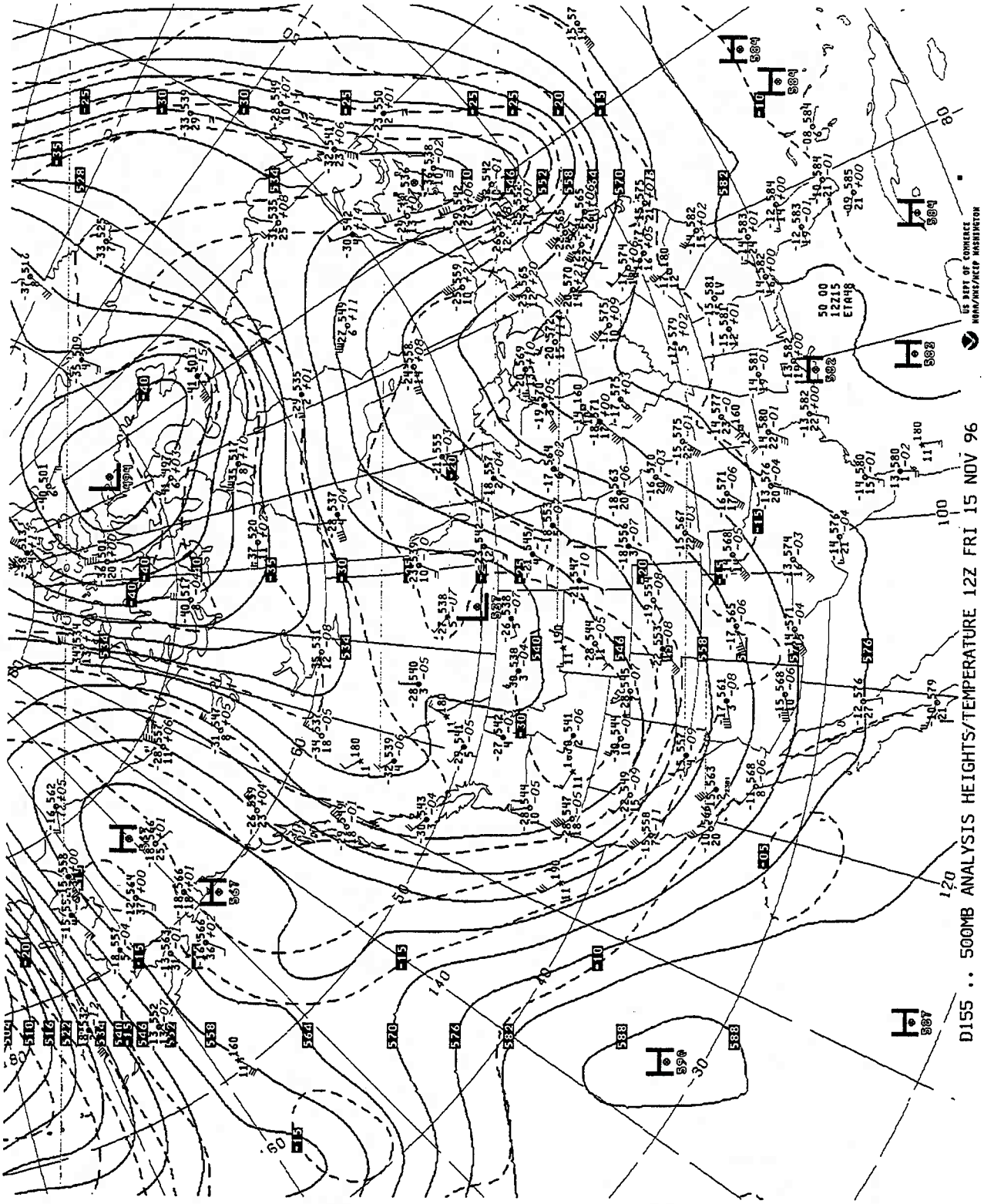

Figure A3-19: 500 mb weather map temporally closest to Test #12, Trial 3200900.

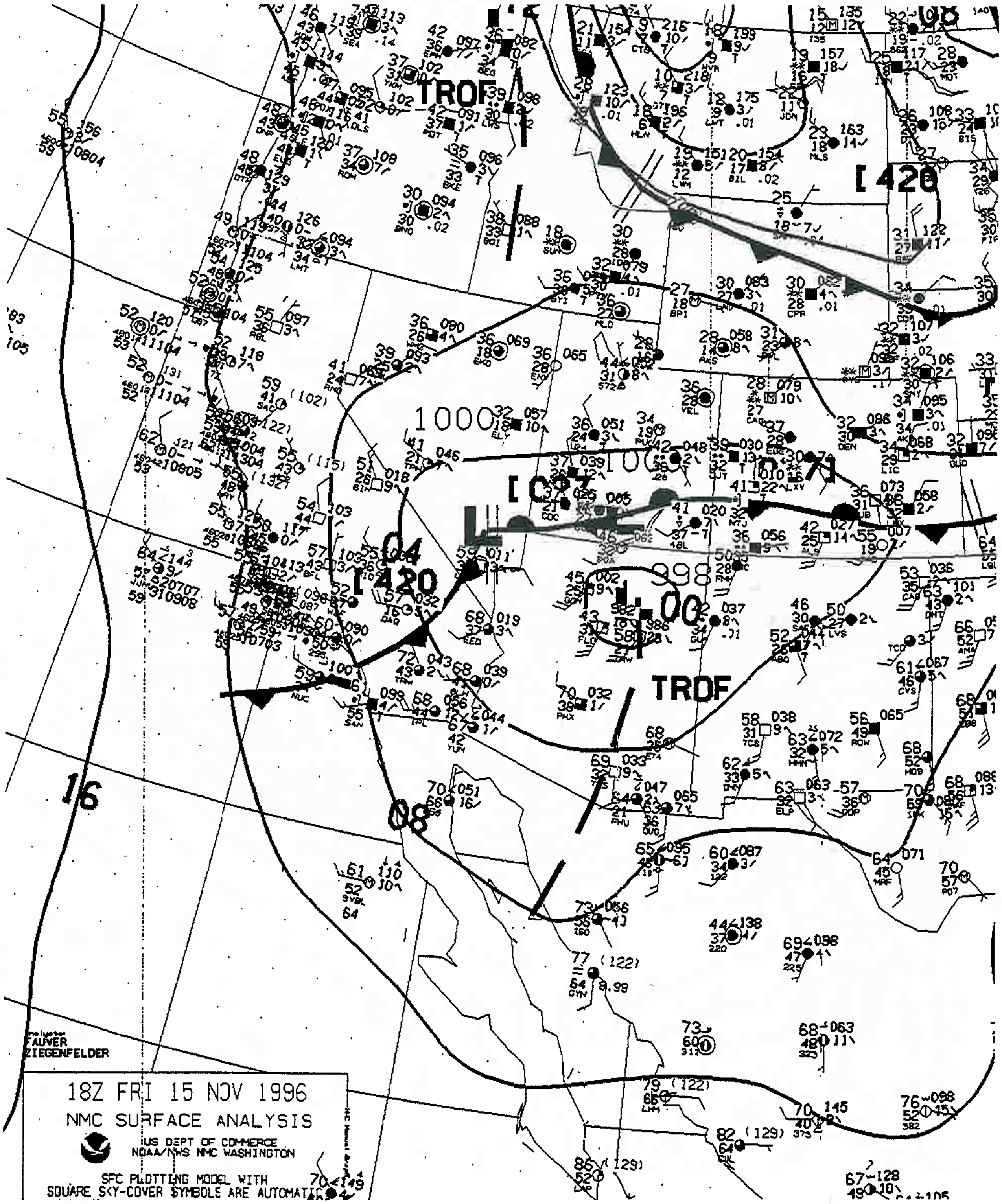

Figure A3-20: Selected portion of surface weather map temporally closest to Test #12.

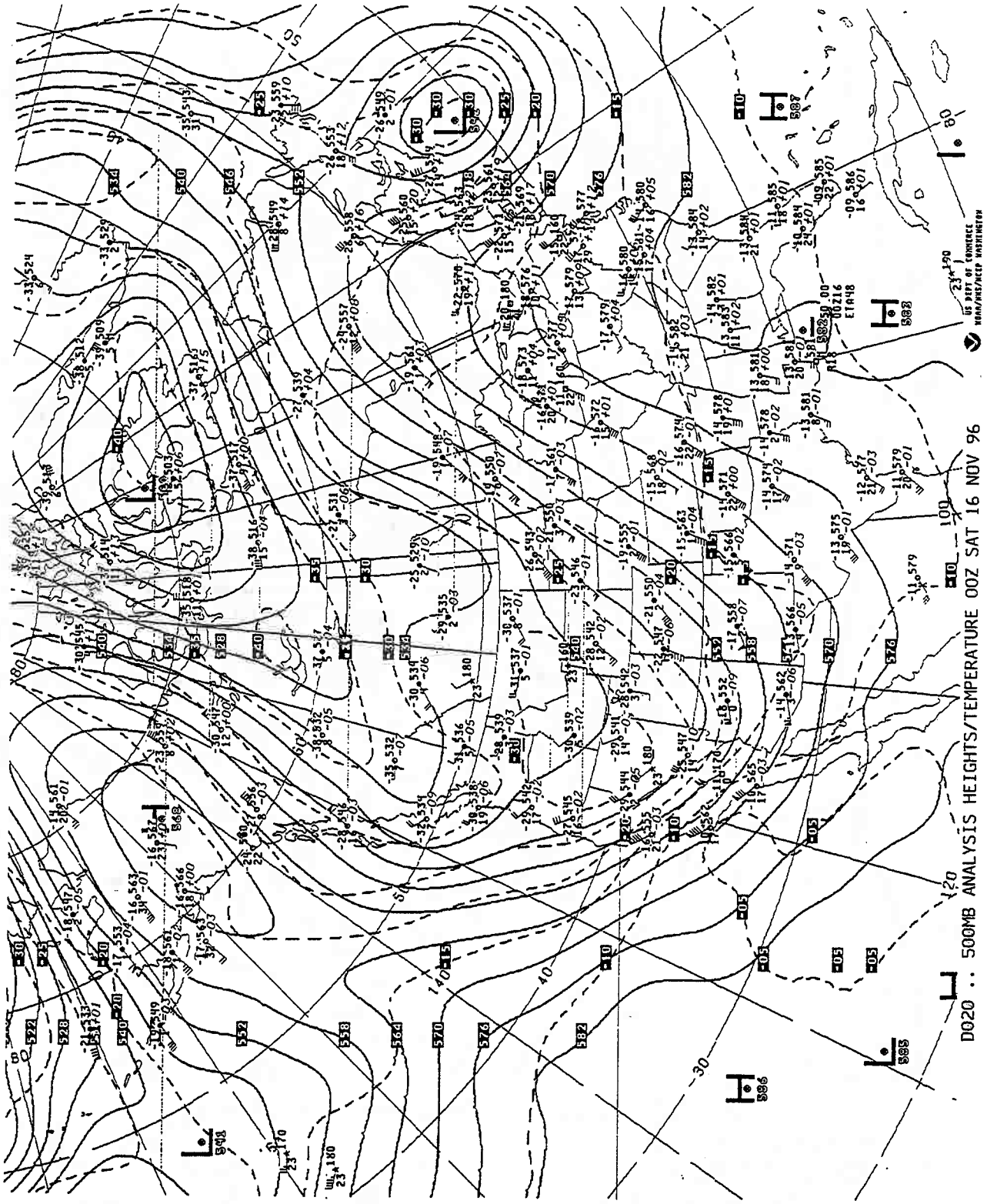

Figure A3-21: 500 mb weather map temporally closest to Test #13, (also closest to Test #12, Trial 3201030).

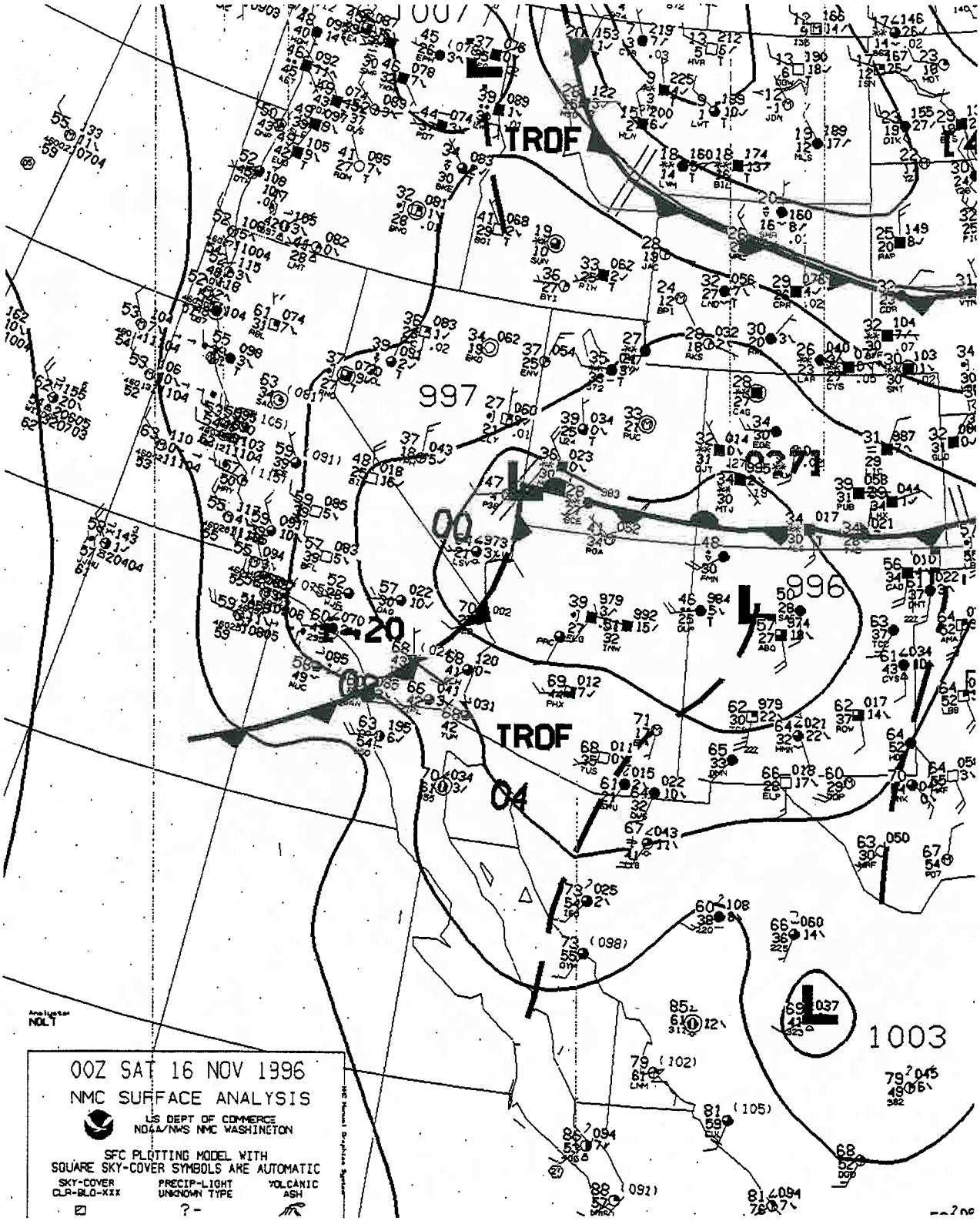

Figure A3-22: Selected portion of surface weather map temporally closest to Test #13.

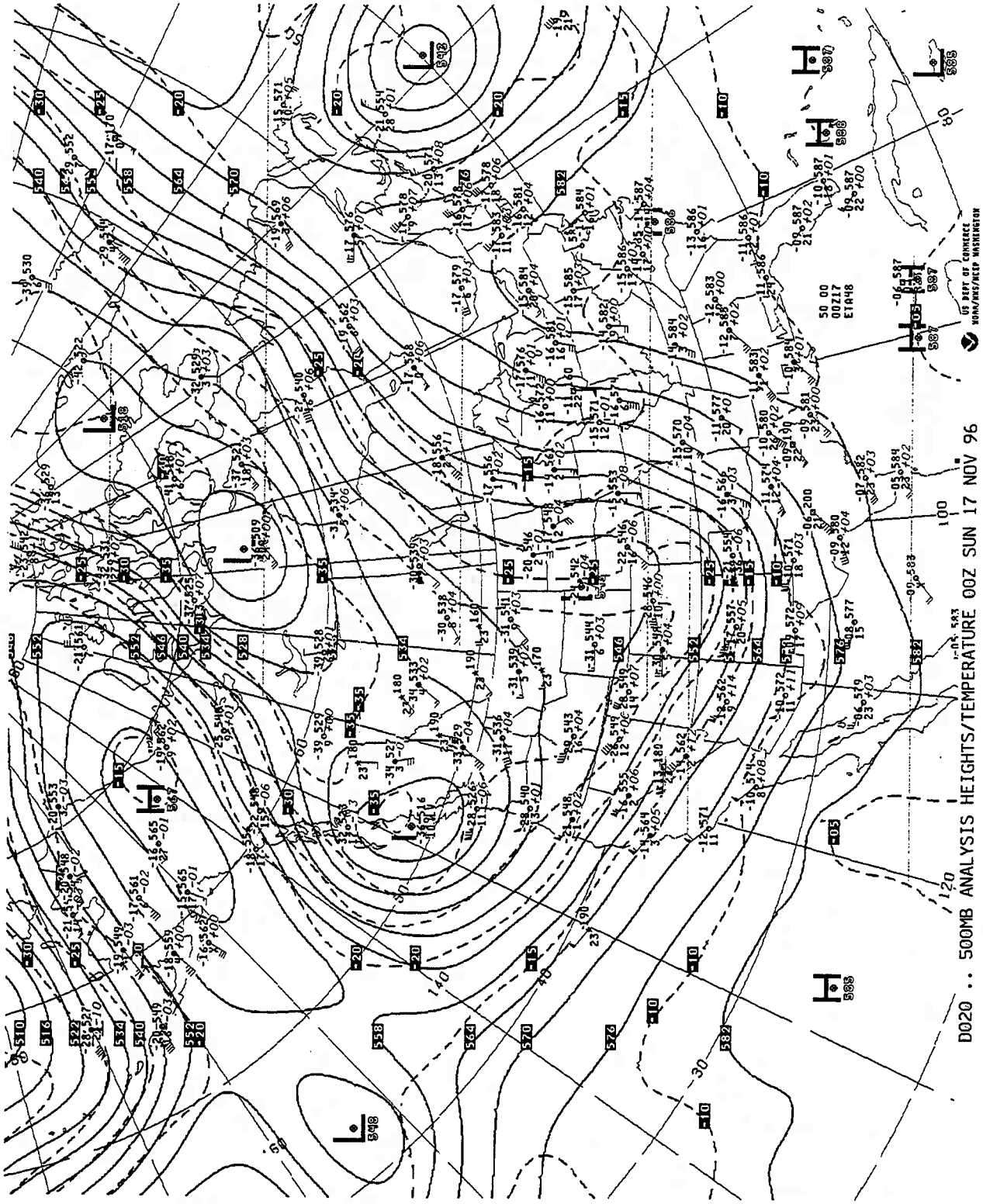

Figure A3-23: 500 mb weather map temporally closest to Test #14.

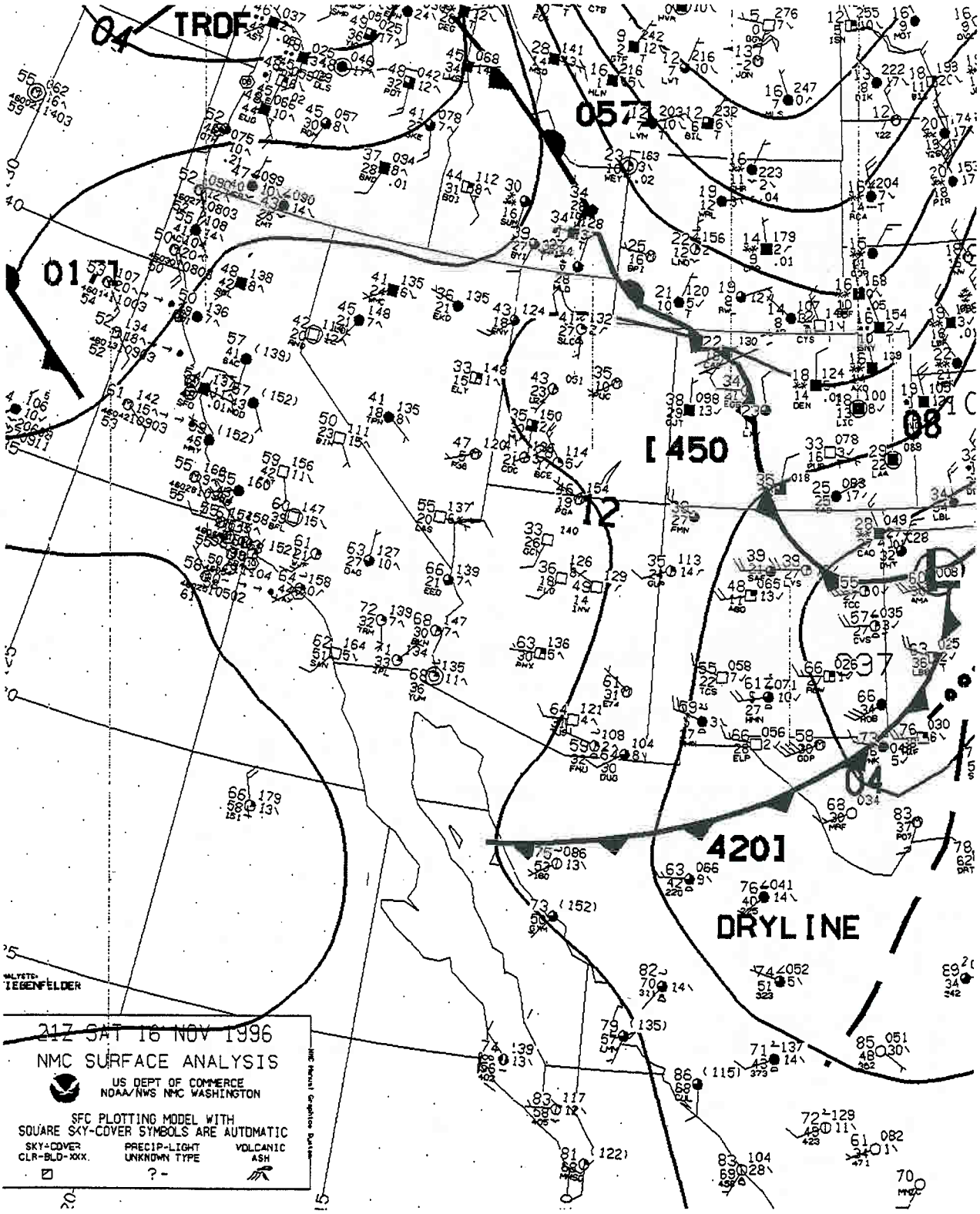

Figure A3-24: Selected portion of surface weather map temporally closest to Test #14.

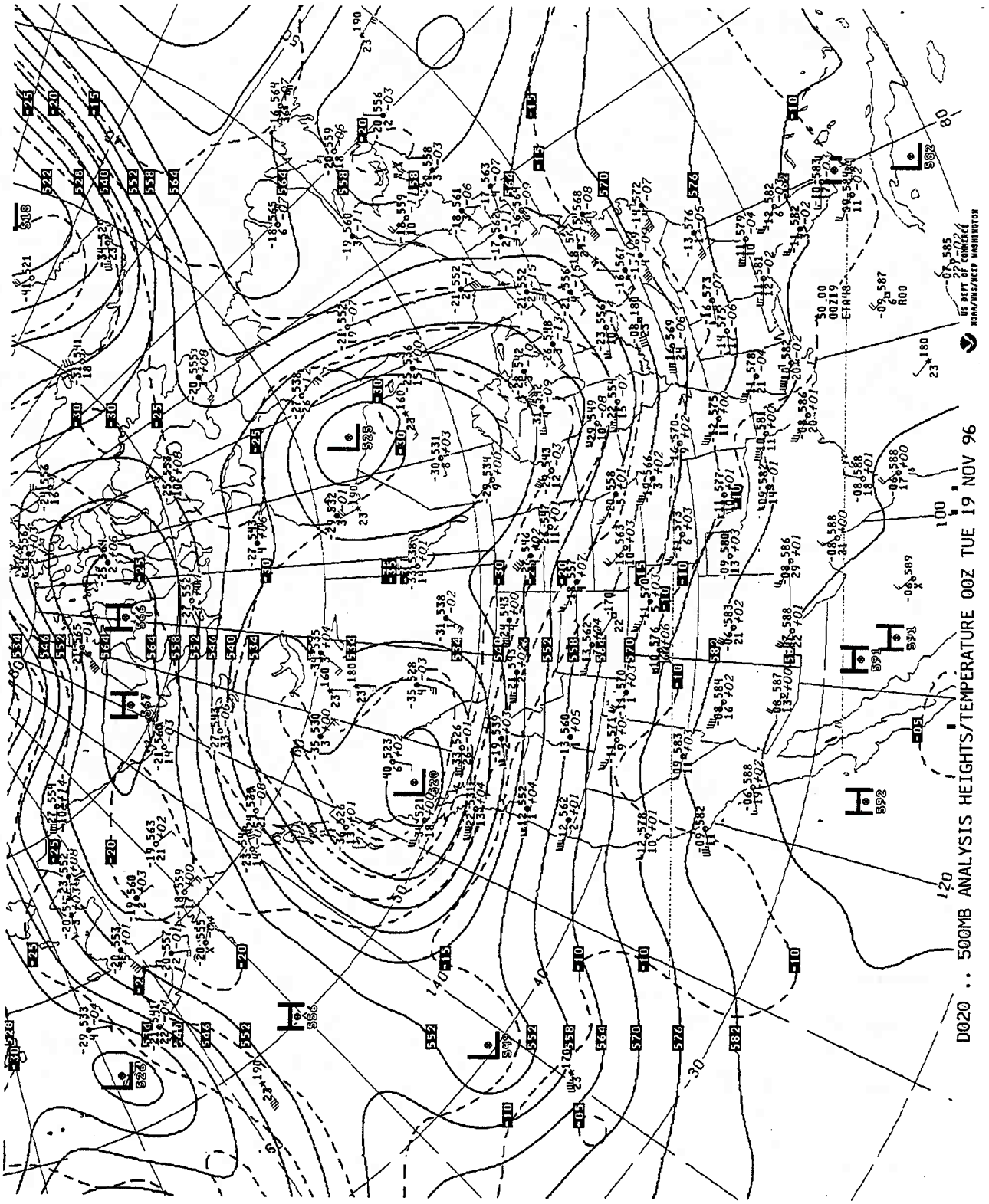

Figure A3-25: 500 mb weather map temporally closest to Test #15.

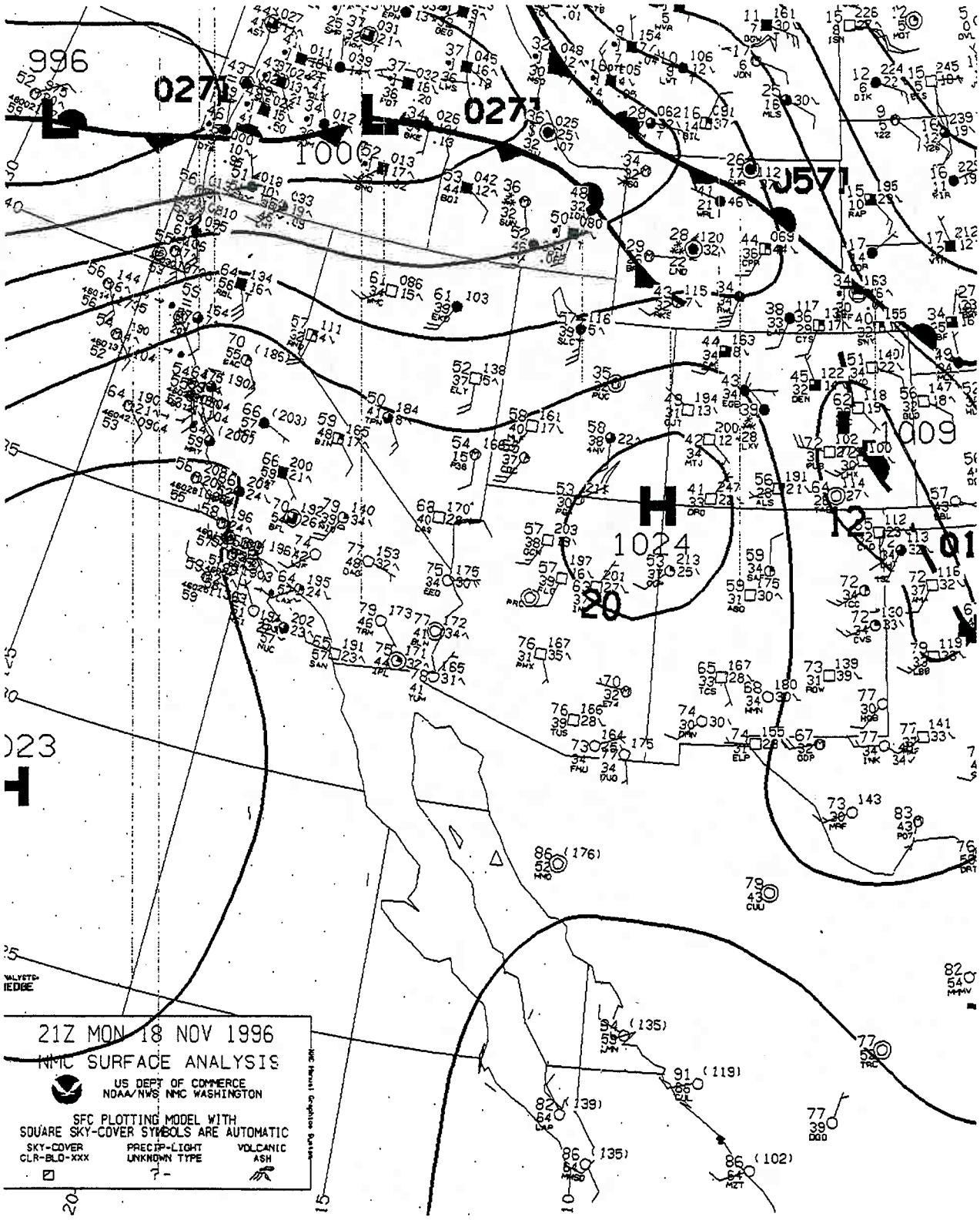

Figure A3-26: Selected portion of surface weather map temporally closest to Test #15.

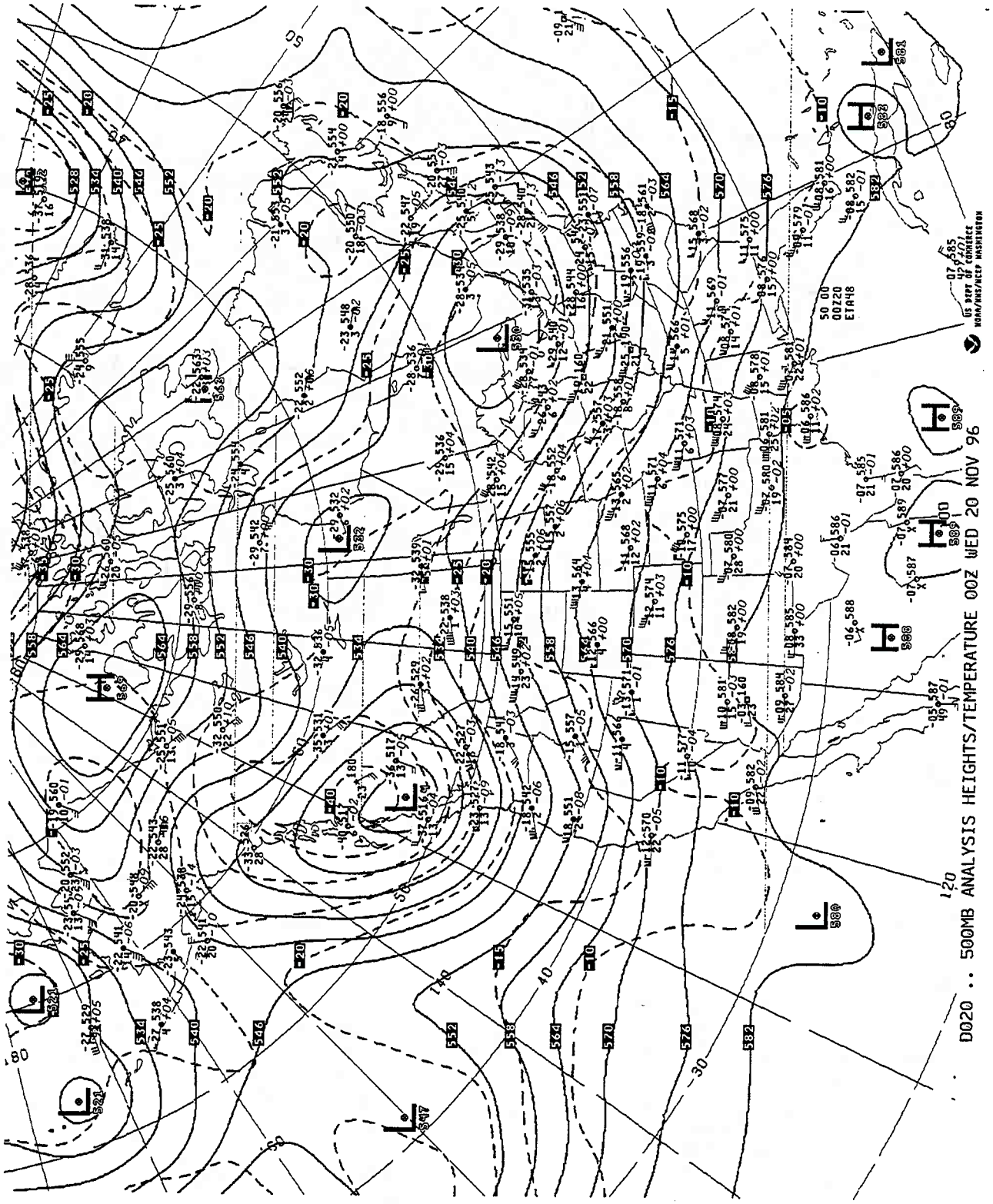

Figure A3-27: 500 mb weather map temporally closest to Test #16.

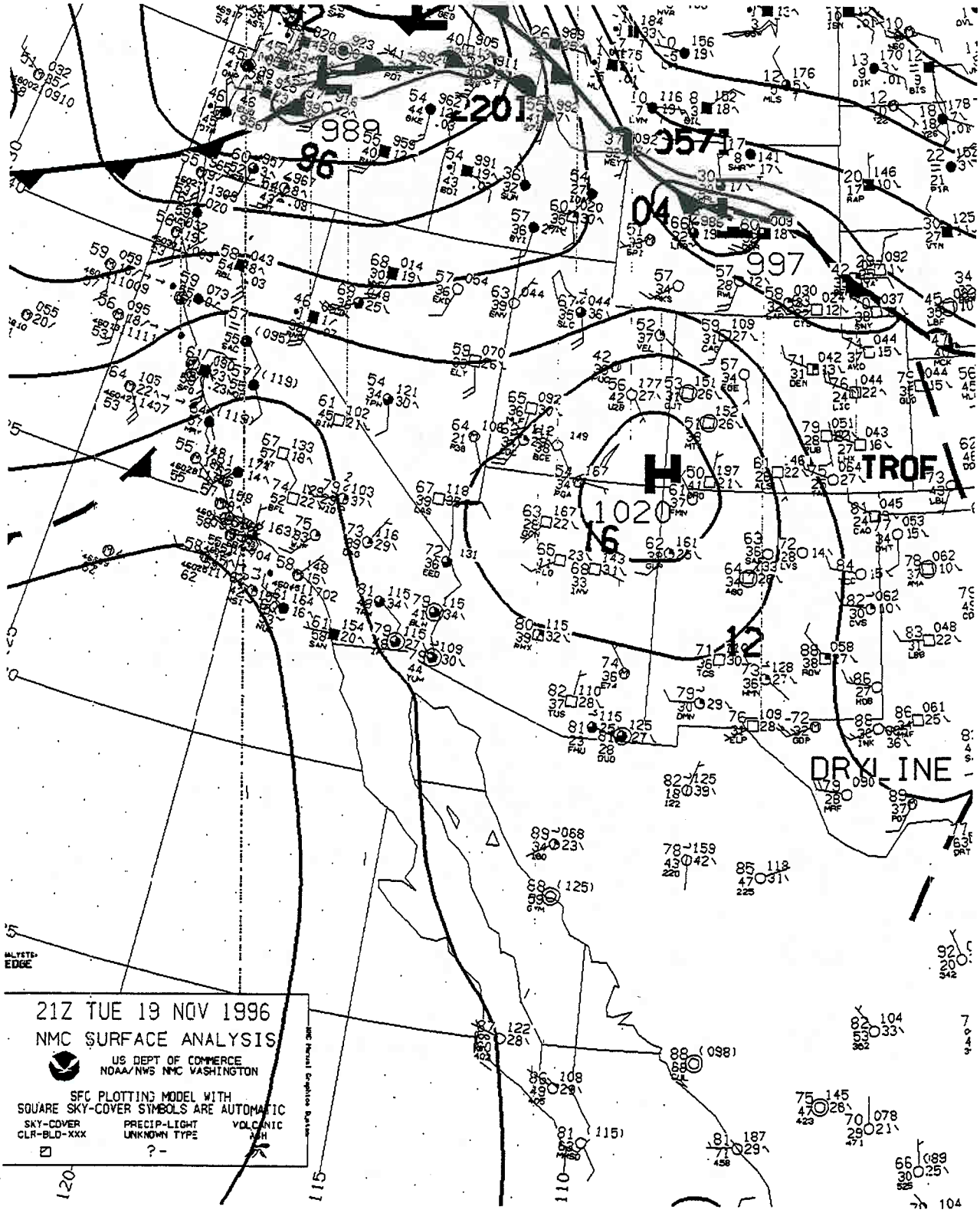

Figure A3-28: Selected portion of surface weather map temporally closest to Test #16.

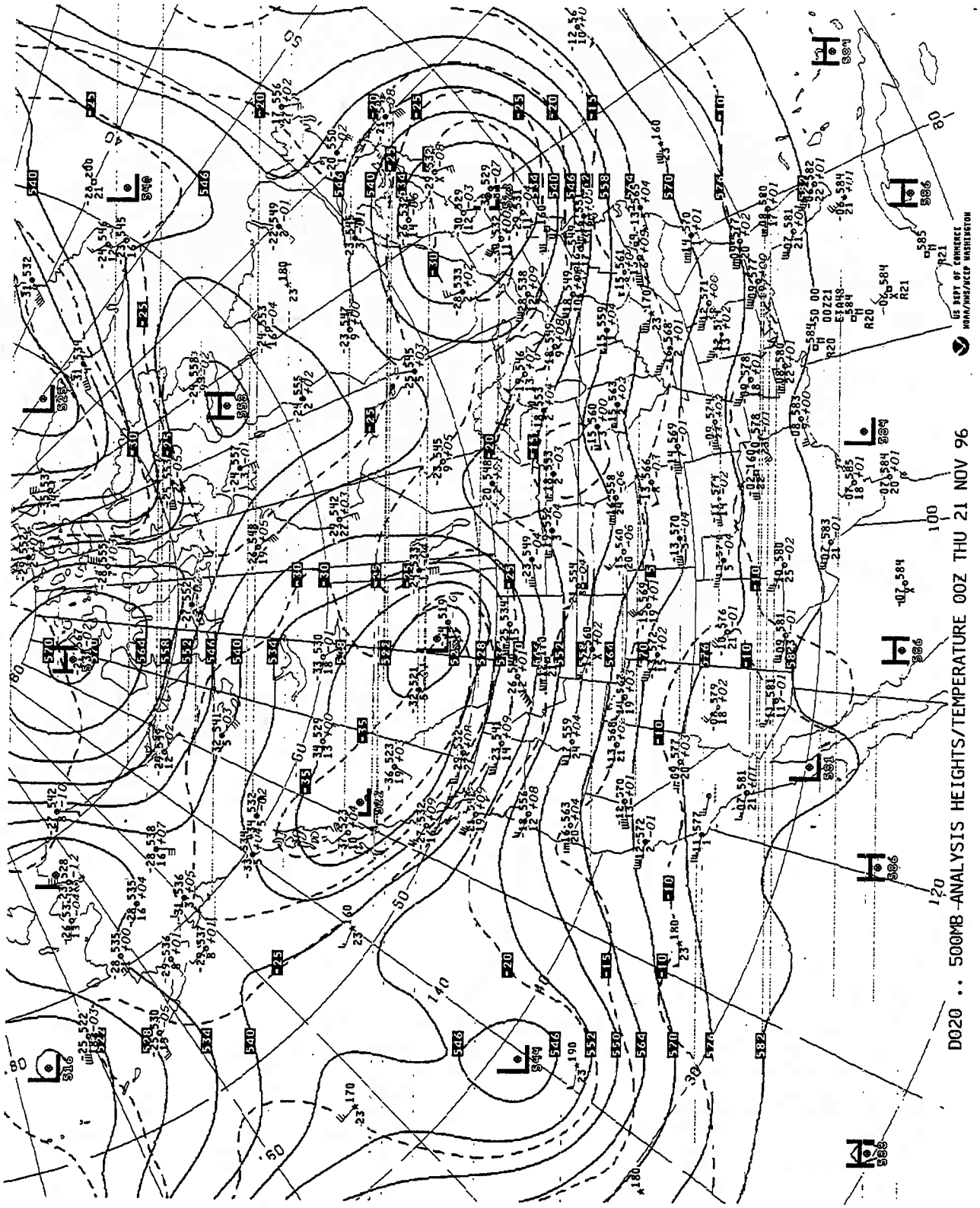

Figure A3-29: 500 mb weather map temporally closest to Test #17.

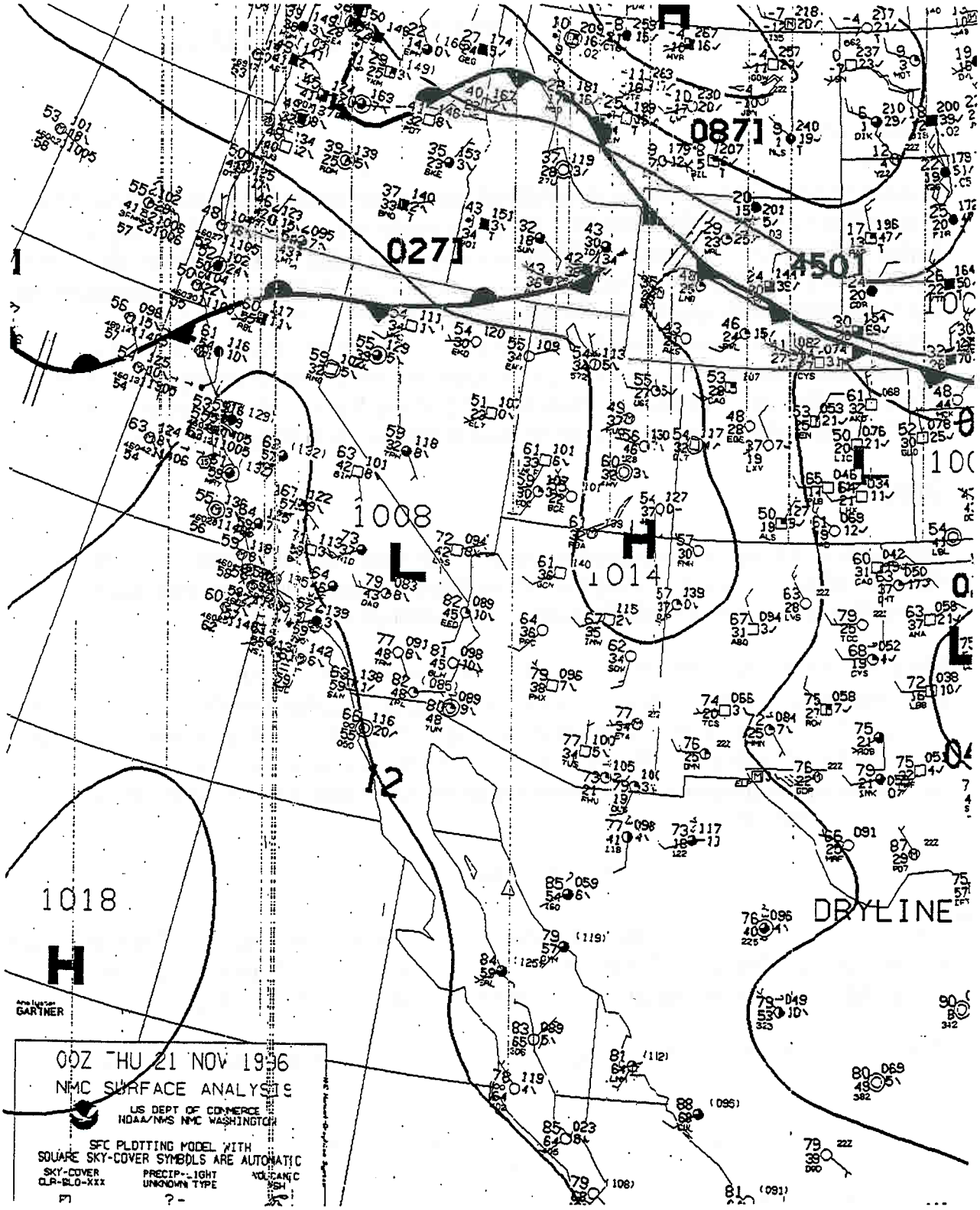

Figure A3-30: Selected portion of surface weather map temporally closest to Test #17, (surface map for 21Z on 11/20/96 unavailable).

APPENDIX 3: DISSEMINATION DATA

Summary

A quick check of the ideal gas assumption used to calculate the mass released for the Dipole Pride 26 test series (Biltoft, 1996) was made using the law of corresponding states. This check indicated a difference in the calculated mass on the order of fifteen percent for a nominal operating point. A more in depth evaluation was conducted to verify the initial calculation. Three independent methods, the law of corresponding states, a Virial, and a Martin-Hou (Mears et al., 1969) equation of state were used that yielded similar results. Therefore, it is suggested that a form of an equation of state other than ideal gas be used. I recommend that the Martin-Hou equation of state be used as it is anchored to experimental data in the range of interest for the experiment.

Discussion

The validity of ideal gas assumption used to calculate the mass released from the dissemination cylinder(s) during the Dipole Pride 26 test series was evaluated by calculation of the compressibility factor for a 'nominal' test point.

The Law of Corresponding States holds well in many instances for molecules that are not polar or hydrogen bonded. The dipole moment for sulfur hexafluoride is zero (Reid et al., 1977) indicating the molecule is not polar. The critical temperature and pressure for sulfur hexafluoride are 318.69 K and 3.77 MPa, respectively. The nominal temperature and pressure were assumed to be 300 K and 1 MPa. The compressibility factor is defined as:

$$Z = Z^{(0)}(T_r,P_r) + w\, Z^{(1)}(T_r, P_r)$$

where $Z^{(0)}$ is the spherical molecule term, $Z^{(1)}$ is a deviation function, and w is the Pitzer acentric factor. The value for the compressibility factor based on the tables and constants in reference 2 is 0.874, i.e., compressibility should be considered.

The van der Waals equation of state was used to calculate the expelled mass. The form of van der Walls equation used was:

$$(p + n^2a/V) (V - nb) = nRT \text{ [4]}$$

The coefficients are:

$$a = 7.857 \text{ bar } l^2 / \text{ mole}^2$$
$$b = 0.08786 \text{ l / mole.}$$

A Virial equation of state may be defined in the form of:

$$\frac{pv}{RT} = \sum_{i=0}^{n} \frac{B_i}{v^i}$$

The first virial coefficient, B_0, is unity and the second virial coefficient, B_1, is defined as (Lide, 1991-1992):

$$B_1 = \sum_{i=1}^{n} a_i \left[T_0 / T - 1\right]^{(i-1)}$$

The values for the coefficients are given as:

i	a_i
1	-278.8
2	-646.8
3	-335.1
4	-71.75

The Martin-Hou equation of state is a variation of a Virial equation of state:

$$P = \sum_{i=1}^{5} \frac{A_i + B_i T + C_i \exp(-KT / T_c)}{(V - b)^i}$$

T is in K, V is in cc/g, P is in bars, K is 6.88302200, T_c is 318.80 K, and b is 0.32736730. The constants are given as:

i	A_i	B	C_i
1	0.0	0.56926365	0.0
2	-4.99043505 10^2	0.54854082	-2.37588665 10^4
3	4.12453944 10^2	-0.334003447	2.81955047 10^4
4	-1.61292746 10^2	0.0	0.0
5	-0.48996987	0.109417750	-3.08268133 10^3

The mass for each trial was calculated using the four equations of state.

The compressibility factor relates the equations of state back to the ideal gas law. The Virial equations of state indicates a fifteen to twenty percent reduction in compressibility for conditions of interest.

Conclusions

A cursory evaluation of the validity of using the ideal gas law to calculate the sulfur hexafluoride mass in the dispersion of cylinder indicated a fifteen to twenty percent difference between assumed equation of states. It is felt that this difference is due to the operating point being close to the critical point. This difference was verified using three different approaches, the Law of Corresponding State, a Virial equation of state, and a Martin-Hou equation of state. The values calculated using a van der Waals equation of state do not agree with the three above approaches. Since the Martin-Hou equation of state is based on experimental data in the region of interest for the Dipole Pride 26 experiment, it is suggested that this formulation be used to calculate the mass, moles, of gas released.

REFERENCES

Lide, David R., 1991-1992. *CRC Handbook of Chemistry and Physics*, 72nd edition, CRC Press.

Mears, W. H, E. Rosenthal, and J. V. Sinka, 1969. Physical Properties and Virial Coefficients of Sulphur Hexafluoride, J. Phys. Chem., **73:**2254-2261.

Reid, Sherwood, and Prausnitz, 1977. *The Properties of Gases and Liquids*, 3rd ed., McGraw-Hill Book Co.

Chris Biltoft, FAX to Gary Ganong / Bill Espander, 19 Dec. 96, "Dipole Pride 26Preliminary Mass Calculations."

Table A4: DIPOLE PRIDE 26 Dissemination Times, Masses, And Comments.

Test #	Date (1996)	Trial* (JJJHHMM)	Sampler Start (PST)	Release Time (PST)	Number of release cylinders	Mass of SF_6 released (kg)	Comments
1	11/4	3091441	14:00	14:41	2	8.0	Bulk of puff missed sampler grid
2	11/6	**********	8:00	**********	1	11.5	SF_6 leak in actuator arm, no release
3	11/8	3130400	4:00	4:00	1	12.3	Plume near ground, 2 segments, pooling at Yucca Lake
4	11/9	3140400	4:00	4:00	1	11.5	Plume near ground, pooling at Yucca Lake
	11/9	3140530		5:38	1	11.5	
5	11/11	3160400	4:30	4:40	1	11.5	Plume lifting off surface
6	11/12	3170400	4:00	4:00	1	11.5	Plume lifting off surface

Test #	Date (1996)	Trial* (JJJHHMM)	Sampler Start (PST)	Release Time (PST)	Number of release cylinders	Mass of SF_6 released (kg)	Comments
7	11/12	3171300	13:00	13:00	2	19.3	1.5 sec between releases,
	11/12	3171445		14:45	1	10.0	Cylinder failed to function at 1445, OK at 1447
8	11/13	**********	9:30	**********			No release
9	11/13	3181400	14:00	14:00	1	10.4	Remote sensing instruments possibly detecting freon
10	11/14	**********	9:00	**********	1	11.3	Winds light & variable
11	11/14	3191430	14:30	14:30	1	10.6	Plume above sampler lines
	11/14	3191545		15:50	1	10.8	Plume in contact with surface
12	11/15	3200900	9:00	9:00	1	11.5	Possible leak,
	11/15	3201030		10:30	1	11.3	tightened gasket

Test #	Date (1996)	Trial* (JJJHHMM)	Sampler Start (PST)	Release Time (PST)	Number of release cylinders	Mass of SF_6 released (kg)	Comments
13	11/15	3201430	14:30	14:30	2	21.6	0.5 sec between releases, plume lofting
14	11/16	3211300	13:00	13:00	2	21.1	0.7 sec between releases
15	11/18	3231130	11:30	11:30	2	10.8	Disseminator leak
	11/18	3231300		13:00	2	20.2	
16	11/19	3241200	12:00	12:00	2	20.3	Plume passing east of samplers
	11/19	3241330		13:30	2	20.3	Plume passing west of samplers
17	11/20	3251200	12:00	12:00	2	20.4	Plume lofting
	11/20	3251330		13:30	2	20.1	Plume west of line, rising over hills nw

APPENDIX 4: PUFF WIDTH ESTIMATES AND CALCULATION METHODS

Cross Wind

Gaussian fits to concentration histograms generated for each sampling line were used to determine "best estimates" of puff width sigmas (σ_y) using the following procedure:

Profiles of the puffs were defined for passage of the SF_6 cloud over each sampling line. The highest SF_6 concentration measured as the cloud passed established the position of the maximum and time interval during which it occurred. Occasionally the highest levels were seen in two adjacent samples and were not significantly different. In this case, the concentration maximum likely passed between or over both sampler positions, and the computation procedure was performed using both locations. Table A5 contains the 15-min averaged puff concentration maxima (C_m) presented in pptv, and as a value normalized by the quantity of SF_6 released. The normalization was performed using a conversion procedure described by ASTM Standard Practice D1914-95[7]. Normalized C_m are rationalized to units of $m^{-3} \times 10^{-18}$.

A puff width histogram was then defined using the concentration data from all samples in the line taken during the sampling period when the identified maximum occurred. All sampler position measurements reporting concentrations above the LOD within this time period were used in the histogram. A total of 40 useful histograms identified in Table A5 by trial name, test name, line number, and bag number, were derived from the data set for the entire test program.

For some trials, above-baseline concentrations were measured at the extreme east and/or west positions of the sampling line, indicating that part of the puff probably missed the sampling line. When the missing data were well within the tail of the distribution, defined as one standard deviation from the peak concentration, the missing part of the histogram was filled in with "best guess" dummy data to permit statistical analysis of the histogram. Brackets in Table 8 indicate histogram statistics affected by this procedure.

Along Wind

Puff width estimates were made only for puff histogram data that met the following criteria: (1) the puff was largely contained on the sampling line; (2) the puff boundaries could be clearly distinguished from background; (3) the puff centroid was at or near the surface. To satisfy criterion (1) the puff center of mass, to include the centroid and at least one standard deviation to each side, must be contained within the sampling line. As a puff disperses downwind, its center concentration diminishes and boundaries become diffuse and difficult to distinguish from background, making a determination of σ_y difficult. Puff boundaries are sometimes defined using one tenth of the centroid concentration. Criterion (2) is satisfied if the centroid concentration exceeds the threshold (background) concentration by a factor of 10 or more. Occasionally, the bulk of a puff lofts over a sampling line. When this happens, the unusually low concentrations measured near the surface are unrepresentative of the actual puff dimensions. Aerospace Corporation provided real-time information on centroid height. Concentration measurements obtained when the centroid was observed to be detached from the surface are not used in the analysis.

Table A5: DIPOLEPRIDE 26 Lateral Dispersion Summary.

Test#	Trial(JJJhhmm)	Line Number	Bag Number	Source Distance (m)	Max[SF_6] (pptv)	Normali-zed[SF_6] $m^{-3}x10^{-18}$	BestFit σ_y	Coeff of Skew (ND)	Coeff of Kurt (ND)	Normal Departure	Crossing Angle (degrees)
3	3130400	1	1	1734	14244	6.577	161	0.091	0.745	6.7	83
3	3130400	2	3	10748	1725	0.795	(1178)	(0.169)	(1.511)	(27.0)	83
3	3130400	3	8	17222	97	0.046	1473	0.589	2.082	41.7	71
3	3130400	3	9	17308	90	0.043	1218	0.267	2.498	19.1	69
4	3140400	1	1	1993	13966	6.762	499	-0.601	2.608	22.4	70
4	3140400	2	3	11479	1304	0.633	1550	0.405	2.281	33.1	70
4	3140400	2	4	12047	1633	0.794	(680)	(0.352)	(3.315)	(15.4)	66
4	3140538	1	8	2569	7823	3.779	590	0.165	2.170	37.9	70
4	3140538	3	11	17577	158	0.075	(2375)	(-0.536)	(0.396)	(96.6)	85
5	3160440	1	3	3953	7093	3.455	277	0.675	4.305	21.7	78
5	3160440	2	6	11776	2148	1.044	(1170)	(-0.016)	(0.429)	(40.4)	73
5	3160440	3	10	18542	672	0.327	(1258)	(0.187)	(0.744)	(56.3)	74
6	3170400	1	2	2289	9889	4.792	433	0.257	1.532	77.9	76
6	3170400	2	7	12832	3240	1.569	531	0.729	3.058	34.6	48
6	3170400	3	10	18926	819	0.400	1745	2.394	7.774	111.7	74
7	3171300	1	4	19898	385	0.104	(2705)	(0.853)	(2.752)	(57.5)	46
7	3171300	2	3	10915	634	0.172	1083	0.127	1.932	32.1	78
7	3171300	3	2	5001	4625	1.262	(534)	(-0.025)	(0.276)	(59.2)	82
9	3181400	1	4	19013	174	0.090	(1448)	(0.136)	(2.302)	(13.7)	72
9	3181400	2	4	10765	661	0.341	974	-0.164	2.152	18.9	70
11	3191551	1	7	2341	27582	13.770	184	-0.028	12.765	3.9	80
11	3191551	2	10	12359	4890	2.441	700	-0.141	1.288	15.1	60

Test#	Trial(JJJhhmm)	Line Number	Bag Number	Source Distance (m)	Max[SF_6] (pptv)	Normalized[SF_6] $m^{-3}x10^{-18}$	BestFit σ_y	Coeff of Skew (ND)	Coeff of Kurt (ND)	Normal Departure	Crossing Angle (degrees)
11	3191551	3	11	18826	924	0.468	1376	0.564	2.365	24.7	73
12	3200900	2	3	13039	133	0.062	2377	0.275	1.849	22.7	73
12	3200900	3	3	19025	125	0.060	(2030)	(0.356)	(2.367)	(20.1)	73
12	3201030	1	7	2923	5173	2.421	240	0.006	2.324	7.5	55
12	3201030	2	8	13060	93	0.044	900	-0.263	0.933	27.1	74
13	3201430	1	1	2443	8190	2.002	123	-3.150	98.607	7.6	78
13	3201430	2	2	13352	303	0.074	601	0.223	4.510	16.2	67
13	3201430	3	1	19261	89	0.022	(722)	(-0.026)	(2.568)	(18.1)	68
14	3211300	1	3	20907	273	0.070	(1435)	(-0.268)	(2.323)	(14.0)	79
14	3211300	3	2	4435	2502	0.647	338	0.4856	4.768	24.0	70
15	3231130	2	4	10135	199	0.099	1320	0.220	2.231	23.7	84
15	3231130	3	2	4223	824	0.410	578	-0.149	0.530	32.9	87
15	3231130	3	7	4305	1154	0.305	279	0.564	3.316	16.8	80
16	3241330	1	8	20426	102	0.027	1746	-0.250	2.332	19.8	80
16	3241330	2	8	10828	894	0.233	478	0.622	4.700	13.5	65
16	3241330	3	7	4205	3555	0.927	276	0.808	3.783	36.7	80
17	3251200	2	3	10785	753	0.193	(812)	(0.489)	(2.210)	(25.3)	87
17	3251330	1	9	20400	170	0.045	(3379)	(-0.148)	(1.956)	(27.2)	85

Table A6: DIPOLEPRIDE 26 Along Wind Dispersion Summary.

Test#	Trial(JJJhhmm)	Position #	Source Distance (m)	Max[SF_6] (pptv)	Normalized[SF_6] $m^{-3}x10^{-18}$	Best Fit σ_y	Coeff of Skew (ND)	Coeff of Kurt (ND)	Normal Departure	Arrival time (hhmms)	Transport Speed (ms^{-1})
3	3130400	206	10747	2891	1.332	215	0.656	2.896	25.0	043519	5.07
4	3140400	224	11841	5088	2.474	134	0.686	3.218	21.6	044331	4.53
5	3160440	201	11460	2475	1.203	918	0.010	2.023	14.0	055545	2.52
6	3170400	212	12329	2875	1.392	969	0.615	2.648	34.0	051209	2.85
7	3171300	224	10835	1803	0.489	104	-0.001	0.104	32.2	134513	3.99
7				1895	0.514	177	0.834	2.802	37.9	134806	
7				4157	1.128	103	0.502	2.361	26.3	153622	
11	3191551	212	12329	6934	3.461	325	0.423	2.786	16.1	165522	3.19
12	3200900	218	13177	352	0.164	214	0.173	2.398	22.0	094148	5.25
12	3201030	218	13177	835	0.389	101	0.437	2.013	35.4	105827	3.76
14	3211300	201	11612	818	0.210	175	-0.195	1.058	36.9	133730	5.16
16	3241200	224	10835	443	0.115	190	-0.316	1.003	36.4	123720	4.84
16	3241330	206	11112	3084	0.804	99	0.009	0.016	30.7	135817	6.55
17	3251200	224	10835	1677	0.430	74	-0.383	1.696	28.5	123639	4.93
17	3251330	201	11612	897	0.230	165	0.428	2.373	20.7	141028	4.78

APPENDIX 5: DATA DIRECTORY STRUCTURE

The Data is divided into three main directories: a directory for the Visualization Images (IMAGES), a directory for the TGA-4000 data (TGA_DATA), and a directory for the whole air sampler data (SAMPLERS). The directory structure is as follows:

IMAGES:

- Lviewpro
- Area.bmp
- Nts.bmp
- Yucca.bmp
- 640x480
  - test01
    - nts_01x
    - .
    - .
    - .
  - test17
    - nts_17x
- 800x600
  - test01
    - dpp_01x
    - .
    - .
    - .
    - .
  - test17
    - dpp_17x

TGA_DATA:

- ttt-u-nn.plm

SAMPLERS:

- dswa01
- .
- .
- dswa17
- test01
- .
- .
- test17
- samplers

The IMAGES Directory contains LVIEWPRO files for image viewing and three shaded surface images: one of Yucca Flat, one of the Nevada Test Site and another of the area surrounding NTS. Two sub-directories entitled 640x480 and 800x600, representing image resolution, reside under the IMAGES Directory. Under each of these sub-directories are the sub-directories for each test. Each test sub-directory contains several files corresponding to individual frames in the animation sequence. These files are arranged alphabetically.

The format of each of the Windows bitmap files is as follows:

IMAGES:

640x480

nts_**x.bmp

800x600

dpp_**x.bmp

where:

** – corresponds to the test number

x – corresponds to letters a through o

.bmp - all files are windows bitmap files

The TGA_4000 Directory contains the processed output for each TGA. Files are comma delimited. Each File Contains: decimal Hours, latitude (degrees), longitude (degrees) altitude (meters), # satellites used in GPS, differential GPS indicator, SF_6 concentration (pptv).

TGA_DATA: ttt-u-nn.plm

"ttt" – the test number

"u" – a tga identifier

"nn" – a sequential plume number.

The SAMPLERS Directory contains the processed sampler data in two file formats and a file containing the sampler locations. Files are comma delimited.

SAMPLERS: dswa**.csv sampler files
** test number

File Contains: an array of SF_6 concentration data
column 1: location number
columns 2-13: SF_6 concentration data corresponding to sampling intervals 1-12.

test**.csv sampler files
File Contains:
column 1: Location number
column 2: bag number with 1/2 hour offset for line 100 or 300
column 3: decimal time
column 4: latitude (degrees)
column 5: longitude (degrees)
column 6: SF_6 concentration (pptv)

samplers.csv: sampler locations.

Line 100 is the North most line.
Line 200 is the middle line.
Line 300 is the South most line.

Each file contains:
column 1: location number
column 2: latitude (degrees)
column 3: longitude (degrees)
column 4: altitude (meters).

APPENDIX 6: INSTRUCTIONS FOR VIEWING IMAGE ANIMATION

Lviewpro is a Microsoft Windows application and has to be run from Windows 3.1, Windows 95 or Windows NT.

1. Double-click the LviewPro Icon.
2. Under File, select Multiple open.
3. The box: List files of type: should have Windows(*.bmp) selected. Under the box: Open destination the Slideshow button should be selected.
4. Select Setup.
5. Under Setup select Cycle Slides, de-select View Full Screen. You can choose to cycle through the frames Automatically with a minimum of 1 second intervals or you can cycle Interactively by clicking on the image with the right mouse button. Select the option you prefer.
6. Select O.K.
7. The left most box contains the image directories. Select the directory by double-clicking.
8. Select the test directory you want to view.
9. A list of files should be visible in the Current path: box.
10. Click the Add all button.
11. Click the O.K. button and the animation sequence will begin. To cycle interactively, use the right mouse button to click on each image.
12. To STOP the animation, click the image with the left mouse button and end the operation.
13. You can select Multiple open to run another test or select exit to end the program.

NOTE: The file Ctl3dv2.dll in the Images directory may need to be placed in the windows\system directory for LviewPro to work properly.

For proper display of the Images, the Color Palette in Windows should be set 256 Colors. This will depict the sampler concentration values in RED.

Also, it may be advantageous to move LviewPro and the underlying image files to your hard-drive for a more responsive operation.

APPENDIX 7: SF6 RELEASE SYSTEM

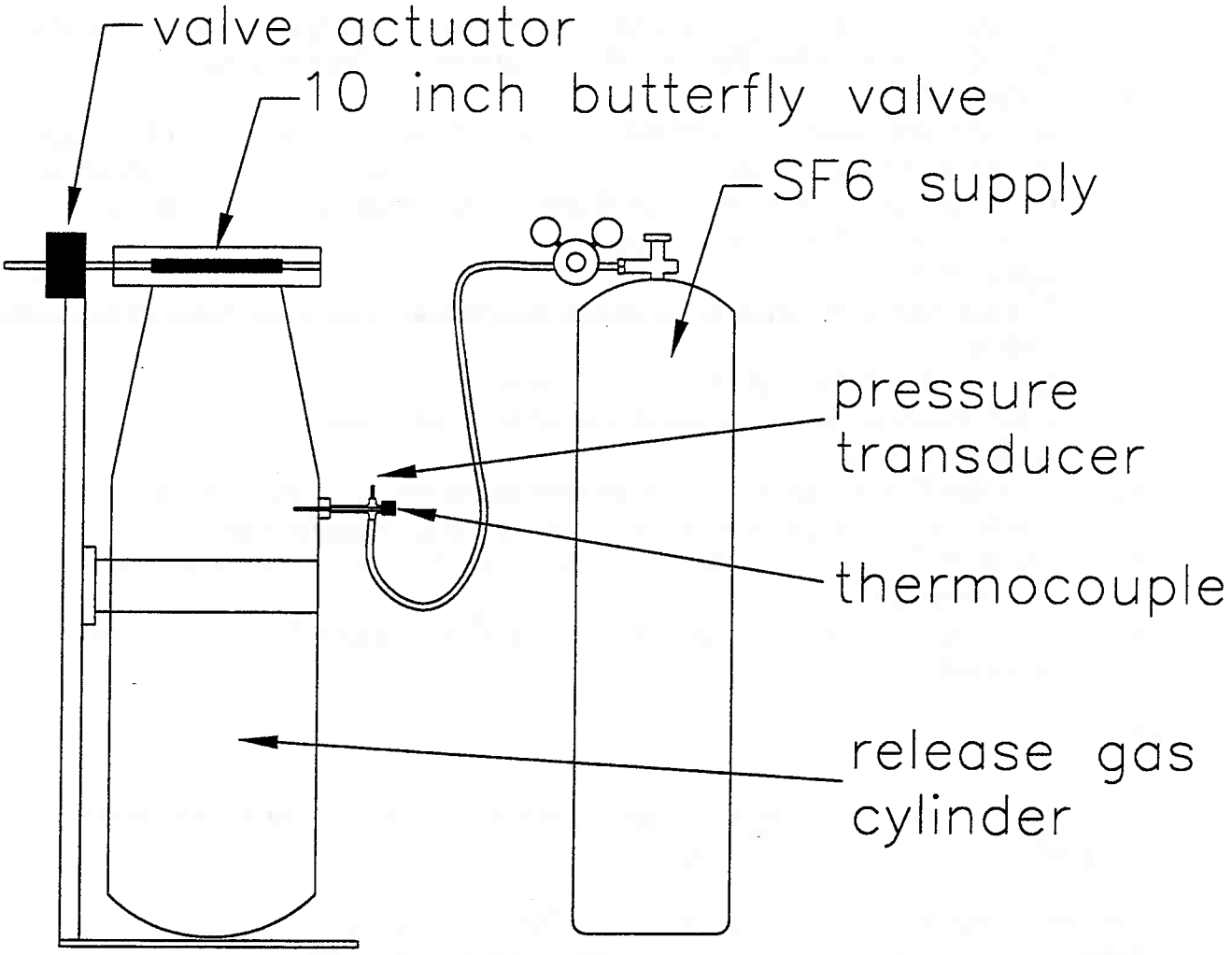

Figure A7: SF_6 release system.